Development of novel cardiovascular biomarkers by MRI assessment of postprandial physiology

Jakob Alexander Hauser

University College London (UCL)

Doctor of Philosophy (PhD)

I, Jakob Hauser, confirm that the work presented in this thesis is my own. Where information has been derived from other sources, I confirm that this has been indicated in the thesis.

Amsterdam, 14 September 2021 _____  _____

i. Abstract

Stress testing is an important concept in cardiovascular medicine. Feeding is a common cardiovascular stressor. Unlike metabolic or immunological stress, the links between feeding-induced haemodynamic stress and cardiovascular risk and dysfunction have not yet been explored in humans.

Therefore, cardiovascular responses to a meal were firstly characterised comprehensively in healthy volunteers using a novel rapid MRI protocol. It was shown that the ingestion of food decreased mesenteric vascular resistance substantially, and that this was compensated for by a rise in cardiac output primarily.

Previous research demonstrated that mesenteric vasoreactivity was blunted in obese animals and those on a lipid-rich diet. This was linked to greater myocardial mass, an important and independent risk factor for cardiovascular disease in early life. Therefore, the proposed protocol was conducted in adolescents of varying weight to investigate links between mesenteric vasoreactivity and indicators of cardiovascular risk. Blunted postprandial mesenteric vasoreactivity was associated with raised systolic blood pressure and greater left ventricular mass. Importantly, this was independent of other factors known to influence these variables, such as pubertal stage, obesity, insulin resistance, and resting blood pressure.

Abnormal vascular resistance of the limbs and the intestine has been described in Fontan-palliated patients with univentricular congenital heart disease, possibly in order to maintain organ perfusion in the presence of low cardiac output and chronic venous congestion. It was hypothesised that this mechanism could interfere with the common cardiovascular responses to feeding. Using the established protocol, vasoconstriction of the legs, but not the intestine, was found in fasting Fontan patients compared to controls. While the mesenteric responses to the meal were similar, Fontan patients had abnormal responses of the celiac axis and the lower limbs.

In conclusion, cardiovascular stress testing by controlled administration of a standardised meal may yield novel biomarkers in different settings of cardiovascular disorders.

ii. Impact statement

The presented research demonstrates that postprandial cardiovascular physiology in humans can be studied safely and in a dynamic fashion using MRI. The proposed study protocol may help reduce, or even obviate, the need for animal trials for *in vivo* cardiovascular studies, and may serve as future basis to investigate the role of vasoreactivity, in particular of the intestine, in various clinical settings and populations.

Exploration of mesenteric vasoreactivity after a meal could yield new diagnostic tools and even, perhaps, lead to interventions in the earliest stages of cardiovascular disease. For example, vascular responses to a high-fat, high-sugar meal could be used to identify young people at increased cardiovascular risk before other more established risk factors are diagnosed, allowing for earlier preventative measures. The links highlighted between altered postprandial vasoreactivity and myocardial hypertrophy may also stimulate further research into new, previously unrecognised mechanisms for cardiovascular risk and dysfunction.

Testing postprandial vasoreactivity may further provide new insights on the long-term complications of the Fontan circulation, such as reduced exercise capacity and protein-losing enteropathy. This may yield new strategies to identify patients at risk before overt derangement of resting (fasting) physiology is seen.

TABLE OF CONTENTS

iii. Acknowledgements

First and foremost, I would like to thank the numerous patients and volunteers who gave so generously of their time and patience to make this research possible.

Of course, I would also like to express my utmost gratitude towards my co-supervisors, Vivek Muthurangu, Andrew Taylor and Alex Jones, who have not only provided me with superb academic guidance, but have also equipped me with invaluable skills, knowledge and critical thinking over the past few years.

I would also like to thank Claudio Cappelli for introducing me to the team and to the department, and for essentially making all of this possible; Jennifer Steeden and Grzegorz Kowalik for developing the MRI sequences and post-processing tools used for my research; Wendy Norman, Rod Jones, Steven Kimberley, Petrina Hetherington and the entire CRF and the NIHR BRC at Great Ormond Street Hospital for their amazing support and assistance with the studies, as well as Bejal Pandya for her help with patient recruitment, and Ina Michel-Behnke for her clinical mentorship throughout the years.

Working with such amazing people has truly been a privilege, inspirational and great fun.

Furthermore, I would like to thank the European Commission for providing the funds for my research as part of the MD-Paedigree project (contract no. 600932), as well as to Cargill Starches & Sweeteners Europe for their kind donation of food-grade maltose syrup to the experiments.

Finally, I thank my friends and family for supporting me throughout the years – and for crucially reminding me that life exists outside of work.

iv. Index of tables

v. Index of figures

vi. Abbreviations

2D	2-dimensional
3D	3-dimensional
AAo	Ascending aorta
b-SSFP	Balanced steady-state free precession
BMI	Body mass index
BP	Blood pressure
Bpm	Beats per minute
BSA	Body surface area
CAD	Coronary artery disease
CHD	Congenital heart disease
CO	Cardiac output
CVD	Cardiovascular disease
CVP	Central venous pressure
DAo	Descending aorta
DBP	Diastolic blood pressure
EF	Ejection fraction
eSBP	Elevated systolic blood pressure
GLP	Glucagon-like peptide
HF	Heart failure
HOMA-IR	Homeostatic model assessment of insulin resistance
HR	Heart rate
IVC	Inferior vena cava
k-t SENSE	*k*-space and time (*k-t*) sensitivity-encoding imaging
LV	Left ventricle / ventricular
LVEDV	Left ventricular end-diastolic volume
LVESV	Left ventricular end-systolic volume
LVH	Left ventricular hypertrophy
LVM	Left ventricular mass
LVM:EDV	Left ventricular mass/volume-ratio
MI	Myocardial infarction
MPR	Multi-plane reformatting
MRI	Magnetic resonance imaging
OGTT	Oral glucose tolerance test
OS	Operating system
PA	Pulmonary artery

PAP	Pulmonary arterial pressure
PCMR	Phase-contrast magnetic resonance imaging
pCO_2	Carbon dioxide partial pressure
PLE	Protein losing enteropathy
pO_2	Oxygen partial pressure
PVR	Pulmonary vascular resistance
PWV	Pulse wave velocity
RAGS	R-R interval averaged golden angle spiral
RAP	Right atrial pressure
RF	Radiofrequency
ROI	Region of interest
RV	Right ventricle / ventricular
SBP	Systolic blood pressure
SD	Standard deviation
SE	Standard error
SENSE	Sensitivity-encoding
SMA	Superior mesenteric artery
SNR	Signal/noise-ratio
SSFP	Steady-state free precession
SV	Stroke volume
SVR	Systemic vascular resistance
T2DM	Type 2 diabetes mellitus
TAC	Total arterial compliance
TCPC	Total cavo-pulmonary connection
TR	Repetition time
V_{enc}	Velocity-encoding
VSD	Ventricular septal defect
VTI	Velocity-time integral
WU	Wood units

Chapter 1. Introduction

1.1. Introduction

Stress testing is one of the cornerstones in the diagnostics, the risk stratification and the pathophysiological understanding of cardiovascular disease (CVD). While various types of cardiovascular stress diagnostics exist (e.g., cardiopulmonary exercise testing, tilt table test, etc.), one important aspect of cardiovascular physiology has remained largely unexplored in the context of CVD: the postprandial state.

Feeding triggers a variety of cardiovascular responses, similar to orthostatic manoeuvres, mental stress, or physical exercise.(1) While the links between the metabolic and immunological responses to a meal and cardiovascular risk are well-established,(2) the significance of the haemodynamic responses have yet to be determined. This raises the possibility that stressing the cardiovascular system with a meal in a controlled setting may reveal previously unrecognised biomarkers of cardiovascular risk and dysfunction, or could identify new mechanisms in the pathophysiology of CVD.

Therefore, the objectives of the research presented herein were:

- To establish a magnetic resonance imaging (MRI) protocol to study cardiovascular physiology dynamically in the setting of feeding;
- To characterise the cardiovascular responses to food ingestion in humans, and
- Based on these findings, to explore new potential markers of cardiovascular risk and dysfunction in 2 different populations with CVD or at risk of it;
- To generate new hypotheses for future research on cardiovascular risk in these populations.

In the first 2 chapters of this thesis, an overview of various aspects and topics relevant for the understanding of this thesis will be provided, including the principles of MRI. Following this, the general methods used universally throughout the conducted experiments will be described in Chapter 3.

Experiments and research findings will be presented in the following 3 chapters. Each contains a brief introduction to set out the scientific context and the study's rationale. Variations in methodology, and study-specific methods will be discussed separately in a brief 'Methods' sub-section. In the final chapter, all findings will be summarised, and perspectives for future research discussed.

The results of this thesis were published in peer-reviewed scientific journals.(3-5) Permissions to use certain elements, such as tables or images, were obtained as necessary.

1.2. The postprandial state

1.2.1. Definition and significance

The term, 'postprandial state', generally refers to the period that comprises and follows a meal. Its onset coincides with the initiation of food intake, as physiological changes can be observed within very short time once feeding starts.(2, 6) No universally agreed definition exists for its duration, as the persistence of the physiological changes varies by organ system and is influenced by meal size and composition (e.g., fat content).(7, 8) Most literature suggests a 4-hour interval by which most physiological responses have normally returned to baseline (fasting) conditions.(8, 9) Considering the eating habits in the industrialised world, this means that most people in Western societies spend the better proportion of the nychthemeral period in the postprandial state.(10)

1.2.2. Metabolic and immunological changes

It is now well-established that impaired postprandial lipid and glucose homeostasis is linked to cardiovascular risk independently of fasting metabolism.(2, 11) For example, measuring the postprandial responses in blood glucose (and insulin) to an oral glucose tolerance test (OGTT) can detect abnormalities in glucose metabolism and identify people at risk of type 2 diabetes mellitus (T2DM) even before disturbances in fasting glucose homeostasis can be detected.(12) Glycaemia after food ingestion has also been

linked to leukocyte activation, and endothelial damage and dysfunction.(13) These factors are also thought to promote CVD, but their significance has yet to be established in prospective or interventional studies.

Similarly to oral glucose challenges, the potential diagnostic and prognostic advantages of assessing lipid metabolism after an oral lipid challenge are now increasingly recognised.(14) For example, postprandial triglyceride-rich remnant lipoproteins have been linked, directly and indirectly, to raised levels of systemic inflammation, platelet activation and greater thrombogenicity, proliferation of smooth muscle cells, as well as to increased adhesion and migration of immune cells to and into the arterial wall.(11, 15) These findings are known promotors of atherosclerosis and CVD. However, as the protocol for such an oral lipid challenge, and the biochemical markers to measure the responses to it, have yet to be agreed upon, this type of test is still less established in clinical routine and research.

In summary, metabolic ‘stress tests’ such as the OGTT are now essential tools in the risk stratification, the diagnosis and for the pathophysiological understanding of CVD and associated disorders.

1.2.3. The cardiovascular system in the postprandial state

The ingestion of a meal triggers a number of cardiovascular responses serving different physiological purposes.(1, 16) Two main phases are differentiated, each characterised by distinct changes.

During the first phase, the anticipation and ingestion of a meal is accompanied by increases in heart rate (HR), cardiac output (CO) and blood pressure (BP), as well as by minor increases in regional vascular resistance of the skin and skeletal muscles.(16) These adaptations appear to be mediated predominantly by sympathetic signalling, which is why this phase is also referred to as the cephalic phase. Physiological changes during this phase prepare the body for the imminent rise in gastrointestinal blood flow, support the production of gastric

acid and supply blood to body regions involved in the process of food ingestion.(16)

The second phase of digestion and absorption typically commences in overlap with the mid-late ingestion phase. It is characterised by a rise in gastrointestinal blood flow, which can be observed within minutes after the onset of feeding.(7, 16) During this phase, segmental increases in regional perfusion of the stomach and the intestine are observed, depending on the location of the chyme. Following a brisk, transient increase in celiac flow, a steady rise in CO and mesenteric perfusion is typically seen, caused by a drop in both splanchnic and total systemic vascular resistance (SVR).(7, 17) Inconsistent data exist regarding the vascular responses of the kidneys and the limbs following the ingestion of a meal.(1, 7, 18-20)

1.2.4. Regulation of cardiovascular responses

Global haemodynamics

The postprandial rise in CO is due to an increment in both, HR and stroke volume (SV), both of which are mediated by sympathetic nervous activity and catecholamine release. Raised sympathetic nervous activity is in part mediated by insulin release postprandially. Insulin has also been shown to have direct positive chronotropic and inotropic effects on the heart.(1) Similar observations have been made for the vasoactive intestinal peptide and glucagon-like peptide (GLP).(1, 21)

Regional vascular function

In the unfed state, blood flow to the abdominal organs is restricted through multiple mechanisms. In the mesenteric and renal arteries (i.e., the large, proximal vessels), blood flow is inhibited mainly centrally via α_1-adrenergic vasoconstrictive signalling from the medulla oblongata and via a number of humoral pathways.(16) This includes hormones that regulate vascular tone systemically, such as vasopressin, and such that are involved in local regulation, such as serotonin. Fasting increases intestinal production of serotonin, which causes mesenteric vasoconstriction through paracrine effects.

Interestingly, intestinal serotonin has also been shown to be up-regulated by a high-fat diet in animals, suggesting that this hormone may be involved in some of the cardiovascular sequelae of an unhealthy diet in humans.(22)

Another gut-specific mechanism that regulates vascular tone of the mesenteric arteries regionally is autoregulation through mechanical and metabolic feedback. Similar to other arteries, such as the renal or the cerebral arteries, vascular tone in the smaller mesenteric arteries responds to changes in transmural pressure (e.g., due to fluctuations in BP). This is mediated by both, L- and T-type Ca^{2+}-channels, which respond to raised wall tension of the vessel with a Ca^{2+}-influx and thus, depolarisation and constriction of the vessel.(23) In the more distal, smaller vessels (e.g., the villus arterioles and submucosal capillaries of the intestine), paracrine factors, such as local endothelin-1, restrict perfusion. Another important mechanism is metabolic autoregulation via partial oxygen pressure (pO_2), which causes changes in vascular tone that are dependent on the metabolic activity of the gut: greater activity reduces pO_2, which diminished O_2-mediated vasoconstriction and, thus, increases delivery of blood. As a result of these mechanisms, only 20-30% of the intestinal capillaries are perfused under fasting conditions, and only a small proportion of CO is commanded by the gut.(16)

A hormone centrally involved in the regulation of splanchnic blood flow is leptin. It exerts both, systemic (as adipocyte-derived hormone) and paracrine effects (as gastric hormone), the 2 of which are mutually distinct. Adipocyte-derived leptin is involved in energy homeostasis and appetite regulation (e.g., upregulation of thermogenesis), as well as in cardiovascular signalling. This includes both, pressor signals (i.e., sympathetic activation) and depressor signals (via endothelial nitric oxide release). Obesity appears to cause resistance to some of the more beneficial of its systemic effects (e.g., nitric oxide release), but less so to the potentially detrimental ones (e.g., sympathetic activation), suggesting that it may play a role in the development of CVD.(24)

Leptin is also stored in gastric epithelial cells and appears to be released acutely within few minutes by feeding as well as by local release of cholecystokinin from the enteroendocrine cells lining the gastrointestinal mucosa. It should be noted that the local concentrations of leptin are several orders of magnitude above those typically measured in the serum and cannot be quantified in the peripheral blood. Following the ingestion of food, the vasoconstrictive signals to the gut and the kidneys described above appear to be inhibited centrally via vagal feedback by these 2 hormones.(24) This 'sympathoinhibitory reflex' triggers vasodilation of the splanchnic and, possibly, the renal arteries. In the limbs, this mechanism is thought to have reciprocal – i.e., sympathoexcitatory – effects, which may be mediated via different synaptic pathways, resulting in an increase in vascular tone and thus, vasoconstriction of the skeletal muscles.(24) Therefore, this mechanism may play a pivotal role in the distribution of blood flow and the regulation of BP in the fed state. Findings from animal studies have also suggested that blunting of this mechanism may be a key mechanism for the development of hypertension in the context of obesity and an unhealthy diet.(25, 26)

In the smaller, more distal vessels, it has been suggested that enzymatic reactions in the intestine, an increased activity of its muscular layer, as well as transportation of nutrients, and active osmotic regulation cause a fall in interstitial pO_2, in pH and osmolarity, as well as a rise in carbon dioxide partial pressure (pCO_2), resulting in a drop in mesenteric vascular resistance through recruitment of previously non-perfused capillaries.(16, 27) Other mechanisms, such as the involvement of cholinergic signalling and molecules of the GLP-family, have been described.(1, 21) GLP-2, for example, is produced by the enteroendocrine cells of the ileum and colon, and is released by the presence of nutrients in the intestinal lumen. Both, food-induced GLP-2 release and GLP-2 administration trigger decreases in mesenteric vascular resistance, accompanied by a rise in CO and HR, that are similar in extent.(28)

The magnitude and the duration of these changes can vary widely. Meal size and calorie load correlate positively with the increase in intestinal blood flow,

and a liquid consistency is believed to accelerate this effect.(29, 30) However, osmolality, volume and consistency of the food bolus alone do not seem to alter intestinal haemodynamics significantly.(30) Meals rich in lipids and carbohydrates appear to provoke a more pronounced and sustained change (especially meals rich in lipids), whereas peptides and amino acids appear to have the smallest effect.(31) The presence of bile salts in the intestinal lumen appears to potentiate the effects of lipids considerably.(16)

1.3. Assessment of postprandial haemodynamics

Overview

Numerous techniques have been established to measure blood flow. Invasive methods such as thermodilution, electromagnetic flowmetry, or the direct Fick method can quantify blood flow with reasonable accuracy, but are associated with patient discomfort and are not without risks. Moreover, many are technically complex and susceptible to measurement error.(32) While invasive techniques have been used in both, human and animal studies in the past, they are now largely considered obsolete for experiments in human volunteers.(1) MRI is the gold standard for the measurement of blood flow as it is largely user-independent, safe and highly reliable, and measures blood flow directly, unlike the other methods discussed.(32)

1.3.1. Invasive methods

Direct Fick method

Based on the assumption that tissue oxygen extraction at rest is directly proportional to blood flow, the arterio-venous difference in blood oxygen can be used to calculate blood flow. This is typically done to measure CO invasively, but can be applied to virtually any compartment in which venous oxygen can be measured. However, this requirement to sample venous blood makes blood flow measurement of the internal organs challenging and bears procedural risk. Moreover, the necessity for frequent blood sampling in multiple compartments as part of a stress protocol could exceed the acceptable safety margins for

blood sampling. Therefore, the direct Fick method has strong limitations as measurement technique of postprandial blood flow in volunteers.(33, 34)

Thermodilution

This method relies on the fact that in the blood pool, variations in temperature caused by the injection of a fluid bolus are inversely correlated to blood flow in that vessel. In practical terms, an ice-cold saline bolus of known volume and temperature is injected into a vessel of interest, and temperature is measured distally to the site of injection. Greater dilution of the bolus (i.e., through greater blood volume circulating in the vessel during the observed period) will cause a smaller drop in temperature at the site of measurement. Flow can be calculated from the observed fluctuations in temperature.

Thermodilution is typically used to measure CO in the pulmonary artery (PA), but can be used in practically any vessel, if large enough to insert a catheter. While technically relatively easy to perform and well-correlated with other techniques such as Doppler-ultrasound, this method has a number of disadvantages. Like most other techniques, thermodilution does not allow for a direct measurement of blood flow, but estimates it from other observations. Flow is not determined in real time, but as an average over several measurements. Therefore, temporal resolution is poor due to the relatively long time required to measure blood flow. As a result, this technique is poorly suitable for dynamic whole-body studies where blood flow must be measured in multiple sites at rapid succession. Moreover, the repeated injection of saline can lead to haemodilution, if many measurements are performed.(32)

Dye-dilution

In analogy to thermodilution, optical dye can be injected (e.g., indocyanine green), and blood flow extrapolated via photo-densitometry from any dilution observed further downstream. Similar to thermodilution, this technique requires vascular access and is, therefore, invasive by default. Moreover, temporal resolution is particularly poor due to the need for dye to clear prior to repeating

a measurement. Allergic reactions to dye can also occur, adding further potential limitation to its use in healthy volunteers.(32)

Electromagnetic flowmetry

The basis for this technique is Faraday's law of electromagnetic induction, according to which a voltage is induced if a conductor moves through a magnetic field. The resulting current is proportional to the velocity and length of the conductor, as well as the density of the magnetic field. If a magnetic field is generated in or around a body part, the blood flowing through it can act as conductor and thus, generate a current. This voltage can be measured and is proportional to flow velocity.

An advantage of this technique is its high temporal resolution, as the electromagnetic signal is picked up in real time. Moreover, electromagnetic flowmetry can, in principle, be performed either invasively or non-invasively. However, in order to measure blood flow of the internal organs, invasive protocols are necessary, hence limiting its use for studies on postprandial blood flow in volunteers.(33) Consequently, this technique has been used mostly in animal studies in this context.(19, 35, 36)

1.3.2. Non-invasive methods

Venous occlusion plethysmography

Venous occlusion plethysmography relies on the observation that following sudden occlusion of the efferent vein(s) of a tissue compartment, the afferent arterial flow to that compartment is proportional to its initial increase in volume. Modern iterations of this technique, originally developed in the early 20th century, have been adapted to measure variations in electric impedance instead of tissue volume. While this method has been used for a considerable amount of time, it does not measure blood flow directly, and is technically limited to assessment of the limbs.(32) Therefore, it is unsuitable for the examination of the intraabdominal organs and thus, studies on postprandial haemodynamics.

Ultrasound

Doppler-ultrasound is the most important non-invasive technique for the measurement of blood flow, and several studies have used it to assess blood flow of the digestive organs.(17, 37-41) It is inexpensive, widely available and well-tolerated by the examinee. The Doppler principle relies on the fact that the frequency of an acoustic wave changes when it is reflected by a moving object (such as erythrocytes in a blood vessel). The shift in frequency is proportional to the velocity of the moving object. Reflection by an object moving in the same direction as the soundwave will stretch it (i.e., lower the frequency of the reflected wave), whereas reflection by an object moving the opposite direction will compress it (i.e., increase its frequency). As the tissue-specific speed of the emitted soundwave is known, the velocity of blood flow can be measured (however, it should be noted that modern devices measure changes in phase to calculate velocities, rather than changes in frequency).

Flow velocity in a vessel is typically measured by pulsed-wave Doppler, as this allows for accurate spatial sampling of the Doppler signal. The resulting velocity-time integral (VTI) is an established estimate for SV.(42) Blood flow is then calculated by multiplication of VTI by the vessel area. However, this method is prone to measurement error for a number of reasons. Firstly, flow velocities are non-uniform across the diameter of a vessel in the presence of laminar flow: velocities in the centre of the vessels are greater than at the periphery. Hence, positioning of the ultrasound sampling volume can affect the measured velocities significantly. Secondly, angulation of the ultrasound probe by an angle β results in underestimation of the measured velocities by a factor of $\cos\beta$ (***Figure 1***).(43) Thirdly, the cross-sectional area of the vessel of interest must be recorded perpendicularly, and any deviation from the perpendicular plane by an angle β will lead to overestimation of the vessel area by a factor of $(\cos\beta)^{-1}$ (***Figure 2***).

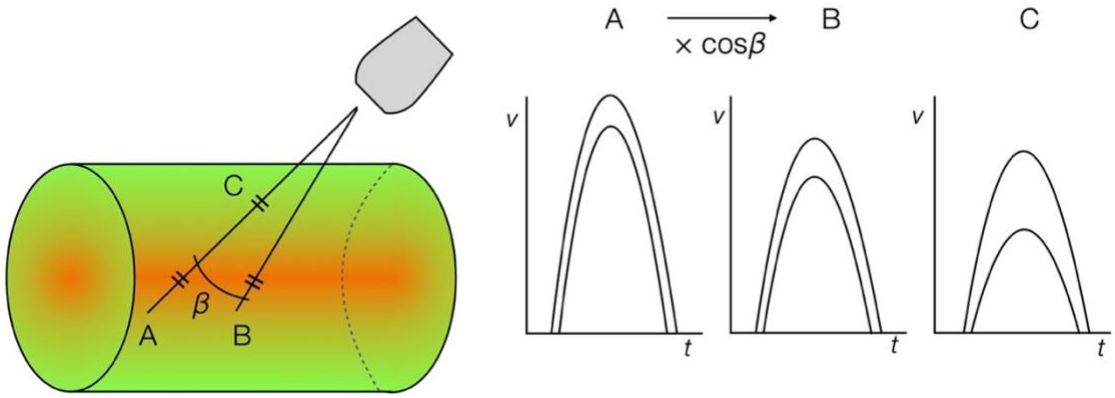

Figure 1. Possible errors in Doppler-based flow measurement.

Red colour represents higher, green lower flow velocities across the vessel. Curves represent velocity-time integrals (VTI).

A: Optimal position of the sampling volume.

B: Underestimation of velocities due to excessive angulation of the probe, and

C: due to off-centre sampling of velocity.

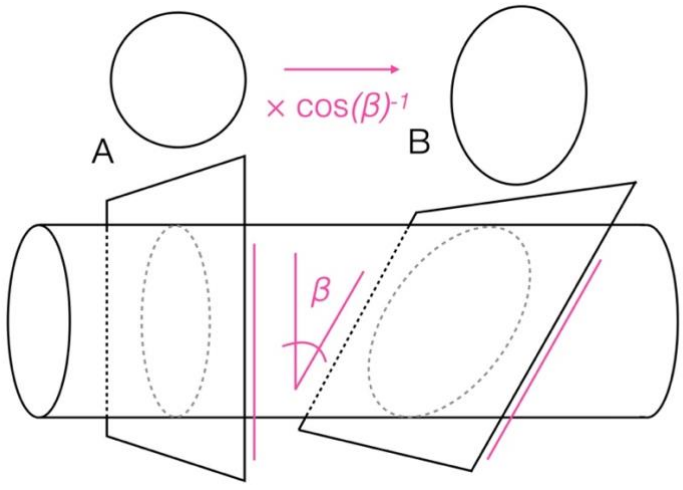

Figure 2. Possible errors in cross-sectional vessel imaging.

A: Correct cross-section of the vessel should be done perpendicular to the vessel.

B: Any deviation from this plane will produce a falsely large vessel area.

As a result, Doppler-ultrasound is a highly user-dependent technique and, therefore, susceptible to measurement error and operator bias. This is particularly problematic for whole-body studies of postprandial blood flow, where the position of the ultrasound probe has to be changed repeatedly in order to record flow in several different locations. This introduces a significant element of measurement variability. Moreover, this technique is highly dependent on the quality of acoustic windows, which can be limited for the abdominal organs, especially in obese patients.

Positron emission tomography

With this functional nuclear imaging technique, a radionuclide tracer is injected intravenously, and positron signals resulting from its decay recorded by gamma-ray detectors which are positioned around the compartment of interest. The kinetics of the signal detected can be used to calculate blood flow. While this method, in theory, allows blood flow to be measured in any compartment non-invasively and with high spatial resolution, its enormous technical complexity and cost, as well as its poor temporal resolution preclude its use for experiments on postprandial physiology.(32)

Magnetic resonance imaging

Phase-contrast MRI (PCMR) is the most widely used MRI-technique to measure flow velocity and volume. It relies on the inherent ability of MRI to encode velocity information into the phase of the detected signal.(44-46) With the availability of novel rapid imaging techniques, this is now an increasingly well-established method for stress imaging.(47-49) The following chapter will discuss the principles of MRI, with particular focus on aspects relevant for cardiovascular stress imaging.

Chapter 2. Magnetic resonance imaging

Introduction

Numerous publications have outlined the physical principles of magnetic resonance and of image generation in MRI. Reference is made to these publications for a basic introduction on the topic.(50-53) The present chapter will focus mostly on the challenges and techniques relevant to this thesis.

2.1. Motion compensation

Overview

The acquisition of MRI data is a relatively time-consuming process (at least using conventional techniques). Hence, as both, the heart and the chest, are constantly in motion in order to exercise their respective functions, mechanisms need to be in place to compensate for motion in order to produce usable images.

2.1.1. Cardiac gating

Because the heart contracts and relaxes over the course of a fraction of a second, acquisition of data has to be timed according to the cardiac cycle. This timing of data acquisition termed ‘cardiac gating’ and is typically done using a vectorcardiogram, as conventional methods to record the electrical activity of the heart are too prone to interference with an MRI system’s main components.(50)

Segmented k-space acquisition

The duration of an image acquisition is determined by the time it takes to fill *k*-space. As discussed earlier, this is proportional to spatial resolution, i.e., the number of phase-encode steps (lines), as well as the interval between successive radiofrequency (RF) excitation pulses (repetition time, TR). For example, to acquire an image at 128 pixels of resolution given a TR of 2.5 ms would, thus, require 320 ms. At a HR of 60 bpm, this would constitute 1/3 of the cardiac cycle, which would preclude ‘freezing’ the motion of the heart to produce a meaningful still image.

Alternatively, *k*-space can be divided into segments, which are filled over several cardiac cycles over a specified, much shorter time window. This time window determines how many lines can be sampled in *k*-space per segment. A longer time window allows the sampling of more data, but in turn increases susceptibility to motion artefact. Inversely, a shorter time window means that more segments are required to fill *k*-space, which in turn implies that more R-R intervals are required to acquire data, increasing the length of the breath hold required to achieve this (see 2.1.2.) Consequently, single phase acquisitions are usually done at mid-late diastole, as this is normally the longest phase of relative cardiac quiescence (however, this is not always true – e.g., in neonates).

Multi-phase acquisitions

In order to produce moving 'cine' images of the heart, the process above can be extended to acquire multiple phases. Prospective gating is one way to accomplish this. With this approach, the cardiac cycle is divided into multiple phases, which ultimately each represent a frame in the cardiac cycle. An event during the cardiac cycle (e.g., the R-wave) is used to trigger data acquisition. Following the filling of a segment in *k*-space of the first phase, data acquisition continues into the following phase to fill a new *k*-space etc. As with single phase acquisitions, the number of lines per segment define the length of a single frame. Consequently, there is an inverse relationship between spatial resolution and temporal resolution. However, if the lines per segment are decreased in order to improve spatial resolution, the number of cardiac cycles needed to fill *k*-space increase. In order to account for variability in R-R duration, a short period at the end of each cardiac cycle is omitted. As a result, this approach is relatively robust to arrhythmia. However, data during late diastole are, therefore, missed.

This can be imaged using retrospective gating, where lines in *k*-space are filled continuously and each line is given a time signature. After completion of data acquisition, lines are then assigned to different sections of the cardiac cycle retrospectively during reconstruction, whereby each R-R interval is stretched or

compressed to fit the mean calculated R-R interval recorded. This technique is more sensitive to arrhythmia, but can acquire data in late diastole, albeit at the cost of longer scan durations.(46)

2.1.2. Respiratory motion

Breath holding

Because data are usually acquired over several cardiac cycles using conventional imaging techniques, breath holding is required to compensate for chest motion. Breaths are usually held at end-expiration as this has been shown to result in better reproducibility. Nevertheless, imaging parameters must be programmed to limit the number of cardiac cycles required, as breath holds are usually limited to 10-15 sec in supine position.(54) Increasing spatial or temporal resolution will increase image acquisition times. By contrast, several strategies exist to shorten them (see 2.2.).

Averaged imaging

As an alternative to breath holding, averaged imaging can be used to acquire data repeatedly over different points of the respiratory cycle. While this technique has less edge sharpness in 2D cine imaging, it is used widely for flow imaging as it mitigates the effects of breath holding on CO. However, this technique comes at the cost of relatively long acquisition times in the range of several minutes.

Respiratory navigator gating

For certain applications it is not possible to keep imaging times short enough for breath held imaging (e.g., acquisition of larger 3-dimensional [3D] datasets). In such cases, respiratory navigating can be used to time image acquisition according to a specific position of the diaphragm. This is typically achieved by placing a navigator (i.e., an additional RF pulse exciting a thin cylinder of tissue) over the right diaphragmatic dome in order to track shifts in phase due to respiratory motion. The diaphragm can subsequently be tracked in real time, and an acceptance window for the acquisition of data is set by the operator.

2.1.3. Rapid imaging

Single shot imaging describes the non-segmented filling of *k*-space within a single cardiac cycle. This can be achieved in a number of ways. Reducing the number of phase-encoding steps (and thus, spatial resolution) is an obvious measure to decrease imaging times, but comes at the cost of image quality. In order to accelerate imaging without compromising on spatial resolution, a number of strategies have been developed (see 2.2.).

If the concept of single shot imaging is extended to multi-phase acquisitions, it is called real-time imaging. Although these techniques are still far from becoming the norm at most centres, they have strong advantages in situations where breath holding is not possible. As their temporal resolution depends critically on the time required to fill *k*-space, they rely strongly on acceleration techniques.(55)

2.2. Acceleration techniques

Overview

A range of strategies to accelerate data acquisition have been developed, to summarise the whole of which lies beyond the scope of this thesis. Therefore, a brief overview of techniques including those applied in the presented research is provided.

2.2.1. k-Space sampling strategies

Imaging time is proportional to the number of lines in *k*-space and to TR. Conventional techniques sample 1 line per phase-encoding step in *k*-space, following a rectilinear (Cartesian) trajectory. This is repeated until all phase-encoding steps have been acquired and *k*-space is filled. Thus, multiple phase-encoding steps are normally required with this approach, which increases image acquisition time proportionally. Other readout schemes, such as radial or spiral trajectories, can sample data in *k*-space more efficiently, and thus reduce acquisition times substantially (***Figure 3***). By sampling more data in the centre of

k-space, they have been shown to be particularly useful for flow imaging, due to their reduced susceptibility to artefact.(56)

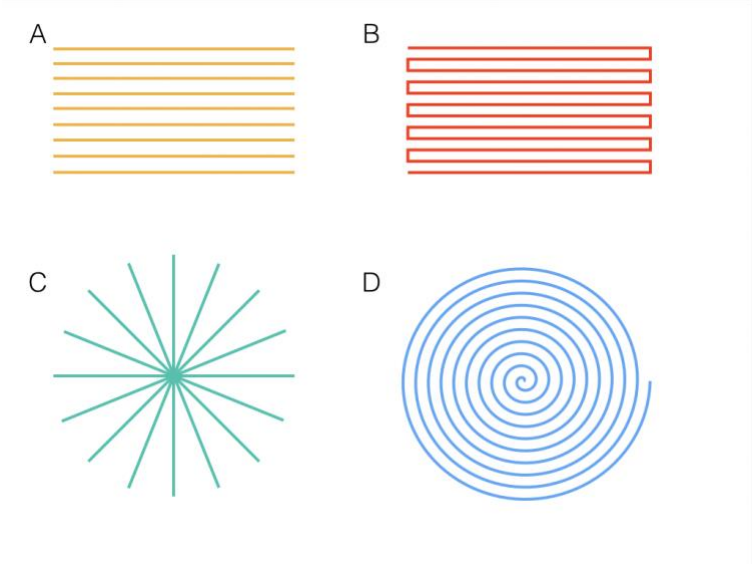

Figure 3. Different trajectories for filling of *k*-space.

A. Cartesian (rectilinear); B. echo planar imaging; C. radial, and D. spiral.
Reprinted with permission from Dr Michael A. Quail.

2.2.2. Parallel imaging

Another approach to accelerate data acquisition is parallel imaging, whereby differences in signal strengths received from each of an array of receiver coils are used to reconstruct images accurately despite under-sampling of data. This relies on the fact that each point in *k*-space includes spatial frequency information about all other points. Sampling data incompletely in *k*-space normally leads to wrapping (aliasing) of the image. One way to overcome this is sensitivity encoding (SENSE), which uses the different spatial sensitivities of the different receiver coils in an array due to their different positions relative to the body to 'un-wrap' under-sampled data in the image reconstruction process (***Figure 4***).(55)

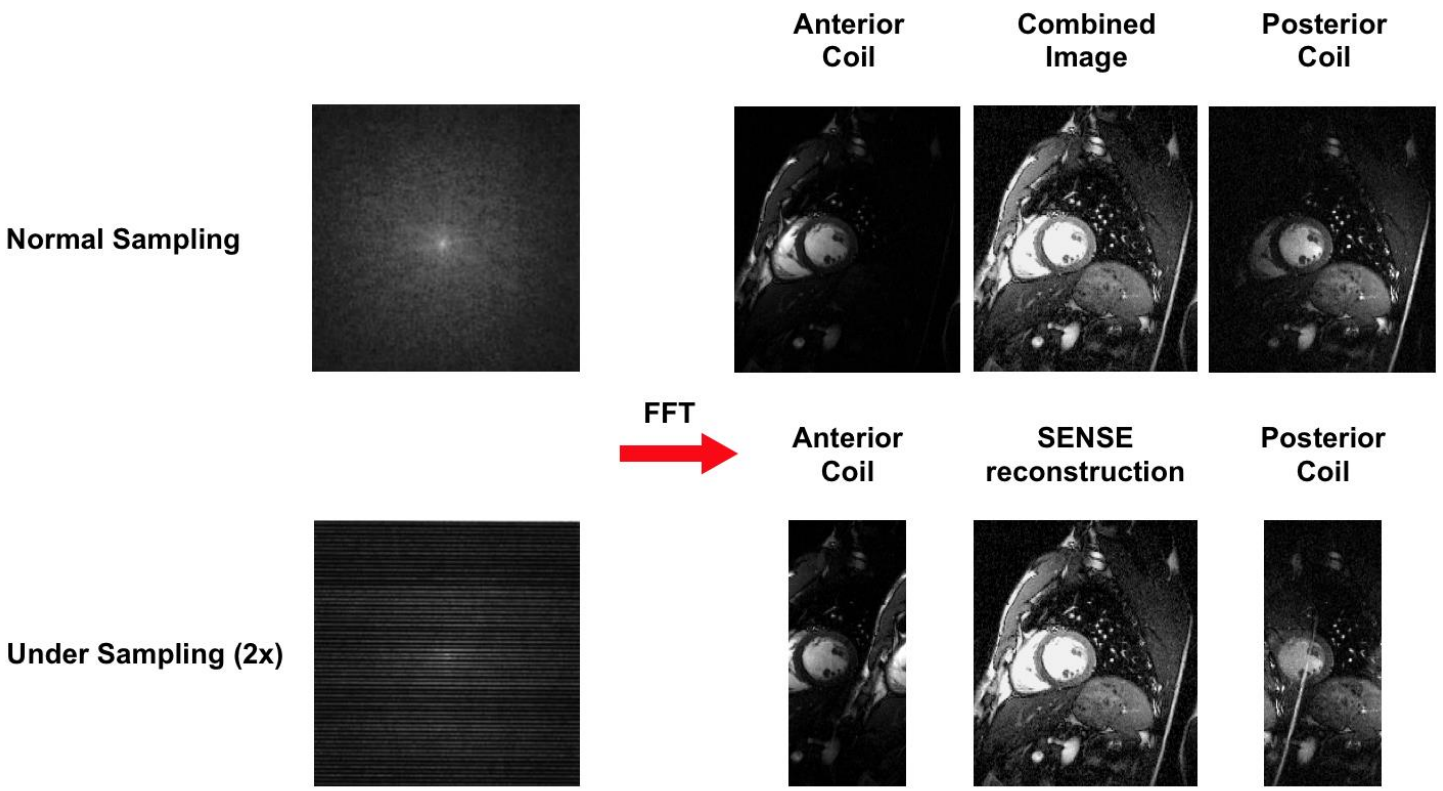

Figure 4. Sensitivity encoding (SENSE) reconstruction.

Under-sampling of data by a factor of 2 halves imaging time but leads to aliasing (fold over) of the reconstructed image. SENSE uses differences in sensitivity of different receiver coils due to their position relative to the body to un-wrap data in the reconstruction process.

From: Bogaert J., Dymarkowski S., Taylor A. M., Muthurangu V. (Eds.): *Clinical Cardiac MRI. Cardiac MRI Physics (Chapter),* (2)1-30.

2.3. Anatomical imaging

2.3.1. Fast gradient echo imaging

Spoiled gradient echo imaging

In gradient echo sequences, excitation by a 90° RF pulse transfers the entire longitudinal magnetisation M_z into the transverse (*xy*-) plane. Consequently, TR is determined by T1, as recovery of longitudinal magnetisation is the prerequisite for the following excitation. This can be accelerated by the application of a partial flip angle of less than 90°, which results in the presence of residual longitudinal magnetisation. This allows for a short TR, making this approach suitable for rapid/dynamic imaging.

Consequently, because M_z has only recovered partially, the available magnetisation to be flipped back into the transverse plane following TR is limited. However, this does not apply to new, unsaturated spins entering the imaging plane, such as blood. Such spins have greater M_z to be excited and thus, will produce greater signal. As a result, this approach produces good contrast between cardiac structures and blood, adding further to its utility for cardiac imaging. However, because this effect depends on the presence of flow, this effect is only present during certain phases of the cardiac cycle.

An issue related to this technique is residual coherent transverse magnetisation prior to the next excitation, which will be added to the transverse magnetisation created by the subsequent pulse, and thus may cause artefact. This can be prevented by ‘spoiling’ any residual transverse magnetisation using RF or spoiler gradients prior to the following repetition.(55)

Balanced steady state free precession imaging

As an alternative to spoiling residual transverse magnetisation, a series of RF pulses can be applied in rapid succession, hence producing a succession of both, gradient and spin echoes. As each will merge into the following, this eventually results in a steady state between longitudinal and transverse

magnetisation, giving rise to this technique's name: steady-state free precession (SSFP). Consequently, the net magnetic vector M_0 is fixed at an angle relative to B_0, around which it precesses. The addition of additional, 'balancing' gradients at multiple steps results in improved coherence of M_0 prior to excitation. As longitudinal magnetisation is never recovered fully, the signal is strongly determined by T1 effects, while also being T2-dependent.(52)

The advantage of this technique is the excellent and always-present contrast between blood pool and cardiac structures. Therefore, balanced SSFP (b-SSFP) has become the standard sequence for cardiac cine imaging. In order to compensate for its inherent susceptibility to field inhomogeneity, TR is typically kept very short (in the range of 2 to 3 ms).

2.3.2. Radial *k-t* SENSE imaging

An excellent approach to obtain anatomical cine imaging data rapidly and at high spatiotemporal resolution is *k*-space and time (*k-t*) SENSE imaging.(55, 57) This technique accelerates imaging by under-sampling *k*-space, and un-wraps the resulting, aliased dataset using sensitivity maps from multiple receiver coils, as well as information of the spatiotemporal correlations of the wrapped data in *k*-space, determined from low-spatial-resolution training data. The combination with a radial sampling trajectory of *k*-space mitigates the artefacts related to under-sampling, resulting in imaging datasets that allow accurate diagnostics even in congenital heart disease (CHD).(55) This technique can be applied in free breathing and uses prospective cardiac gating.

2.4. Flow imaging

2.4.1. Phase-contrast MRI

Flow measurement by PCMR is based on spoiled gradient echo imaging, with the addition of a velocity-encoding gradient along the direction of blood flow. When such a gradient is applied, the magnetic moments of spins will be de-phased along its direction. If an inverse gradient is applied subsequently, the spins will re-phase, resulting in no net phase shift – provided that they have

been stationary. However, as spins move through the field (e.g., blood along a vessel), spins in the imaging plane will have been replaced by spins from a different location along the field gradient by the time the second, inverse gradient is applied. As a result, spins (blood) moving into the imaging plane will be in different phase than the slice (stationary, surrounding tissue) they move into. Because the change in phase of these moving spins is proportional to the physical distance they travel along the field gradient, the net change in phase is proportional to their velocity.(45, 46)

In practical terms, data are acquired in a plane that is orthogonal to a region of interest (ROI; e.g., a vessel), and a velocity-encoding gradient applied along the *z*-direction. As the product of the duration and the field strength of the gradient applied determines the shift in phase, stronger gradients are typically used in order to keep imaging times as short as possible.(46) After application of the 2 bipolar gradients exemplified above, the signal is acquired, and the moving spins will exhibit a change in phase that is proportional to their velocity. Additionally, the same data are acquired without the addition of the velocity-encoding gradient, and subtracted from the first dataset. This is done in order to neutralise the effects of phase due to other causes (e.g., field inhomogeneity).

Once reconstructed, PCMR typically produces 2 images: a phase image, which contains information about the direction and velocity of flow, and a magnitude image containing anatomical information (***Figure 5***).(45, 46)

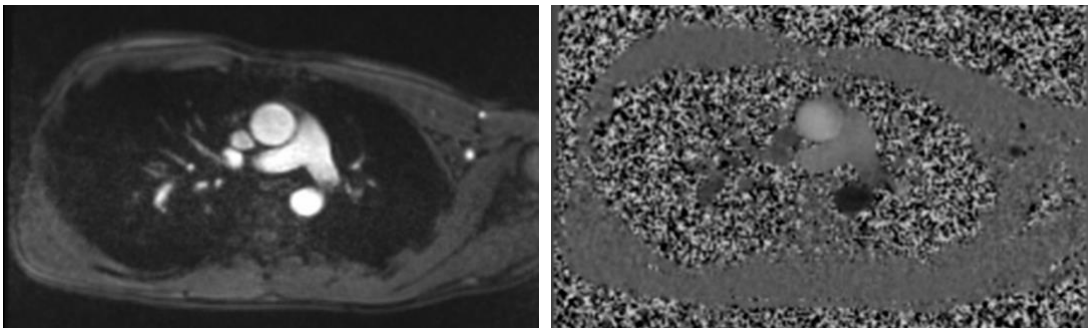

Figure 5. Phase-contrast MRI of the ascending aorta.
Left: magnitude (modulus) image; right: phase image.

Velocity encoding

The velocity-encoding gradient parameter (V_{enc}) defines the range of velocities, which the flow acquisition is sensitive to, and is determined by the strength and duration of the field gradient applied. It is set by the operator and corresponds to the maximum velocity that can be registered in either direction of the imaging plane without aliasing of velocity data. Changes in phase (in this case, V_{enc}) can range from 0 to 180°. If the measured velocity exceeds the V_{enc}, phase will rotate past 180° and back to 0°, resulting fold over (aliasing) of the registered velocity. Conversely, if the V_{enc} set too high, signal/noise-ratio (SNR) worsens.

Temporal resolution

Flow data are usually sampled in a discrete (frame-wise, time-resolved) manner by multi-phase acquisition. In order to resolve flow-curves accurately, data must be sampled at sufficient temporal resolution. At normal HR, the typical temporal resolution required is 30-40 ms for imaging of large vessels with pulsatile flow. Lower temporal resolution may smoothen flow curves and thus, underestimate velocity and flow volumes.(46) Consequently, higher HR necessitate greater temporal resolution. Because breath holding has been shown to affect haemodynamic measurements, free breathing sequences are often used as an alternative.(58)

Anatomical planning

Data should be acquired perpendicularly to the vessel, as deviation from its axis at an angle β reduces the measured velocities by a factor of cosβ, and increases the apparent area of a vessel by a factor of $(\cos\beta)^{-1}$, with partial volume effects as consequence (see also ***Chapter 1, Figure 2***). Deviations of less than 15° from the orthogonal plane of a vessel do not result in a significant measurement error.(46)

In conventional (i.e., 2D) flow imaging, the imaging plane is usually defined using anatomical imaging, such b-SSFP single shot imaging, for large vessels. Single shot ‘scout’ images are acquired firstly at pre-defined planes throughout the body (this is normally done at least in transverse orientation, but can be

done in any orientation). Based on the resulting images, landmarks are used for orientation in order to set standard imaging planes of the vessels of interest. Additional single shot images may be acquired to aid slice location.

For smaller vessels, 3D ‘whole heart’-imaging can be used alternatively. Three-dimensional data can be reformatted freely by the operator using 3 orthogonal planes (multi-plane reformatting, MPR). Accurate (i.e., perpendicular) planning is achieved by aligning 2 of these planes with the vessel of interest for orientation (see ***Chapter 3, Figure* 8**). The third plane is then perpendicular to that vessel, and can be moved along it to determine the position for data acquisition, if possible on a straight segment.

Reliability and comparison with other techniques

The advantage of PCMR is that it is highly reliable, safe and largely operator-independent. Intra- and interobserver variability has been reported to be as low as 2% and 3%, respectively, and *in vivo* validation studies (e.g., comparing aortic with pulmonary blood flow) typically show very low variability within the range of 3-5%.(46) No adverse effects are known, and the only relevant issue related to tolerability are anxiety and claustrophobia in the scanner, which are relatively rare.

2.4.2. Small vessel imaging

Challenges in stress imaging

In a cross-sectional image of a vessel, the lumen is represented by a number of voxels, depending on the spatial resolution set by the operator. If resolution is low, a proportionately greater number of voxels will cover both, intravascular and extravascular space at the edges of a vessel, resulting in underestimation of velocity and flow data (partial volume effect). A minimum number of voxels relative to the vessel diameter are therefore required to ensure accurate acquisition of flow data.(45) Consequently, smaller vessels require greater spatial resolution and as a result, longer scans. As the resulting imaging times exceed those compatible with breath holding, respiratory navigator gating is

necessary. This narrows the window for data acquisition further and thus, extends imaging times additionally.

As a result, for example, measuring blood flow in a renal artery using conventional cardiac gated, respiratory navigated PCMR takes ~5 min, or longer.(47) This makes conventional imaging techniques unsuitable for stress imaging, where data must be sampled frequently enough to record dynamic changes over time accurately. This is especially problematic for the assessment of whole-body responses, where flow is measured in several different locations in rapid succession. (Importantly, measuring flow responses by Doppler-sonography in such a protocol would neither be a suitable technique due to its user-dependency and poor reproducibility. This is even more relevant in whole-body stress imaging due to the need to change the position of the ultrasound probe repeatedly, resulting in greater variability.)

Averaged imaging for rapid organ blood flow measurement

In stress imaging, the temporal resolution of single blood flow datasets is of secondary importance, as absolute flow data, acquired with high repetition to describe dynamic changes over time, are of greater interest than the description of flow curves. Therefore, temporal resolution can be omitted entirely by using averaged imaging in order to overcome the long acquisition times of conventional, time-resolved sequences for blood flow imaging of organ specific vessels. This can be achieved by R-R interval averaged imaging, which acquires flow data over an integer number of R-R intervals in an ungated fashion, providing single, ‘time-averaged’ magnitude and phase images. By dividing flow by the number of R-R intervals recorded, it provides the average flow per beat over the time period assessed. Park *et al.* demonstrated that this method could be used to measure blood flow in relatively small vessels, such as the renal arteries, within substantially shorter time than using conventional, time-resolved techniques (typically in the order of ~6 sec, within a single breath hold).(59) Pairing this approach with a spiral readout scheme was further shown to convey a number of key advantages.(60)

This is due to the fact that spiral trajectories start at the centre of *k*-space and spiral towards the periphery. This is more time-efficient than other sampling strategies (e.g., echo planar imaging) and ensures that important low-spatial frequency flow information is always sampled, independently of HR. By contrast, other sampling patterns, such as Cartesian trajectories or echo planar imaging (***Figure 8***), may populate the periphery of *k*-space but under-sample the centre at higher HR, and thus cause aliasing of low-spatial frequency information. Spiral trajectories have moreover been shown to be more robust to ghosting artefact in the presence of pulsatile flow, which is a key advantage in small vessel flow imaging.(60)

R-R interval averaged golden angle spiral PCMR

An iteration of this technique is R-R interval averaged golden angle spiral (RAGS) PCMR, which was subsequently proposed by Steeden *et al.*(47) One of the novelties of their approach was that it used the vectorcardiogram-system of the MRI setup to track R-waves, whereas previous, ungated techniques estimated R-waves from the MRI-dataset itself.(60) This approach was chosen to facilitate image reconstruction. Moreover, their technique employed a golden angle spiral ordering scheme, in which each consecutive spiral interleave was rotated by 222.5º, rather than a pseudo-random or manual spiral ordering scheme in order to fill *k*-space optimally and flexibly at all HR.(60)

Using this technique, data were combined over ~5 R-R intervals to produce a single ‘time-averaged’ image. As a result, continuous PCMR data were acquired with very high spatial resolution (0.78 × 0.78 mm), and acquisition times typically lasting only ~6 sec (***Figure 6***). The use of a golden angle spiral readout scheme resulted in superior SNR and a comparable edge sharpness to that of conventional techniques.(47)

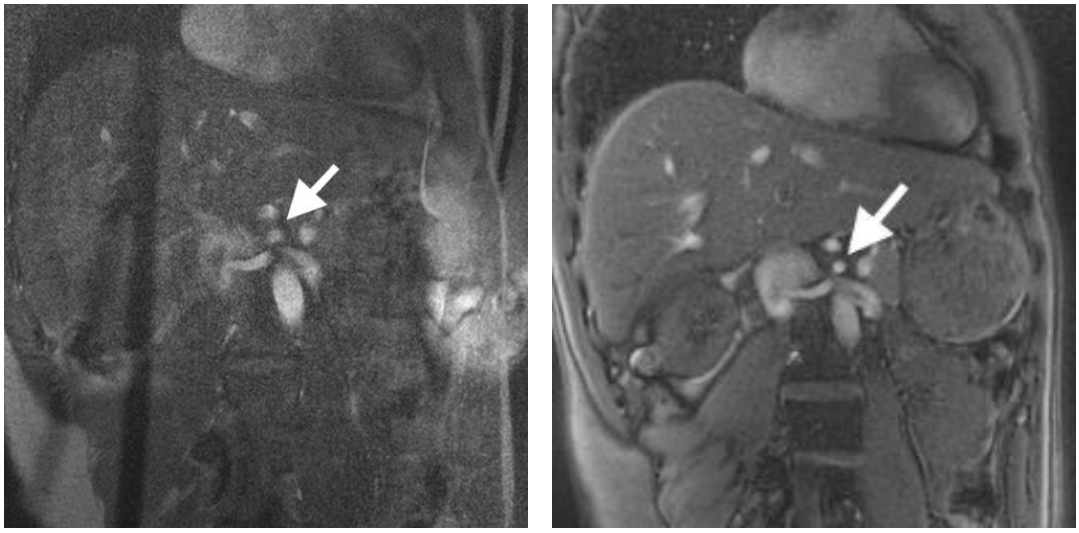

Figure 6. Respiratory triggered, cardiac gated (left) *versus* R-R interval averaged golden angle spiral (RAGS) (right) phase-contrast MRI of the superior mesenteric artery (arrows; magnitude images).

Image acquisition times were ~7 min versus ~6 sec.

In the renal arteries, the authors demonstrated excellent agreement of flow data with conventional high-resolution respiratory-navigated cine techniques using, both, correlation (r = 0.9823) and Bland-Altman analysis (bias: 0.01 $L.min^{-1}$; limits of agreement: -0.04 to 0.06 $L.min^{-1}$). However, the authors noted that HR, as well as radial and translational vessel movement had to be within certain boundaries for the technique to be accurate.(47) This was demonstrated by an *in silico* simulation, in which the authors determined that the effect of HR was likely a result of the asymmetric nature of translational motion, expansion, and flow. It was shown that at lower HR, vessel translation caused spatial misalignment, as the phase image, which was used to calculate flow, was influenced predominantly by systole, while the magnitude image, which was used for segmentation, was determined more by diastole. Furthermore, vessel expansion caused phase information to be dispersed over a larger area than in the magnitude image. At higher HR, the cardiac cycle becomes more symmetrical, hence mitigating this issue. However, translational movement of the vessel caused blurring of the vessel and hence affected accuracy at high HR. Therefore, while it was acknowledged that this technique may be less

suitable for large, pulsating vessels such as the aorta, it was proposed as a good technique for imaging of the abdominal vessels, such as the celiac or the SMA.

Validation of the imaging technique

Reliability and reproducibility of RAGS PCMR were confirmed for the purpose of this thesis. In order to assess intra- and interobserver variability, SMA flow data of 16 randomly selected cases from Chapter 5 were re-segmented by 2 independent investigators. Intraclass correlation analysis demonstrated very good intra- and interobserver agreement, with intraclass correlation coefficients of 0.95 [95% CI: 0.86, 0.98] and 0.91 [95% CI: 0.76, 0.97], respectively.(4)

Further, reproducibility of data acquisition using RAGS PCMR was assessed using 2 independent fasting datasets from 10 subjects from Chapter 4 (fat/sugar experiment and water experiment). Bland-Altman analysis showed good reproducibility of this technique (bias: 0.04 $L.min^{-1}$; limits of agreement: -0.56 to 0.48 $L.min^{-1}$; ***Figure 7***). It should be noted that the 2 measurements used for this analysis were acquired several days apart and thus, part of the variance may be explained by inter-day variability.

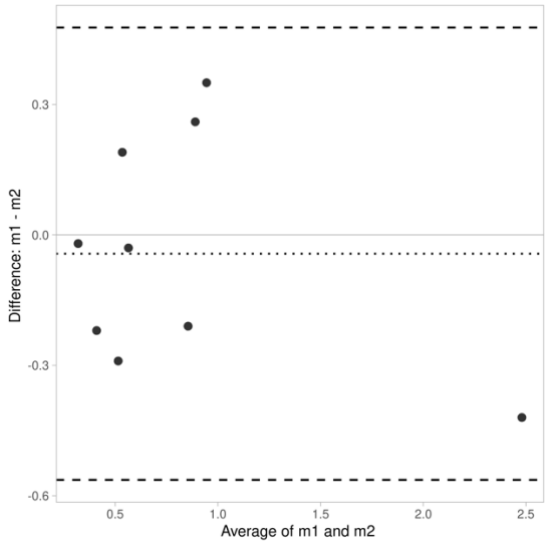

Figure 7. Bland-Altman plot for reproducibility of splanchnic blood flow acquisition.

2.4.3. Aortic imaging

Challenges in aortic imaging

In order to characterise aortic physiology accurately, a number of factors must be considered. Firstly, data must be acquired at high enough spatial and temporal resolution to describe physiological changes in vessel motion, expansion, and flow accurately and without artefact.

Secondly, cardiovascular functions, such as vessel expansion, pressure, and blood flow over time are 'analogue' signals, which can be described mathematically by continuous, oscillating, wave-like functions. Due to the technical nature of MRI explained earlier, data from these signals can only be sampled at discrete timepoints, whereby the sampling frequency is determined by temporal resolution. The higher sampling frequency (temporal resolution), the more accurate the digital representation of the analogue signal (e.g., time-area curve). Conversely, data sampling of a signal at less than 2 times the frequency of the highest frequency component results in misrepresentation of data, when using them to reconstruct a continuous function (Nyquist-Shannon theorem)(61). Therefore, in order to describe physiological functions such as pressure or flow accurately, imaging data must be sampled at high temporal resolution. For simple cardiovascular applications, such as the description of aortic flow curves, a temporal resolution of 30 ms is usually sufficient. However, for cardiovascular functions that oscillate at higher frequencies, such as the early systolic upstroke in aortic cross-sectional area, temporal resolution must be 10 ms, assuming a normal HR at rest.(62)

High spatiotemporal resolution gated spiral PCMR

To cover the technical requirements needed to resolve such cardiovascular functions, Steeden *et al.* proposed a prospectively triggered spiral PCMR sequence accelerated with SENSE.(56) This sequence used a uniform-density spiral trajectory with 36 spiral interleaves, under-sampled by a factor of 3, resulting in only 12 spiral interleaves being acquired in each cardiac phase. Two spiral interleaves were acquired per R-R interval, resulting in 6 R-R intervals being used for the entire data acquisition. For each cardiac phase, the

sampling pattern was rotated, so that 3 consecutive cardiac phases resulted in a fully sampled *k*-space with 36 spiral readouts.

The proposed sequence resulted in significantly shorter imaging times compared to a reference technique (~5 sec *vs.* ~16 sec), making it more suitable for paediatric imaging, where long breath-holds are oftentimes not feasible. The authors measured SV in a range of vessels in a population of adults and children with congenital heart disease using a standard sequence and spiral SENSE PCMR imaging and found good agreement between the 2 (spiral breath-hold PCMR: 20.7 mL; standard breath-hold PCMR: 20.5 mL; limits of agreement: 24.4 mL, 2.9 mL *vs*. 210.3 mL, 9.3 mL, respectively; correlation $r = 0.998$ *vs.* $r = 0.984$, respectively). Quail *et al.* subsequently used this technique to derive central aortic systolic pressure from aortic area-distension waveforms.(62)

Chapter 3. General methods

3.1. Oral stress protocol

3.1.1. Protocol

In order to investigate the cardiovascular effects of food ingestion non-invasively and comprehensively, a novel MRI-based oral stress protocol was developed. It was subsequently validated and published in peer-reviewed publications.(3-5)

On the evening prior to study attendance, participants were instructed to eat a standardised meal (margarita pizza), and to then fast overnight and consume nothing but water until after the experiment. Subjects were also asked to abstain from tobacco, alcohol, recreational drugs, caffeine and formal exercise for the preceding 24 h due to possible effects on endothelial function and postprandial blood flow.(63-65)

Study visits took place at 9:00 a.m. after at least 12 h of fasting. An MRI assessment of ventricular volumes, segmental aortic and organ-specific blood flows was performed at baseline (see 3.2.2.). After baseline scanning, the subjects were asked to sit up on the scanner table and drink a standardised liquid meal. Subjects were instructed to finish this within less than 5 min. After returning to supine position, flow measurements were repeated subsequently every 7-10 min for up to 1 h of follow-up. BP was recorded non-invasively before the meal, and repeatedly every 5 min thereafter.

Exclusion criteria were: Chronic diseases requiring hospital management; endocrine or congenital obesity; known or possible pregnancy; MRI-incompatible metal implants; regular use of medication, and known dairy allergy.

All experiments were conducted at Great Ormond Street Hospital for Children, London, UK.

3.1.2. Study meal

The standardised liquid meal consisted of 300 mL of double cream (Waitrose, Bracknell, UK), 89 g of maltose syrup (C*Sweet M 10170, Cargill, UK) and natural custard flavouring (Foodie Flavours Ltd., Tring, UK). Maltose syrup was used due to the relatively lower sweetness compared to glucose and the subsequently better tolerance.(66) At a total fluid volume of ~350 mL, this amounted to the following nutritional contents: fat 142 g, protein 5.1 g, glucose equivalent 75 g, energy 1,635 kcal.

3.2. Imaging

3.2.1. Imaging setup

All MRI was performed on a 1.5 T system (Avanto, Siemens AG, Berlin, Germany) using 2 spine coils, 1 neck coil, and 1 body matrix coil, resulting in 12 coil elements in total. A vectorcardiogram was used for cardiac gating and HR monitoring.

3.2.2. Stress imaging protocol

Image planning and protocol

Imaging planes for aortic and cranial blood flow measurements were planned by 2D b-SSFP single shot imaging. After acquisition of ~15 images each in axial, sagittal and coronal orientation (slice thickness 8 mm, gap 8 mm), an additional stack of ~5 images were obtained of the neck in perpendicular orientation to the common carotid arteries (slice thickness 10 mm, gap 10 mm). This was done in order to select the optimal slice for neck vessel imaging (defined as mid-cervical slice on a straight segment, where the vertebral and the common carotid arteries were clearly visible).

Subsequently, images were obtained of the left ventricular (LV) and the right ventricular (RV) long axes, as well as at basal valve level. These data were used to plan 4-chamber cine imaging. The 4-chamber view and the LV long axis were used to plan LV short axis stack cines. Additional images were obtained of the LV outflow tract to plan ascending aortic blood flow measurement. This was

done at the sinotubular junction. Blood flow of the descending aorta was planned at the level of the diaphragm.

In order to plan blood flow to the legs, an image of the abdominal aorta was acquired in coronal orientation, and an imaging plane proximal to the iliac bifurcation selected using a sagittal view for additional orientation.

Respiratory navigated, cardiac gated, 3D b-SSFP ('whole heart') data were acquired from the diaphragm to the base of the kidneys in order to plan flow measurement of the smaller, abdominal vessels (spatial resolution 1.6 × 1.6 × 1.6 mm).(3) Imaging planes were planned by MPR using 3 perpendicular planes. This was accomplished by aligning each vessel of interest with 2 orthogonal imaging planes, resulting in the third plane being perpendicular to the vessel. The plane for flow imaging was then set to be located on a straight segment (***Figure 8***). The planning process took approximately 10-12 min.

Planning was repeated after meal ingestion due to patient movement and displacement of abdominal contents by the meal. The average interval between bouts of MRI data acquisition was 7-10 min. The last imaging cycle started between 40 and 50 min after ingestion of the meal, resulting in a postprandial scanning time of ~50 min to ~1 h. Total scanning time was ~90 min.

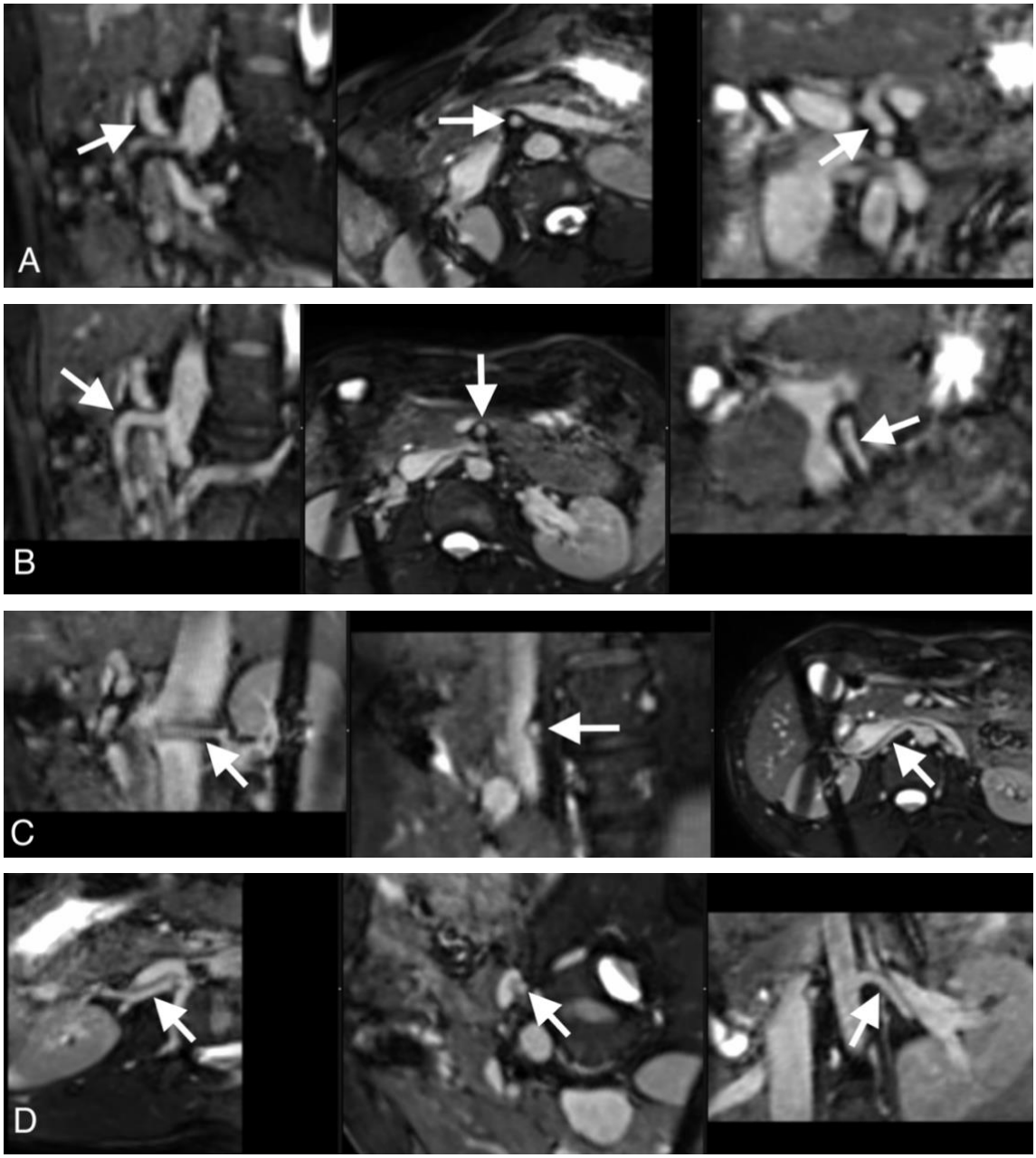

Figure 8. Multi-plane reformatting of 3D balanced SSFP data of the abdomen.
Imaging planes for flow measurements (centre panes) were set using 2 orthogonal cross-sectional views of the vessel of interest for orientation (arrows).
A: Celiac artery;
B: superior mesenteric artery;
C: right, and
D: left renal artery.

Aortic blood flow measurement

Aortic blood flow was measured using in-house high-spatiotemporal resolution cardiac gated spiral PCMR (***Figure 9, A & B***).(56) This sequence uses efficient spiral trajectories (with 36 spiral interleaves required to fully sample *k*-space) combined with data under-sampling (SENSE, factor of 3) in order to achieve high spatial and temporal resolution imaging (spatial resolution 2.1 x 2.1 mm; temporal resolution 9.6 ms) in a breath hold of ~11 sec.(56) Blood flow to the legs was measured proximal to the iliac bifurcation using standard cardiac gated PCMR (spatial resolution 1.56 x 1.56 mm; temporal resolution 32 ms) in a short ~5 sec breath hold; ***Figure 9, C***).

Next page:

Figure 9. Cardiac gated phase-contrast MRI of the aorta.

Note the difference in phase depending on the direction of blood flow (white: cranial flow; black: caudal flow). Top: magnitude (modulus) image; bottom: phase image.
Arrows:
A: Ascending aorta, above the sinuses;
B: descending aorta, diaphragm level;
C: distal aorta, proximal to iliac bifurcation.

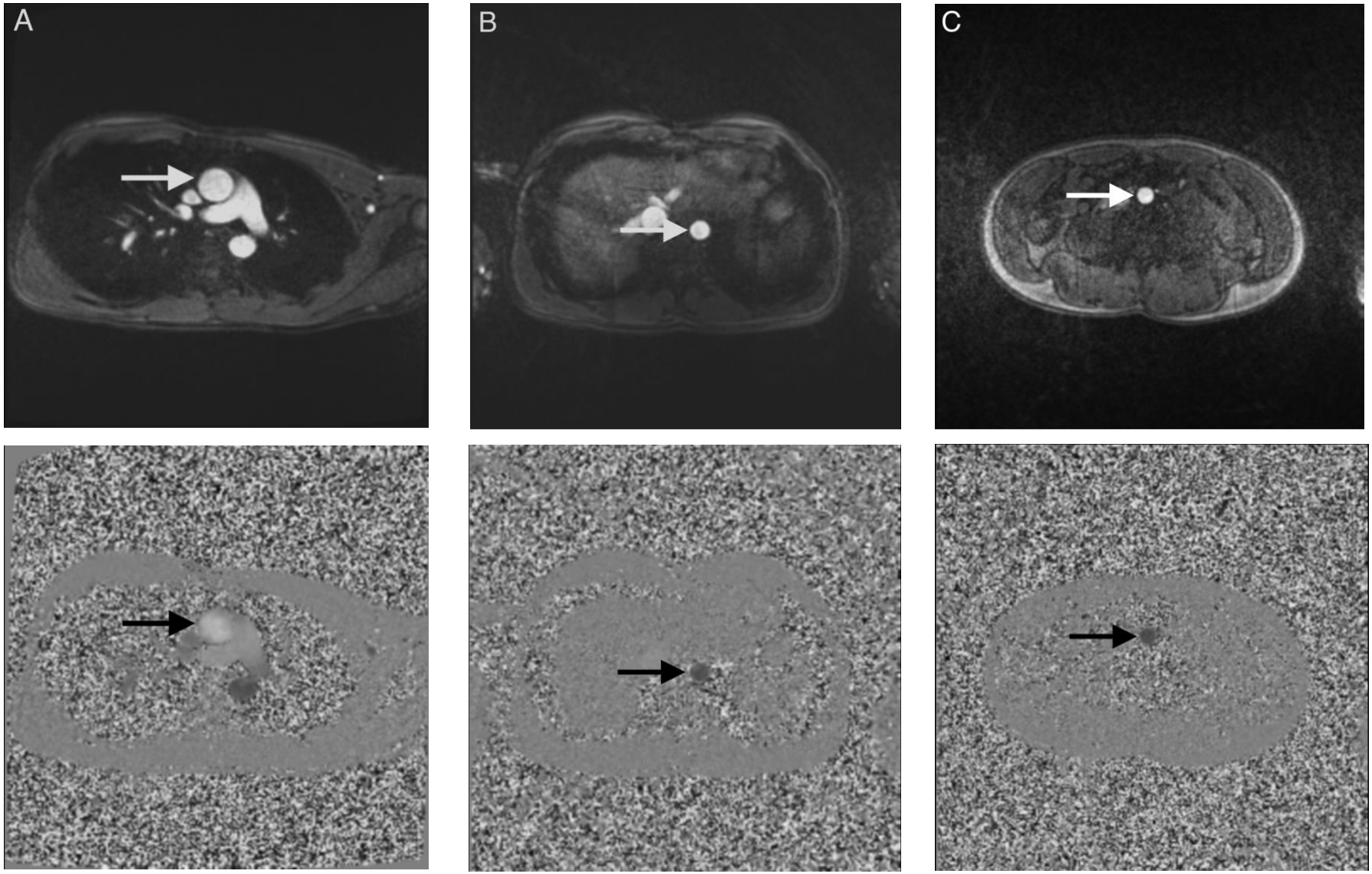
A
B
C

Organ-specific blood flow measurement

In-house RAGS PCMR was used for rapid and accurate measurement of blood flow in the carotid and vertebral arteries, the celiac trunk, the SMA, as well as the renal arteries.(47) This sequence acquires continuous spiral PCMR data with very high spatial resolution (0.78 × 0.78 mm) over a short breath-hold of ~6 sec. A golden-angle ordering scheme was used (where each consecutive spiral interleave was rotated by 222.5º) to produce even filling of *k*-space at all HR. The resultant data is then simply combined over ~5 R-R intervals to produce a single 'time-averaged' image (see 2.4.2.).

Intraclass correlation analysis of SMA flow data from 16 randomly selected cases, which were re-segmented by 2 independent investigators, showed very good intra- and interobserver agreement, with intraclass correlation coefficients of 0.95 [95% CI: 0.86, 0.98] and 0.91 [95% CI: 0.76, 0.97], respectively. Reproducibility of data acquisition was assessed using 2 fasting datasets from 10 subjects (fat/sugar *vs.* water, Chapter 4). Bland-Altman analysis showed good reproducibility of this technique (bias: 0.04 $L.min^{-1}$; limits of agreement: -0.56 to 0.48 $L.min^{-1}$; ***Figure 7***).

Following 2 pages:

Figure 10. R-R interval averaged golden-angle spiral phase-contrast MRI.
This technique acquires data over ~5 R-R intervals to yield a single 'time-averaged' image that can be used to calculate mean flow through a vessel (resolution 0.78 × 0.78 mm, breath hold ~6 sec). Top: Magnitude (modulus) image; bottom: phase image.
Arrows:
A: celiac artery;
B: superior mesenteric artery;
C: left, and
D: right renal artery;
E: common carotid and vertebral arteries.

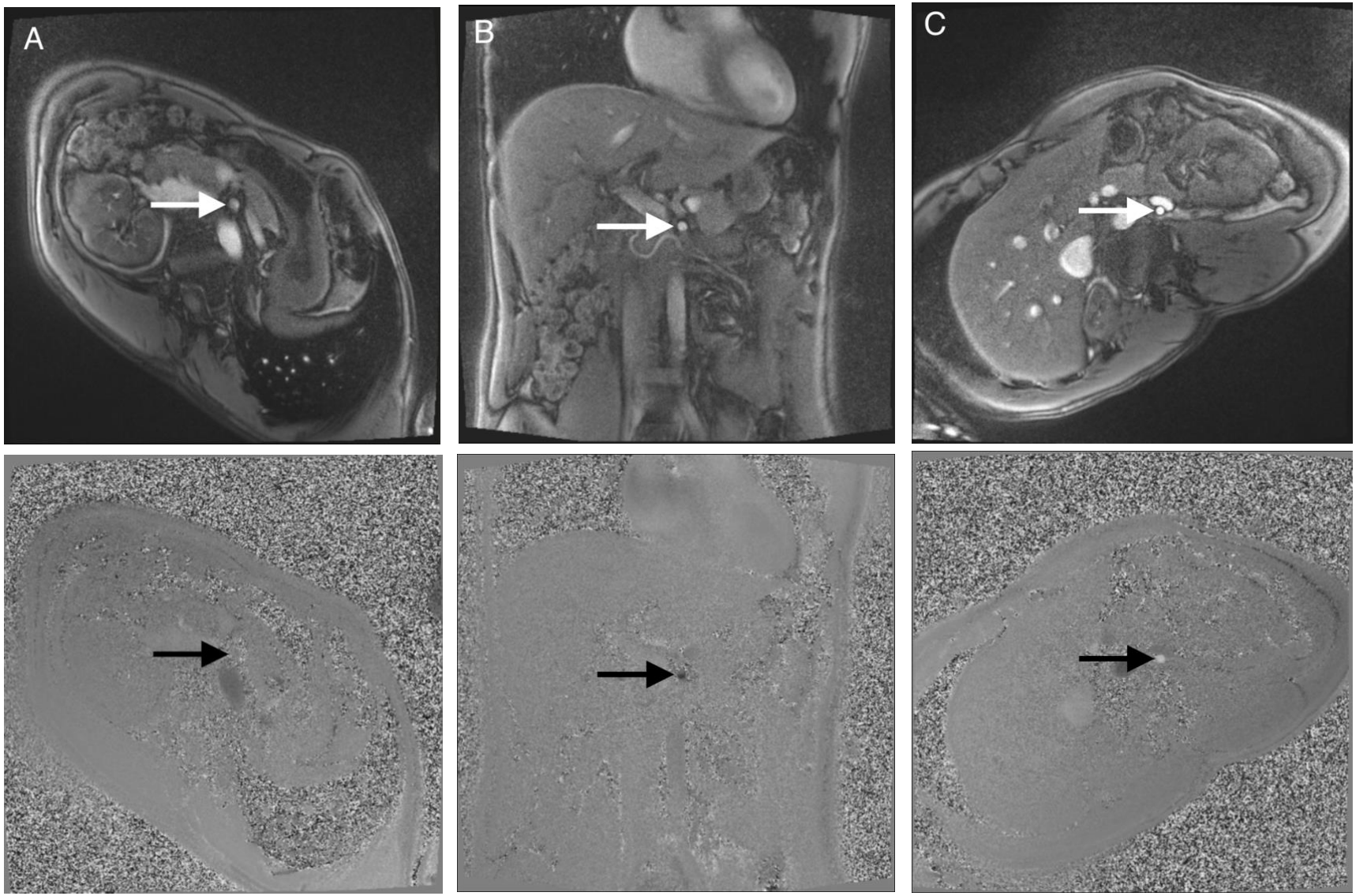
A
B
C

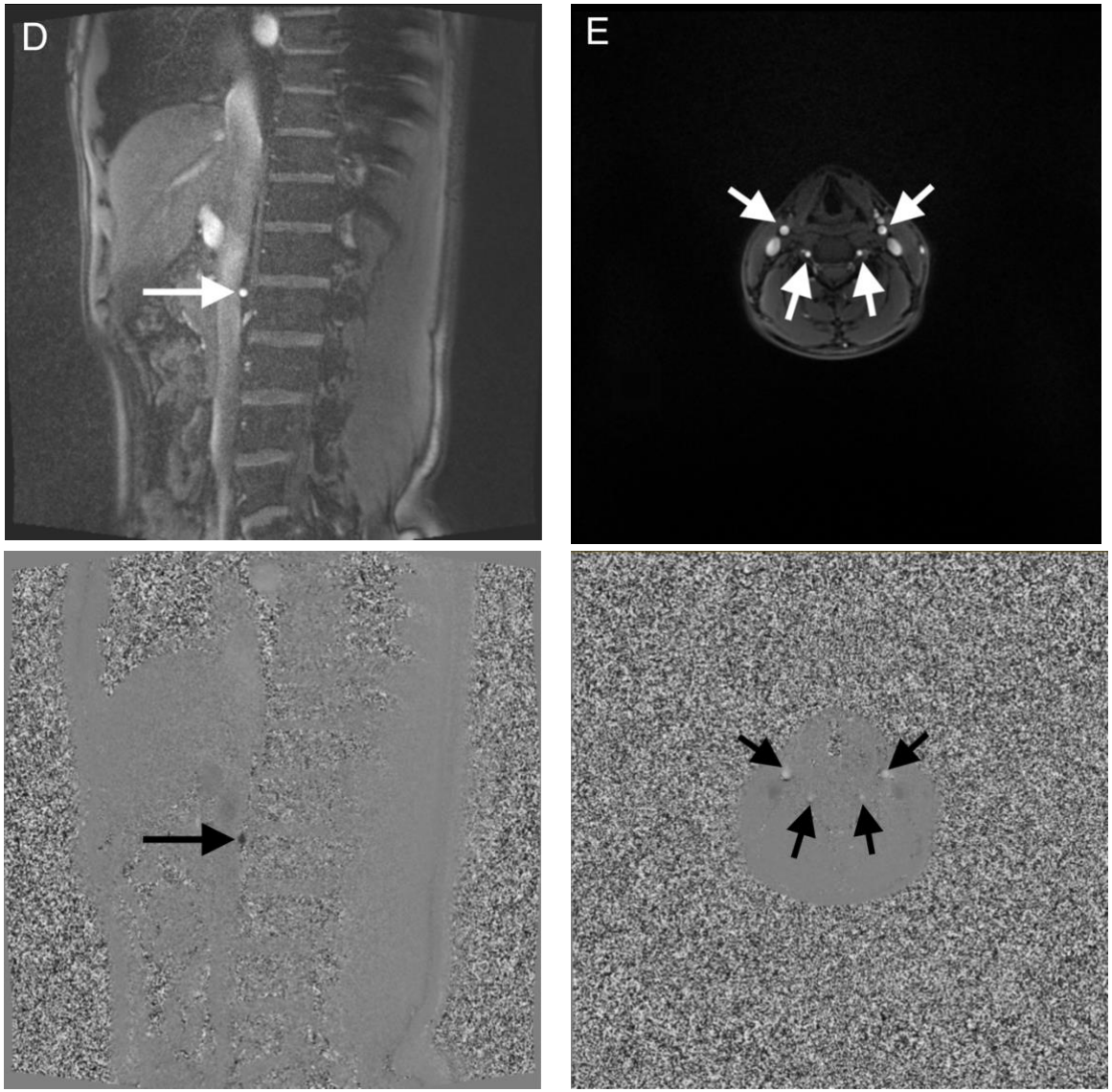
D
E

Anatomic imaging

LV volume and mass were acquired from a stack of short axis cine images encompassing the heart from the apex to the atria using real time radial b-SSFP *k-t* SENSE during free breathing (128 radial spokes per slice, with *k-t* SENSE under-sampling factor of 8; ***Figure 12***).(55) Eleven to 13 contiguous slices were acquired in the short axis to ensure coverage of the LV. An additional 4-chamber view was acquired to allow for identification of the basal slices during the post processing (***Figure 11***). Real-time data for each slice was acquired for 1.5 sec and the slice was then automatically moved down the ventricle. This resulted in scan time of ~30 sec, with good spatial and temporal resolution (3.1 × 3.1 × 10.0 mm / 35.7 ms, respectively).(55) While this technique may not be optimal for the morphological assessment of the atrioventricular (AV-) valves, it is nevertheless a key sequence used for volumetric assessment in some centres (e.g., Great Ormond Street Hospital for Children, where the studies for this PhD were conducted), and excellent agreement has been demonstrated with b-SSFP breath-held cine imaging.(55) Moreover, using a conventional technique with higher spatial resolution would have come at the cost of unacceptably longer acquisition times.

Figure 11. Four-chamber view of the heart.

This cine image was acquired to identify the base of the heart and the atrioventricular valves during postprocessing (i.e., to distinguish ventricular volume from atrial volume).

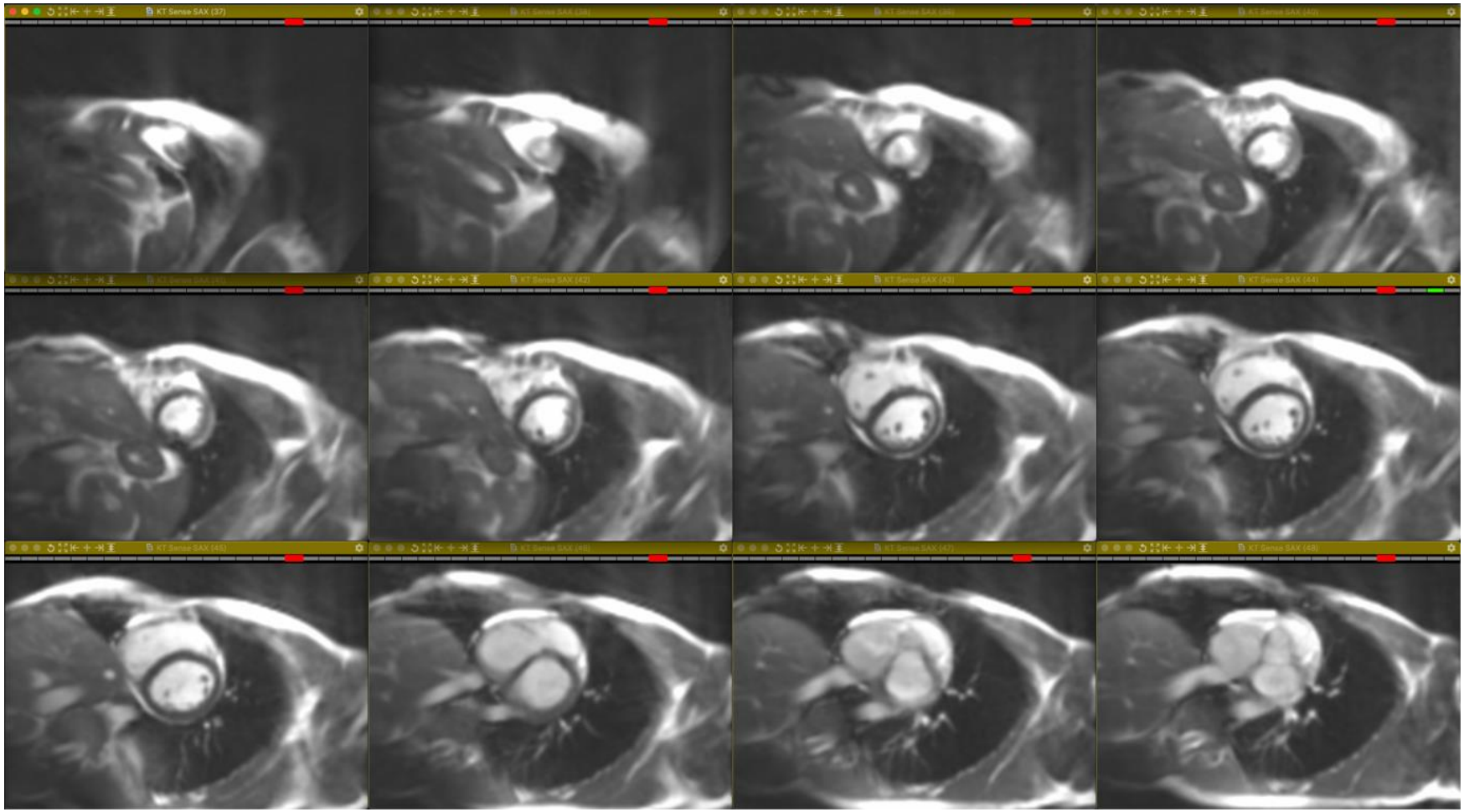

Figure 12. Short axis stack cine images of the left ventricle.

Cine images were acquired in a series perpendicular to the long axis of the heart, reaching from the apex (top left) to the left atrium (bottom right) at a slice thickness of 10 mm using *k-t* SENSE during free breathing.

Image post processing

Imaging data were processed offline using custom plugins for OsiriX software for Mac OS X, version 6.5.2 or later (Pixmeo, Bernex, Switzerland). LV myocardial volume was obtained by manual contouring and subtraction of the endocardial from the epicardial volume (***Figure 13***). Papillary muscles were included in the myocardial volume. LV mass (LVM) was calculated by multiplying myocardial volume by a density estimate of 1.05 g/mL. LV volume was measured by manual segmentation of the endocardial borders in diastole and systole, whereas diastole was defined as the frame that coincided with closure of the AV-valves, and systole as the frame preceding their opening. A cine image in 4-chamber view was used to identify the AV-valves.

Segmentation of aortic magnitude and phase images from PCMR was performed in a semi-automated fashion using an in-house algorithm, followed by manual, frame-wise adjustments of the contours. Organ-specific blood flow was derived from the mean volume flow across one cardiac cycle within the ROI on the respective, single RAGS PCMR magnitude image.

Figure 13. Short axis cine image (diastolic frame, midventricular slice).
LV myocardial volume was obtained by manual contouring and subtraction of the endocardial (orange) from the epicardial volume (blue).

3.3. Blood pressure

BP was measured every 5 min in the non-dominant arm in supine position with each study participant's arms by their side while in the scanner, using an oscillometer device (Datex Ohmeda, General Electric, Boston, MA, USA).

3.4. Anthropometry

Height was measured to the nearest 1 mm using a calibrated stadiometer, without shoes and with the Frankfurt plane of the participant's head aligned by eye to be parallel to the ground. Weight was measured to the nearest 10 g, using a calibrated scale, with the participant wearing only light clothing and no shoes. Waist and hip circumferences were determined using a flexible measuring tape according to standard practice.(67) Body surface area (BSA) was calculated using Du Bois' formula in adults (BSA = 0.007184 × weight [kg]$^{0.425}$ × height [m]$^{0.725}$), and using the Haycock formula in adolescents (BSA = 0.024265 × weight [kg]$^{0.5378}$ × height [m]$^{0.3964}$). Body mass index (BMI) was calculated as weight [kg] / height [m]^2.

3.5. Statistics

3.5.1. Software

Statistical analyses were performed using Stata SE software for Mac OS X, version 13 or later (StataCorp, College Station, TX, USA).

3.5.2. Descriptive statistics

Normally distributed data are expressed as mean ± standard deviation (SD). For non-normally distributed data, the median (interquartile range [IQR]) is presented. Group comparisons were done with Student *t*-test or Mann-Whitney-U test, as appropriate. Skewed data were log-transformed prior to parametric testing and group means were back-transformed to geometric means for presentation in natural units.

Blood flow, SV and LVM were indexed to BSA, unless indicated otherwise. Indexed variables are indicated by an ‘i’-suffix, e.g. SVi.

3.5.3. Regression analysis of longitudinal data

To account for variations of synchronisation between measures, BP and MRI data were linearly interpolated at 10-min intervals, starting from the beginning of meal ingestion, and truncated at 50 min. Changes in data over time and the effect of various covariates (e.g., sex, BMI) were assessed using repeated measures mixed models. These models account for the correlated nature of repeated measures over time. The coefficients of these models for each time point after baseline represent the time-dependent change from baseline, and their *P*-values represent the significance of that change. These *P*-values are reported to illustrate the significance of postprandial responses.

A significance level of $P \leq 0.05$ was assumed, and 95% confidence intervals (CI) are provided where applicable.

3.6. Ethics

All experiments were conducted in accordance with the Declaration of Helsinki. Ethics approval was sought and obtained from National Research Ethics Service London – Queen Square prior to initiation (reference no. 13/LO/1750 and 16/LO/1649). Informed consent was obtained from all participants and/or their parents, as applicable.

Chapter 4. Cardiovascular responses to food ingestion in humans

Abstract

Ingestion of food is known to increase mesenteric blood flow. However, whether this increased flow demand is compensated for by a rise in CO alone, or by redistribution of blood flow from other organs, is unclear. To test this, a new comprehensive imaging method to assess the human cardiovascular response to food ingestion was developed and validated in the following chapter.

Blood flow in segments of the aorta and in organ-specific arteries, and ventricular volumes were assessed in 20 healthy adults using MRI under fasting conditions and repeatedly for up to 50 min following ingestion of a high-energy liquid meal. After meal ingestion, SVR fell substantially and CO rose significantly. BP remained stable. These changes were driven predominantly by a rapid fall in mesenteric vascular resistance, resulting in over 4 times more intestinal blood flow. Renal vascular resistance also declined but less dramatically so. No changes in celiac, brain or limb perfusion were observed.

The following chapter is the first study to fully characterise systemic and regional changes in vascular resistance after food ingestion in humans. It was shown that the postprandial drop in SVR is fully compensated for by increased CO and not by redistribution of blood from other organs in healthy adults. With the exception of a modest increase in renal blood flow, there was no evidence of altered perfusion of non-digestive organs. Moreover, it was demonstrated that the proposed oral stress protocol can be applied safely in an MRI environment, allowing further, detailed study of the involvement of the gut in systemic disorders or CVD.

4.1. Background

4.1.1. Gaps in knowledge in postprandial physiology

Overview

The cardiovascular responses to food ingestion have been the subject of extensive research in, both, humans and animals over the past several decades.(1, 7, 16, 20) While the global haemodynamic responses are well-understood, several unknowns and inconsistencies exist regarding the regional vascular responses to a meal. This may be because previous human studies have had to rely upon observer-dependent and inconsistent measurement techniques, and have been limited in sample size.(7, 20)

As already set out in Chapter 1, the ingestion of food triggers a transient, moderate drop in celiac vascular resistance, followed by a more sustained and substantial decrease in mesenteric vascular resistance. This is accompanied by a simultaneous rise in CO in order to maintain BP whilst providing the additional blood flow commanded by the intestine. There is debate about whether this is achieved by increasing CO alone, or whether there is blood flow redistribution from non-digestive organs. Such redistribution would require regional disparities in vascular resistance.

The MRI techniques described in Chapter 2 allow rapid and accurate flow measurement in vessels that are too small for dynamic stress studies using commonly used sequences. These techniques now allow to address the open questions about the cardiovascular responses to food ingestion in humans.

Cardiac output responses

Data on the CO responses after food ingestion vary. Using radionuclide cardiography in a small sample of 8 volunteers, Kelbaek *et al.* demonstrated a 62% increase in CO after ingestion of a sizeable ~1,500 kcal mixed meal.(68) Using Doppler ultrasound, other authors administered meals of varying composition to volunteers, and found a 32% increase after a carbohydrate-rich meal, compared to 22% following a lipid-rich meal of the same calorie-load

(~600 kcal).(7) Other studies confirmed that the magnitude of the postprandial increase in CO depends on meal size and composition.(69)

Mesenteric blood flow

Under fasting conditions, mean blood flow to the SMA has been reported to vary widely from 0.22-0.54 $L \cdot min^{-1}$ in different studies.(41) However, few authors reported this measurement relative to indices of body size (e.g., BSA), making meaningful comparison between studies challenging.

Considerable variability has also been reported on postprandial increases in SMA blood flow, ranging from 58-64%(17) to 125-164%(37, 38) assessed by similar methods after liquid meals of similar energy content. Larger meals of 750 to ~1,150 kcal have been reported to provoke increases of up to 240-250% of fasting blood flow.(37, 70) A very informative and concise overview by Someya *et al.* demonstrates that a liquid consistency, higher calorie content, as well as a mixed composition of, both, lipids and carbohydrates induce more pronounced rises in mesenteric blood flow.(41)

Differences in the time course of these responses are generally attributed to consistency and meal composition, in particular to protein content. This was addressed by one of the larger studies related to this topic, which demonstrated that the timing, but not the magnitude, of the postprandial increase in SMA blood flow was determined by meal composition.(17)

Renal blood flow

Data on renal blood flow changes after the ingestion of a meal have been inconsistent and sparse. Avasthi *et al.* used transabdominal Doppler ultrasound and validated it against an invasive Doppler measurement technique in animals. Subsequently, this group administered 3 different meals of different compositions (protein, carbohydrate, and water with electrolytes), and found that all meals increased renal blood flow, albeit to different extent and over differing time courses. However, the authors highlighted the complexity of the Doppler measurement technique they employed. Moreover, their study was

limited by a small sample size (N=5).(20) Others have compared a single postprandial MRI measurement of renal blood with fasting measurements and found a moderate increase.(71)

By contrast, Iwao and colleagues found evidence of increased renal vascular tone in a substantially larger cohort following the ingestion of a liquid meal.(18)

Limb blood flow

Previous research suggests that meals of different composition may alter limb blood flow in different ways. Using venous occlusion plethysmography, one study showed a decrease in calf blood flow postprandially. Meals high in lipid content provoked a greater and more sustained fall in limb blood flow than meals high in carbohydrates did. As the high-lipid meal also resulted in a more pronounced and prolonged increase in mesenteric blood than the high-carbohydrate meal did – despite an equal rise in CO in both meals – this finding suggests that blood flow is redistributed from the limbs in order to cover the increased blood flow demand of the digestive organs postprandially.(7) However, this study was limited by a small sample size (N=6), as well as the small effect size demonstrated relative to the reproducibility of the method used. Moreover, blood flow to the upper extremity was not assessed.

This was investigated by a more recent study, which confirmed that blood flow decreased postprandially.(41) Others found similar decreases in lower limb blood flow postprandially.(71, 72)

However, these findings were contrasted by a study in a slightly larger sample using thermodilution, which found that blood flow to the legs actually increased after the ingestion of glucose.(73) By contrast, an experiment in dogs using radioactive microbeads showed that blood flow to the limbs did not change postprandially.(74)

4.1.2. Purpose of the study

To test the hypothesis that, following ingestion of a meal, blood flow to the gut is driven by organ-specific falls in vascular resistance, and compensated for by increased CO, without any redistribution from other organs.

4.1.3. Publication

Findings from this chapter were published as original article in the *American Journal of Physiology: Regulatory, Integrative and Comparative Physiology*.(3)

4.2. Methods

4.2.1. Subjects

Twenty healthy adults (7 female; mean age 30 ± 9 years, range 18-52 years) took part in this study. Staff members volunteered for this experiment.

4.2.2. Study protocol

The experiment was conducted as detailed in 3.1. and repeated with a volume of water equivalent to that of the liquid meal in 10 randomly selected subjects. These ‘control’ experiments took place on a different day, either before or after the liquid meal experiments at random, to control for the influence of past experience with the protocol.

4.2.3. Imaging

Aortic blood flow was acquired at sinus level, at diaphragmatic level, and proximal to the iliac bifurcation, and regional blood flow was acquired for the common carotid and vertebral arteries, the celiac artery, the SMA, and each renal artery, as described in 3.2. Flow to the arms was estimated by subtraction of the neck- and descending aortic blood flows from total CO. SV at all time points was obtained using PCMR, but at 3 postprandial time points, it was also calculated as the difference between LV end diastolic volume (LVEDV) and LV end systolic volume (LVESV) and the values were compared to ensure internal consistency.

Vascular resistance was calculated by division of mean arterial pressure (MAP [mmHg]) by indexed blood flow, and expressed as Wood Units (WU) × m^2. Ejection fraction (EF, %) was obtained with the formula EF = (SV / LVEDV) × 100. Total arterial compliance (TAC) was calculated as SVi / (systolic BP [SBP] – diastolic BP [DBP]).(75)

4.2.4. Statistics

Repeated measures mixed models for the assessment of quantitative changes in physiological data over time (as described in 3.5.) included sex, BMI, age and control (water) as covariates.

4.3. Results

4.3.1. Systemic haemodynamic responses

Demographics and resting data are shown in ***Table 1***. After ingestion of the study meal, BP remained stable throughout the entire observed period. From 10 min onwards, mean SVR fell continuously until the end of the experiment (20% fall, $P<0.001$). There was a parallel rise in CO of 20% ($P<0.001$), which was predominantly driven by a continuous rise in HR. This association was significant from 20 min onwards ($P<0.001$). At 60 min, a mild decrease in LVEDV was seen (6% fall, $P<0.05$) and there was a trend towards an increase in EF (8% increase, $P=0.052$). Ingestion of water had no effect on any of the measured metrics (***Figure 14***).

Table 1. Subject characteristics and resting data.

N=20 (7 female)	Mean ± SD	Minimum	Maximum
Age (y)	30 ± 9	18	52
Height (m)	1.76 ± 0.1	1.57	1.93
Weight (kg)	79 ± 19	52	118
Body mass index	25.5 ± 5.5	18.7	39.9
Heart rate (bpm)	63 ± 10	46	89
Stroke volume ($mL \cdot m^{-2}$)	49 ± 7	36	63
LV diastolic volume ($mL \cdot m^{-2}$)	80 ± 13	58	105
LV systolic volume ($mL \cdot m^{-2}$)	32 ± 8	23	45
LV ejection fraction (%)	60 ± 5	51	68
TAC ($mL \cdot mmHg^{-1} \cdot m^{-2}$)	0.58 ± 0.1	0.40	0.78
Systolic BP (mmHg)	118 ± 7	104	131
Mean BP (mmHg)	87 ± 5	81	97
Diastolic BP (mmHg)	65 ± 6	56	81

BP = blood pressure; LV = left ventricle; SD = standard deviation; TAC = total arterial compliance. Adapted and reprinted with permission from: (3)

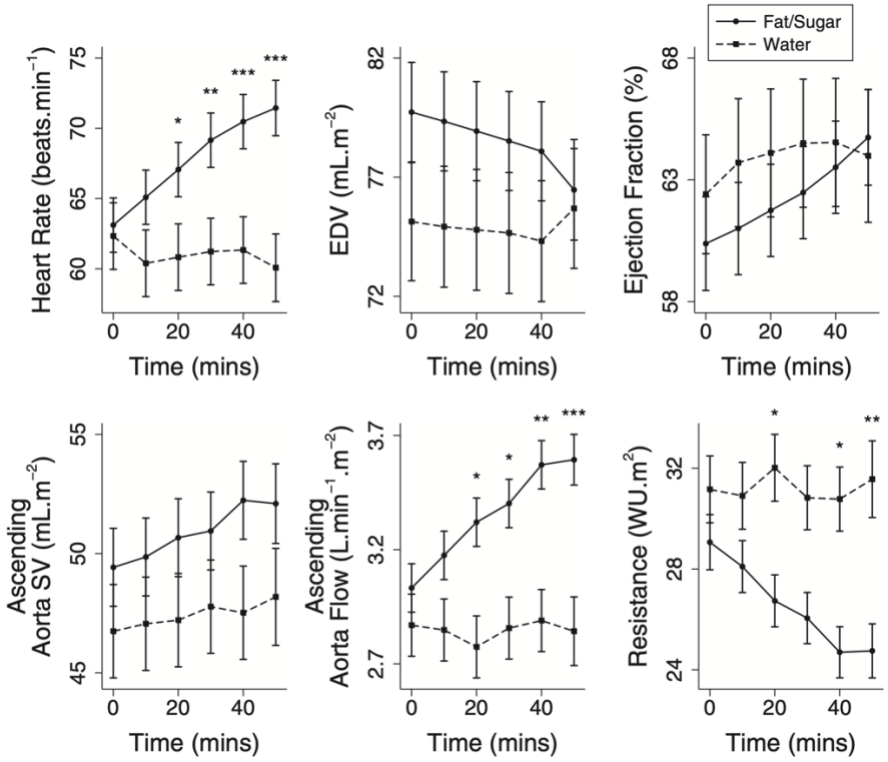

Figure 14. Haemodynamic changes over time.

Repeated measures mixed model adjusted for sex, body mass index, and age. The solid line shows changes after ingestion of the sugar/fat liquid meal (N=20); the dashed line shows responses to the control experiment (water; N=10). Resting metrics did not differ significantly. *P*-values are for differences between groups at each time point with respect to baseline: **P*<0.05; ***P*<0.01; ****P*<0.001. Standard error bars are used. EDV = end-diastolic volume; SV = stroke volume; WU = Wood units. Adapted and reprinted with permission from: (3)

4.3.2. Regional vascular responses

Baseline resistance and blood flow data are shown in ***Table 2***. Vascular resistance of the SMA decreased substantially from 10 min after ingestion of the sugar/fat meal and exhibited a continuous decline until the end of the observed period, resulting in a flow increase to more than 4 times the resting value (360% increase after 50 min; *P*<0.001). There was a modest but significant, steady decrease in renal vascular resistance, resulting in an increase in renal blood flow of 23% (*P*<0.01 after 20 min). By contrast, vascular resistance of the celiac artery territory, the brain, the legs and the arms did not change significantly

(***Figure 15***). Water had no measurable effect on regional organ perfusion or vascular resistances.

Table 2. Resting haemodynamics

		Fat/sugar (N=20)		Water (N=10)	
		Mean ± SD	Range	Mean ± SD	Range
AAo	*BF*	3.0 ± 0.5	2.2-4.3	3.0 ± 0.4	2.5-3.5
	R	30 ± 5	20-38	30 ± 3	25-36
DAo	*BF*	1.8 ± 0.3	1.3-2.4	1.8 ± 0.4	1.5-2.3
Brain	*BF*	0.60 ± 0.15	0.37-0.86	0.62 ± 0.19	0.30-0.93
	R	143 ± 35	99-205	170 ± 66	105-312
Limbs	*BF*	1.1 ± 0.3	0.7-1.4	1.2 ± 0.6	0.4-2.4
	R	86 ± 24	60-117	100 ± 69	38-263
Celiac	*BF*	0.38 ± 0.25	0.15-1.04	0.43 ± 0.26	0.16-1.13
	R	299 ± 156	93-644	281 ± 156	86-586
SMA	*BF*	0.15 ± 0.08	0.02-0.38	0.18 ± 0.07	0.08-0.28
	R	676 ± 403	256-1,828	605 ± 316	304-1,075
Renal	*BF*	0.60 ± 0.24	0.35-1.35	0.68 ± 0.36	0.20-1.61
	R	168 ± 54	72-268	173 ± 94	55-292

AAo = ascending aorta; BF = blood flow ($L \cdot min^{-1} \cdot m^{-2}$); DAo = descending aorta; R = resistance ($WU \cdot m^2$); SD = standard deviation; SMA = superior mesenteric artery; WU = Wood unit.

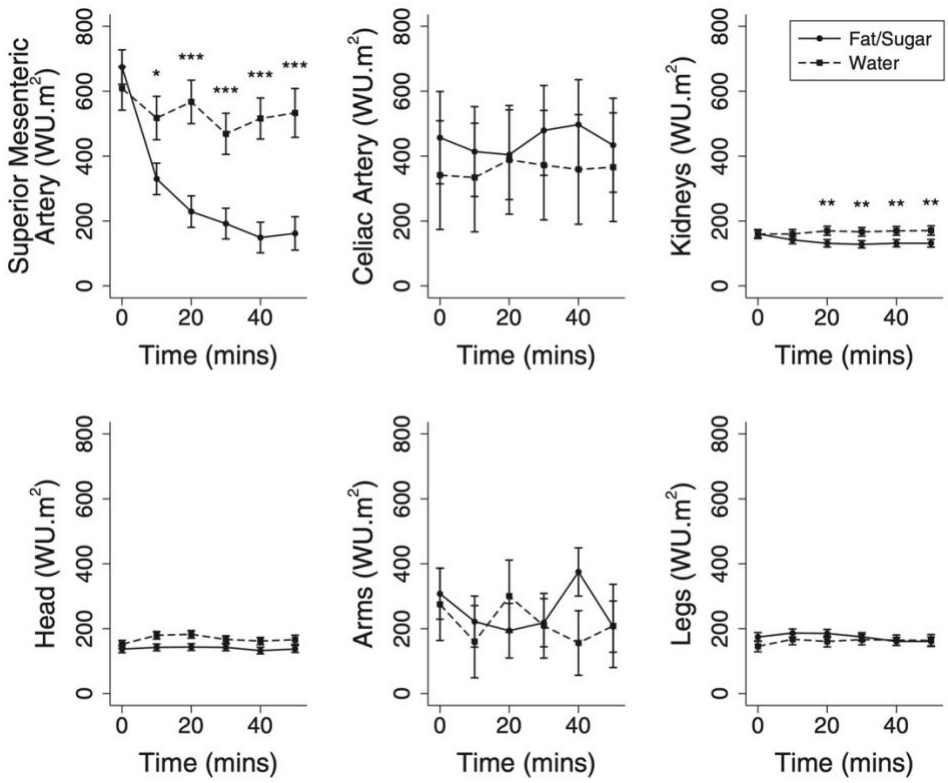

Figure 15. Changes in regional vascular resistances over time.
Repeated measures mixed model, adjusted for sex, body mass index and age. The solid line shows changes after ingestion of the sugar/fat liquid meal (N=20); the dashed line shows responses to the control experiment (water; N=10). Resting metrics did not differ significantly. *P*-values are for differences between groups at each time point with respect to baseline: **P*<0.05; ***P*<0.01; ****P*<0.001. Standard error bars are used. Adapted and reprinted with permission from: (3)

4.4. Discussion

4.4.1. Overview

This is the first comprehensive and non-invasive description of the cardiovascular responses to a high-calorie meal in humans. Using a novel, dynamic MRI approach, it was shown that the substantial drop in SVR seen after food consumption is compensated for by an increase in CO alone, without significant vasoconstriction in other territories. In healthy subjects, this compensatory process was well balanced, with BP remaining stable throughout the experiment. The reported findings were not due to volume (cardiac preload)

effects as there were no haemodynamic effects of ingesting water with the same volume as the liquid meal.

4.4.2. Comparison with existing literature

In this experiment, mesenteric blood flow increased to more than 4 times its pre-prandial value. This effect was more pronounced than suggested by previous findings from Doppler-based studies, where SMA perfusion rose to 200-300% of the baseline values.(7, 17) It is likely that the high carbohydrate and fat content of the study meal used, as well as its liquid consistency, led to the rapid and pronounced surge in mesenteric flow observed in the present cohort. In an MRI study published by Muthusami *et al.* subsequently to the present study, responses of comparable magnitude were found.(71) However, that study only measured blood flow at a single time postprandially and, thus, did not characterise postprandial haemodynamic responses in a time-resolved manner.

Interestingly, this experiment could not replicate the increases in celiac blood flow described previously.(41) However, the celiac response to feeding has been reported to occur almost immediately after the initiation of feeding, lasting only a short duration before returning to fasting levels. Thus, it is possible that the expected decrease in celiac vascular resistance was not detected appropriately, as the acquisition of MRI data required to re-plan imaging planes was still ongoing in the early postprandial period. In the MRI study published by Muthusami *et al.*, a change in celiac blood flow was similarly absent, supporting this hypothesis.(71)

Previous experiments on the vascular response of both splanchnic and non-digestive organs to the ingestion of food have been predominantly undertaken in non-human primates and dogs, and only few studies have been made in humans.(7, 17, 20, 29) These experiments have typically employed a combination of Doppler ultrasound and occlusion plethysmography in order to estimate small vessel blood flow. By nature, these techniques are not able to detect brisk changes in blood flow in different body regions at very similar time

points and track changes reliably over time. Thus, Doppler ultrasound and occlusion plethysmography techniques do not allow for a complete haemodynamic assessment and may be unable to accurately or reliably determine regional haemodynamics as a result. Earlier studies have also been small (N≤10) and reliant on methods, such as ultrasound, that are vulnerable to observer bias.(7, 29)

Nonetheless, the existing literature suggests that blood flow to the legs declines in order to compensate for the increased blood flow demand of the gut, especially after a fatty or protein-rich meal.(7, 76) In this comparatively larger group of 20 subjects, this change was not observed. Differences in meal composition, methodology or sample size may explain this discrepancy. Considerations made for the lack of an apparent celiac responses may also apply.

The role of renal blood flow in the haemodynamic response to food ingestion has been controversial. Avasthi *et al.* demonstrated that renal perfusion increased during the digestive phase and that the extent and duration of this effect correlated with the protein content of a meal.(20) However, those findings are in contradiction to results from a larger study, where renal perfusion was found to drop following ingestion of a meal.(18) Findings from animal studies have been similarly equivocal.(19, 76) In the present experiment, there was a modest but significant decrease in renal vascular resistance, which led to a sustained rise in renal blood flow. Contrary to the conclusions of Avasthi *et al.,*(20) this effect was present throughout the observation period despite the low protein content of the study meal used. Therefore, it is speculated that the steady rise in renal blood flow was the consequence of increased nutrient or metabolic breakdown products that result from ingestion of large amounts of sugar and fat, and not due to the modest volume of the meal, as there was no change in renal vascular resistance following the water fluid challenge alone.

This study's finding that cranial blood flow did not change postprandially is in line with previous work.(71) It is likely that autoregulation of cerebral blood flow prevents any significant changes following ingestion of a meal.

4.4.3. Clinical implications

Stress imaging

Most haemodynamic investigations in the healthy and in disease groups rely upon one-off measurements of global vascular physiology, usually taken at rest. In established diseases, such resting measurements may be sufficient to reveal abnormalities. However, in some disorders, or in early disease, such measurements are often normal.

Stress tests can provide additional information as they can unmask dysfunction that is otherwise compensated for, or that only manifests under certain conditions. For example, exercise tests are a central tool in cardiovascular diagnostics, as they assess cardiovascular responses to physical stress on a global level. However, this includes metabolic, endocrine, mental or neuromuscular components of physical stress responses. Therefore, exercise tests can only describe stress responses in a comprehensive fashion. By contrast, other cardiovascular challenges exist that test autonomic responses in a more focussed manner.(77) Such stress tests interrogate neuronal and neuroendocrine reflexes (e.g., vascular tone) to specific physiological triggers (e.g., postural manoeuvres). Different stress tests address different reflex arcs involved in the autonomic homeostasis of the cardiovascular system.(78) The protocol proposed in this chapter examines an autonomic reflex that has not been previously investigated systematically in humans and may, therefore, be a useful additional tool in cardiovascular diagnostics.

Techniques with better ability to characterise dynamic physiology and to resolve haemodynamic behaviour in organ-specific vascular beds noninvasively are now emerging.(48, 49, 79) Using such novel methodology, this study demonstrated that people can undergo an oral challenge in an MRI-environment safely to examine the vascular physiological responses to food

ingestion. Future studies may use this proposed new technique to resolve vascular physiological abnormalities in patient groups, such as, for example, those with autonomic failure, hepatic portal venous hypertension, or metabolic disorders (e.g., obesity).

Postprandial hypotension

As age progresses, attenuation of the cardiovascular responses to cardiovascular stress, such as exercise or orthostasis, can be observed.(80) Blunting of the normal CO increase following a meal has been linked to falls and syncope in the elderly. Failure to maintain an adequate cerebral perfusion pressure in compensation for the postprandial drop in SVR has been discussed as a likely mechanism.(81) Although risk factors for such events have been identified (e.g., heart failure [HF]), they can occur even in the absence of cardiovascular disorders as a result of autonomic dysregulation. Moreover, abnormal regulation of peripheral vascular tone has been demonstrated in subsets of patients, supporting the need for further dynamic study of regional vasoreactivity.(82, 83)

Postprandial angina

Chest pain can be triggered by the ingestion of food in certain populations. This is typically seen in patients with coronary artery disease (CAD) and, less commonly, in patients with hypertrophic cardiomyopathy.(84-86) The underlying mechanisms are not fully understood. Postprandially raised myocardial contractility may cause relative ischaemia in patients with CAD, where coronary flow reserve is decreased.(87) Additionally, a blunted CO increase after a meal may cause angina when the postprandial drop in SVR cannot be compensated for sufficiently in order to maintain coronary perfusion pressure.(86) The postprandial increase in HR may further aggravate coronary perfusion in these subjects.(84)

Similar observations have been made in patients with hypertrophic cardiomyopathy.(85) In this disorder, myocardial hypertrophy and abnormal myocardial microvasculature necessitate a comparatively higher coronary

perfusion pressure. This may be compromised when SVR falls postprandially. Moreover, an increase in pressure gradient in the LV outflow tract can be observed after the ingestion of food, with increased LV wall strain and decreased coronary blood flow as consequences.(88)

4.4.4. Strengths and limitations

Study protocol

A standardised, validated MRI food challenge protocol of high-fat, high-sugar food was used.(3) The study protocol controlled for time of day, caffeine, exercise and other potential confounders for physiological responses. Each participant ate a standard meal and then fasted for a similar duration.

The MRI sequences used in the proposed setup have been validated for the rapid assessment of ventricular volumes and the measurement of small vessel blood flow in humans.(3, 4, 47, 55) In contrast to the direct quantification by electromagnetic probes used in animal experiments, flow measurement by MRI is non-invasive. This may obviate or reduce the need for animal studies in future cardiovascular research.

Study meal

The meal used for this study has a number of advantages. Diets high in fat and sugar are now common in the modern era, particularly in the obese, and have been implicated in LVH development.(89) Maltose syrup was used to enhance palatability and decrease sweetness and osmolality, reducing the risk of nausea or vomiting. It is metabolised to dextrose by amylases and hepatic maltase so rapidly that the blood glucose response is virtually identical to that following ingestion of an equivalent quantity of glucose but with approximately half the sweetness of glucose.(90) The meal was well-tolerated generally in the studied population but one person reported nausea immediately after consumption and one person reported late vomiting, several hours after the experiment. Nausea and vomiting are well-recognised complications of the standard OGTT.(91) Given the equivalent carbohydrate load in the meal used in this study, together

with a high fat content, tolerance of this mixed meal is considered good, and comparable to the OGTT.

4.4.5. Conclusions

I. The ingestion of food causes a drop in SVR due to mesenteric vasodilation.

II. This is compensated for by an increase in CO, without any significant vasoconstriction in non-digestive compartments.

III. The proposed protocol can be applied safely in humans and can be used to study the involvement of the gut in systemic disorders or CVD.

Chapter 5. Postprandial vascular dysfunction and links to cardiovascular risk in adolescents

Abstract

LV hypertrophy (LVH) is a major risk factor for CVD, including HF. Although linked to obesity and hypertension, its aetiology is multifactorial. Blunted postprandial sympathetic regulation of gut blood flow has been observed in overweight animals and suggested as a promotor of hypertension and LVH. It was hypothesised that blunted postprandial superior mesenteric blood flow responses would be more common in overweight humans, and associated with increased BP and LVH.

To test this, LV dimensions and haemodynamic responses to a standardised high-calorie liquid meal were measured in healthy adolescents by MRI. Covariates such as BMI, BP, Tanner score, and an index of insulin resistance were included in multiple regression models to examine the independent associations of mesenteric flow response with BP status and LVH. Food ingestion increased CO and SMA flow. A blunted mesenteric flow response was associated with increased LVM and concentric LVH, independently of known determinants of LVH, including BMI. It was also associated with elevated SBP but this link did not explain the association with LVM.

In conclusion, postprandial mesenteric vascular dysfunction is associated with LVH and hypertension, independently of common risk factors for those conditions. The findings presented in the following chapter highlight a new, independent marker of cardiovascular risk in the young.

5.1. Background

5.1.1. Cardiovascular disease

Definition

The term, ‘cardiovascular disease’ (CVD), summarises a number of diseases:

- coronary artery disease (CAD);
- cerebrovascular disease;
- peripheral arterial disease;
- cardiomyopathy;
- heart failure (HF);
- hypertensive heart disease;
- inflammation of the heart;
- aortic aneurysm;
- arrhythmia;
- rheumatic heart disease;
- valvular heart disease;
- congenital heart disease (CHD), and
- deep vein thrombosis, and pulmonary embolism.

Due to their similar pathophysiology and their epidemiological predominance, the term is also often used colloquially to refer to atherosclerotic CVD (i.e., CAD, cerebrovascular disease and peripheral arterial disease).

Epidemiology and significance

CVD is one of the main health burdens, and the leading cause of death, in the world. The World Health Organisation estimated that 17.9 million people died from CVD in 2016, representing 31% of all global deaths. Of these deaths, 85% were attributable to myocardial infarction and stroke. Of note, over ¾ of CVD-related deaths were reported in low- and middle-income countries, highlighting that CVD is not a problem that affects the industrialised world predominantly.(92) In the European Union, it caused 1.8 million deaths in the same year, representing 35.7% of all deaths and making it considerably more

lethal than the second most frequent cause of death, cancer (26.0%). Of note, this figure was higher in women (38.4%) than in men (33.1%).(93)

Risk factors and pathophysiology

Several factors promote the development of CVD, including overweight and obesity, lack of physical activity or exercise, tobacco smoke consumption, dyslipidaemia, diabetes, elevated BP, and alcohol consumption. CVD risk also increases with age and family history. However, the strong predominance of modifiable risk factors has shown that CVD is largely preventable.(94)

The main pathophysiological hallmark of most CVD (i.e., CAD, cerebrovascular disease and peripheral arterial disease) is atherosclerosis, a complex disorder of the arterial wall characterised by (sub-)endothelial inflammation and retention of lipoproteins. This process typically develops over decades and eventually results in thickening of the arterial wall, and formation of atheromatous plaques in the intimal layer of the arteries. As these processes advance, the vessel lumen narrows, impeding blood flow to end organs.(95) Chronic undersupply with blood and oxygen may trigger symptoms of ischaemia, such as angina or claudication, or cause progressive end organ damage, such as ischaemic heart disease. Rupturing of plaques may cause sudden, potentially life-threatening ischaemia and subsequent organ failure, such as myocardial infarction (MI) or stroke. However, improved management of stroke and MI have lowered their mortality and shifted the health burden of CVD towards chronic conditions such as HF.(96)

One prominent autopsy study revealed that early atherosclerotic changes are already abundantly present in childhood and adolescence, and that these changes were correlated with the presence of cardiovascular risk factors.(97) This led to the understanding that CVD has its origins much earlier in life than previously thought, and that improved strategies to understand and prevent CVD in the young are needed.(94) Paediatric obesity, in particular, plays a key role in the development and prevention of CVD.

5.1.2. Overweight and obesity

Definition

Obesity is a complex disorder characterised by excess body fat (adiposity). Adiposity is estimated grossly by measuring body weight. However, as body weight is also determined by factors other than adipose tissue (e.g., body height, or lean mass), it is usually corrected for frame in some way. BMI (weight [kg] / height [m]^2) is the most widely used estimate for obesity that adjusts for body size partly. However, although easy to obtain and consistently linked to CVD in population studies, it is limited by the assumption that the proportion of adipose tissue among individuals with similar weight and height is equal. This is particularly problematic among children, where lean mass accrued through somatic growth has been shown to correlates more strongly with BMI than adipose mass.(98, 99) Nevertheless, BMI remains the most widely accepted marker to assess overweight and obesity. In adults, overweight is defined as BMI ≥25.0 and <30.0, whereas obesity is defined as BMI >30.0. In children and adolescents, overweight is defined as a BMI z-score ≥1.04 (85th centile), and obesity as a BMI z-score of ≥1.64 (95th centile).(100)

Obesity and cardiovascular risk

Obesity is one of the most important risk factors for CVD. Although it also increases CVD risk directly, much of the association is mediated by a number of secondary cardiometabolic and endocrine disturbances it entails.(101) Greater deposits of adipose tissue, especially of the viscera, trigger oxidative stress and the release of pro-inflammatory mediators. These alterations lead to inflammation of the arterial wall, which promotes atherosclerosis and vascular stiffening, and thus, hypertension.(102) Adiposity also leads to progressive insulin resistance, with T2DM as long-term consequence, as well as to dyslipidaemia. Both promote atherosclerotic remodelling of the arterial wall further.

Paediatric obesity

Obesity in childhood and adolescence is a major, global health issue of growing importance. In Europe, the prevalence of overweight/obesity in children between 2 and 13 years of age increased from 20.6% in the period from 1999 to 2006, to 21.3% between 2011 and 2016. Within this timeframe and population, the prevalence of obesity rose from 4.4% to 5.7%.(103) In the United States, the prevalence of obesity in children and youth between 2 and 19 years of age increased from 14.5% in 1999/2000, to 17.3% in 2009/2010. In 2012, the prevalence of overweight and obesity combined was ~32%.(104) Although the trends observed in recent years appear to be flattening in some Western countries, the prevalence of paediatric obesity remains on the rise in many parts of the world.(105) These developments are projected to cause an alarming surge in CVD in the near future.(106)

Whether paediatric obesity is an independent risk factor for CVD later on in life, or increases cardiovascular risk by persisting into adulthood, is not yet fully resolved.(107, 108) Nevertheless, substantial increases in cardiometabolic derangements promoting CVD, such as T2DM, dyslipidaemia, LVH, or high BP, have been reported as a consequence of the rising trends in obesity in the paediatric population.(109)

5.1.3. High blood pressure

Overview

BP plays a central role in the development of CVD. Hypertension can cause CVD directly by inducing concentric remodelling and hypertrophy of the LV via raised afterload. This can progress into hypertensive heart disease and HF (through progressive LV dilation), as well as to atrial fibrillation (through left atrial dilation due to raised LV filling pressure). Raised BP is also one of the main risk factors for atherosclerotic CVD, valve disease, and aneurysm, as it promotes fibrotic remodelling of the arteries due to raised shear stress. Vascular stiffness is one of the hallmarks of raised BP. However, the association is complex and not fully understood. For example, it has been

shown that vascular stiffness can be both, a consequence of high BP (through fibrotic remodelling of the arterial wall), and a cause for it.(110)

Obesity and blood pressure

Two of the main determinants of BP are body weight and body composition. Although the links between raised body weight and BP are not yet fully understood, several mechanisms have been proposed. In obese young adults, raised SVR appears to be the main determinant of high BP.(111) This may be due to the poorer vascularisation of adipose tissue. Raised sympathetic nervous activity and greater circulating volume may also play an important role.(112) With increasing age, cardiometabolic derangement associated with obesity may further aggravate this through progressive stiffening of the arteries. By contrast, in the lean, raised CO is the hallmark of elevated BP. It has been suggested that aortic compliance may be enhanced at a young age to counteract this, and that these mechanisms progressively fail with ageing and arterial stiffening.(113, 114)

5.1.4. Left ventricular hypertrophy

Overview

LVH is defined as raised myocardial mass of the LV. It is often a secondary phenomenon of other CVD risk factors, such as T2DM, age, or raised BP. These factors can cause cardiac remodelling by stimulating cardiomyocyte growth either directly (e.g., hyperinsulinaemia), or through abnormal cardiac loading (e.g., stiffening of the aorta). Other important, non-modifiable determinants of LVM include genetics and ethnicity. For example, LVH is more common in Black people than in White people. However, whether this association is independent of other factors known to increase LVM, such as BP, is not yet fully resolved. Heritability is another key factor that affects LVM, and appears to be driven by genes encoding proteins that are involved in BP regulation, skeletal growth, metabolism, calcium homeostasis, and other important variables that can alter cardiomyocyte growth.(115)

Importantly, increased LVM is also an independent cardiovascular risk factor that can be present before other cardiometabolic abnormalities are diagnosed.(116, 117) Various other forms of LV remodelling exist and may involve enlargement of the LV cavity, with or without raised LVM. Different patterns of cardiac remodelling have been linked to different cardiometabolic phenotypes, and predict different cardiovascular complications.(118) One important factor influencing cardiac mass and geometry is obesity.

Obesity and left ventricular hypertrophy

Obesity causes adverse cardiac remodelling in adults.(119) Changes in LVM and geometry develop as this process advances. LVH is the eventual result and is a major risk factor for CVD, including diastolic and systolic HF, atrial fibrillation, MI and stroke.(117, 120) Indeed, childhood obesity has been identified as a strong risk factor for developing HF, in particular in adulthood.(121) LVH may develop before other risk factors – such as hypertension – are diagnosed, highlighting its importance as an independent marker of early cardiovascular risk.(116) In children, increased LVM has been linked independently to adiposity before other potential contributing factors such as hypertension or hyperinsulinemia were seen, indicating that the process starts earlier in life than previously thought.(118, 122, 123) The increasing global prevalence of childhood obesity necessitates early identification of such pathology and a better understanding of its underlying mechanisms in order to improve prevention of HF and CVD.(124)

The link between childhood obesity and LVH remains poorly understood.(118, 122) Animal experiments have revealed a new potential mechanism to explain the association.(24, 125) A lipid-rich diet and obesity were both linked to disordered arterial control in the splanchnic vascular bed in rats.(125) Reflex vasodilation in this vascular bed is the typical response to food ingestion, but blunting of this reflex was found in obese rats(3) and was associated with hypertension and increased LVM.(125) Despite a widespread preference for high-calorie diets in Western countries and the observation that most people spend the greater proportion of their day in a postprandial state,(10) this link

has not been demonstrated in humans before. Limited conventional techniques may have prevented such investigation.

Given that LVH is a major risk factor for cardiovascular morbidity and mortality and that it appears early in the disease process, understanding factors that drive its emergence in young people is vital for the development of effective CVD prevention.

5.1.5. Purpose of the study

The purpose of this study was to test the hypothesis that abnormal postprandial mesenteric vascular function is linked to increased BP and adverse LV remodelling in adolescents with varying degrees of adiposity.

5.1.6. Publication

Findings from this chapter were published as original article in *Circulation: Cardiovascular Imaging*.(4)

5.2. Methods

5.2.1. Subjects

Healthy adolescents, aged 13-19 years, were recruited via newspaper advertisements and through an obesity clinic (University College London Hospital, London, UK) between September 2014 and May 2016.

5.2.2. Study protocol

Participants underwent the oral stress protocol as detailed in 3.1. Prior to the meal challenge, a fasting blood sample was collected. Baseline BP was assessed after participants had been resting for 15 min (IQR 12-17 min) and before any interventions or blood tests. BP measurements obtained successfully in this quiescent period were averaged (mean 2.5 measurements; range 1-6). The timing of meal ingestion was recorded and the meal was typically consumed within 2 min (IQR 1-3 min). Flow measurements were repeated for at least 40 min postprandially. Pubertal (Tanner) stage was self-

assessed by the participants.(126, 127) This method has been shown to have good levels of agreement with physician examination in a large paediatric population.(126)

5.2.3. Imaging

Aortic and regional blood flow, HR and LVM were measured as described in 3.2. Cranial blood flow was not assessed in all but a small number of initial subjects after 2 events of vomiting in the early stages of the study raised concerns that the neck coil could prevent subjects from turning their heads to the side in case they vomited (however, no more vomiting events were observed after this).

Pulse wave velocity (PWV) was derived from ascending and descending aortic flow (Q) and area (A) curves as described previously.(62) This method relies on the fact that PWV = $\Delta Q / \Delta A$ in the reflection-free part of early systole. Thus, PWV was calculated by robust linear regression of the initial linear segment of unfiltered and non-interpolated data points in both the Q and A curves, and by division of the resulting gradient for Q by that of A.

5.2.4. Statistics

Data Adjustments

Blood flow and SV were indexed to height [m] raised to powers of 0.92 and 1.45, respectively.(128, 129) LVM was indexed to height [m] to the power of 2.7. These adjustments correct for the influence of skeletal size with minimal confounding by obesity, and are preferred over adjustment for BSA in this context.(123, 130)

To address limitations of reference MRI data in children, normal values were generated within the study population using an established technique.(123) First, LVMi was adjusted for age and sex by linear regression. LVH was defined as an adjusted LVMi above the 95th centile in a subpopulation with a normal BMI distribution (N=55, BMI z-score mean 0.17, SD 0.94, range -1.96 to 1.87). This centile and its 95% CI were found by a bootstrap method. LVM to LVEDV-

ratio (LVM:EDV) was calculated and an upper limit for this measure was defined using the same approach. Eccentric LVH was defined as LVMi >95th centile, and concentric LVH was defined as LVM:EDV >95th centile and LVMi >95th centile.(123)

BMI was converted to age- and sex-specific z-scores in adolescents using published data.(131) Overweight was defined as a BMI z-score ≥1.04 (85th centile) and obesity as a BMI z-score of ≥1.64 (95th centile), according to current guidelines.(100)

In accordance with current guidelines,(132) elevated SBP (eSBP) was defined as SBP >120 mmHg but <130 mmHg, and DBP <80 mmHg. Hypertension was defined as SBP ≥130 mmHg or DBP ≥80 mmHg.

Response analysis

The postprandial SMA flow response (ΔSMA) was calculated by area-under-the-curve (AUC) analysis using the trapezoidal rule on non-interpolated measures. Each AUC was divided by the time difference between meal ingestion and the last measure, yielding a time-weighted mean to control for individual variations in experiment duration. ΔSMA was calculated by subtracting resting values from these means. Responses recorded for less than 40 min were excluded in the final model (n=7).

Repeated measures mixed models to assess quantitative changes in physiological data over time (as described in 3.5.) included sex and BMI z-scores as covariates. Marginal mean estimates were then calculated from these models at 3 values of BMI z-score representing the normal range (-2, 0, and +2) to illustrate the time-varying, continuous associations found in these models. Haemodynamic responses to the meal are presented initially both unindexed and indexed for a power of height to show that the findings do not depend on this adjustment.

Multiple linear regression was used to assess the effects of ΔSMA on LVM, independently of known determinants of LVM, i.e. sex, Tanner stage, BMI, age, resting SBP, SV, and homeostatic model assessment of insulin resistance (HOMA-IR). A similar model was used to assess the effects of ΔSMA on SBP accounting for the same potential confounders, except resting HR was included as an independent variable as marker of sympathetic activity, and BP was not. Logistic regression was used to determine the risk of LVH and eSBP on the basis of ΔSMA. These models were repeated with the inclusion of other potential determinants, as for LVM, to test for independent effects. Goodness-of-fit tests were carried out for linear and logistic models to ensure that the models did not contravene model assumptions.

5.2.5. Laboratory analysis

Blood samples were obtained using standard techniques, following at least 20 min of rest in the supine position. Samples were immediately centrifuged and stored at -80°C before batch analysis.

Fasting glucose was measured using a Vitros 5600 Clinical Chemistry analyser (Ortho Clinical Diagnostics, Raritan, New Jersey, USA), and fasting insulin was determined using a chemiluminescent immunoassay (Immulite 2500, Siemens Diagnostics, Berlin, Germany). HOMA-IR was calculated as (fasting glucose × fasting insulin) / 22.5.

5.3. Results

5.3.1. Study population and resting data

Eighty-two participants were enrolled (36 female; median age 16 [IQR 14-18] years). Data from 2 participants who vomited during the MRI scan were excluded from longitudinal analyses. The remaining 80 completed the protocol without side effects. Thirty participants were obese and a further 9 were overweight. At baseline, overweight/obese participants had significantly higher COi, HOMA-IR, SBP, LVM and LVMi and lower indexed SMA flow (SMAi) than normal weight comparators (***Tables 3, 4 & 5***). They were also more likely to have

LVH and eccentric hypertrophy, but not concentric hypertrophy, and they were more likely to have hypertension. Linear associations of BMI z-score with COi (r=0.39; *P*=0.0003), SVi (r=0.48; *P*<0.0001), SBP (r=0.30; *P*=0.009) and SMAi (r=–0.23; *P*=0.04), supported these findings. BMI z-score did not correlate with diastolic or mean BP, PWV in any aortic segment, or HR.

Table 3. Cardiometabolic measures.

	All	**Normal weight**	**Overweight / obese**	***P***
N	82	43	39	
Age (years)	16.2 ± 2.0	16.1 ± 1.9	16.3 ± 2.1	0.814
Female	36 (43.9%)	20 (46.5%)	16 (41.0%)	0.617
BMI*	24.6 ± 7.5	20.0 ± 2.4	31.0 ± 6.6	<0.001
BMI z-score	1.0 ± 1.6	-0.2 ± 0.8	2.5 ± 1.1	<0.001
HOMA-IR*	1.44 ± 2.87	0.92 ± 1.17	2.18 ± 3.77	0.003
LVH	11 (13.4%)	1 (2.3%)	10 (25.6%)	0.002
Concentric LVH	6 (7.3%)	1 (2.3%)	5 (12.8%)	0.068
Eccentric LVH	5 (6.1%)	0	5 (12.8%)	0.015
LV mass (g)	122.9 ± 36.9	109.0 ± 30.8	138.3 ± 37.4	<0.001
LV mass ($g \cdot m^{-2.7}$)	28.8 ± 6.5	26.3 ± 4.8	31.6 ± 7.1	<0.001
LV EDVi ($mL \cdot m^{-2}$)	80.0 ± 14.0	84.8 ± 11.5	74.5 ± 14.8	<0.001
LV ESVi ($mL \cdot m^{-2}$)	30.3 ± 7.0	32.0 ± 6.5	28.3 ± 7.9	0.008
Hypertension	7 (9.5%)	1 (2.6%)	6 (17.1%)	0.032
eSBP	12 (16.2%)	5 (12.8%)	7 (20.0%)	0.403
PWV_{AAo} ($m \cdot s^{-1}$) (IQR)	4.3 (3.4, 5.3)	4.0 (3.3, 5.2)	4.3 (3.4, 5.3)	0.924
PWV_{DAo} ($m \cdot s^{-1}$) (IQR)	3.9 (3.1, 5.1)	3.9 (3.1, 4.9)	3.8 (3.1, 5.0)	0.947

P-values are for comparisons with normal weight group by student *t*-test (except X^2 for sex and blood pressure [BP] and LVH parameters). *Geometric mean. BMI = body mass index; EDV = end-diastolic volume; eSBP = elevated systolic BP; ESV = end-systolic volume; HOMA-IR = homeostatic model assessment of insulin resistance; IQR = interquartile range; LV = left ventricular; LVH = LV hypertrophy; PWV = pulse wave velocity. Adapted from: (4)

Table 4. Pre-prandial, resting cardiovascular measures.

	All	Normal weight	Overweight / obese	*P*
Systolic BP (mmHg)	114.6 ± 10.4	111.7 ± 8.5	117.7 ± 11.5	0.013
COi ($L \cdot min^{-1} \cdot m^{-0.92}$)	3.8 ± 0.7	3.6 ± 0.7	4.1 ± 0.5	<0.001
HR (bpm)	68.1 ± 11.1	68.3 ± 11.7	67.8 ± 10.5	0.839
SMAi ($L \cdot min^{-1} \cdot m^{-0.92}$)*	0.17 ± 0.12	0.21 ± 0.13	0.15 ± 0.12	0.041

*Geometric mean. BP = blood pressure; CO = cardiac output; HR = heart rate; SMA = superior mesenteric artery.

Table 5. Post-prandial, time-weighted mean (AUC) cardiovascular responses

	All	Normal weight	Overweight / obese	*P*
∆Systolic BP (mmHg)	2.0 ± 4.0	2.5 ± 3.5	1.4 ± 4.5	0.213
∆COi ($L \cdot min^{-1} \cdot m^{-0.92}$)	0.28 ± 0.38	0.25 ± 0.35	0.31 ± 0.42	0.579
∆HR (bpm)	5.0 ± 4.5	5.5 ± 4.5	4.4 ± 4.6	0.160
∆SMAi ($L \cdot min^{-1} \cdot m^{-0.92}$)	0.47 ± 0.22	0.51 ± 0.23	0.41 ± 0.18	0.031

AUC = area under the curve; BP = blood pressure; CO = cardiac output; HR = heart rate; SMA = superior mesenteric artery.

Overweight/obese subjects also had significantly lower vascular resistance the legs and, subsequently, greater blood flow to the legs, as well as higher SMA resistance and renal blood flow, but no significant corresponding differences in SMA flow and renal vascular resistance (***Table 6***).

Table 6. Fasting haemodynamics.

		Normal weight (N=43)		Overweight/obese (N=39)	
		Mean ± SD	Range	Mean ± SD	Range
AAo	*BF*	3.5 ± 0.7	2.2-5.2	4.0 ± 0.5*	3.1-5.5
	R	24 ± 4	15-35	21 ± 3$^{\#}$	14-28
Legs	*BF*	0.7 ± 0.3	0.3-1.6	0.9 ± 0.3$^{\#}$	0.5-1.6
	R	127 ± 58	52-334	97 ± 24$^{\#}$	44-154
Celiac	*BF*	0.48 ± 0.26	0.11-1.36	0.43 ± 0.22	0.10-0.98
	R	232 ± 172	72-794	248 ± 183	80-944
SMA	*BF*	0.23 ± 0.13	0.04-0.82	0.19 ± 0.12	0.04-0.55
	R	434 ± 281	100-1,862	639 ± 444†	159-2,393
Renal	*BF*	0.61 ± 0.19	0.35-1.35	0.75 ± 0.26$^{\#}$	0.21-1.72
	R	146 ± 44	74-261	126 ± 60	54-416

Group comparisons were performed by student *t*-test. *P<0.001, $^{\#}P$<0.01, $^{\dagger}P$<0.05. AAo = ascending aorta; BF = blood flow (L·min^{-1}·m$^{-0.92}$); CO = cardiac output; R = resistance (WU·m$^{0.92}$); SD = standard deviation; SMA = superior mesenteric artery; WU = Wood unit.

5.3.2. Postprandial haemodynamics and associations with adiposity

Both unindexed and indexed mean CO increased significantly within 10 min of meal ingestion, plateaued at 40 min (time-weighted mean unindexed ΔCO 0.45 [SD 0.62] L·min^{-1}; P=3.8x10^{-8}) and did not fall significantly before the end of the experiment. With the exception of the 10 min timepoint, where BMI z-score was associated with a smaller increase in HR and thus, in COi, the magnitude of the COi increase did not differ significantly by BMI z-score (***Figure 16***). It was driven predominantly by an increase in HR and, to lesser extent, by an increase in SVi at 10 and 20 min.

SBP also rose in response to the meal (time-weighted mean Δ 1.96 mmHg; P=7x10^{-5}) and was significantly greater than baseline from 10 min onwards (P<0.05 at 10 min, P<0.01 at 30 min, and P<0.001 at 20, 40 and 50 min; ***Figure***

16). Baseline SBP was associated with increased BMI z-score (*P*=0.006) but the magnitude of the postprandial response was not, if baseline SBP was accounted for. DBP rose to similar extent following ingestion of the meal, and this increase was weakened slightly by greater BMI z-score (<1 mmHg lower increase per BMI z-score, *P*<0.01 at 10 and 20 min). As a result, BMI z-score was linked to a slightly attenuated response in mean BP.

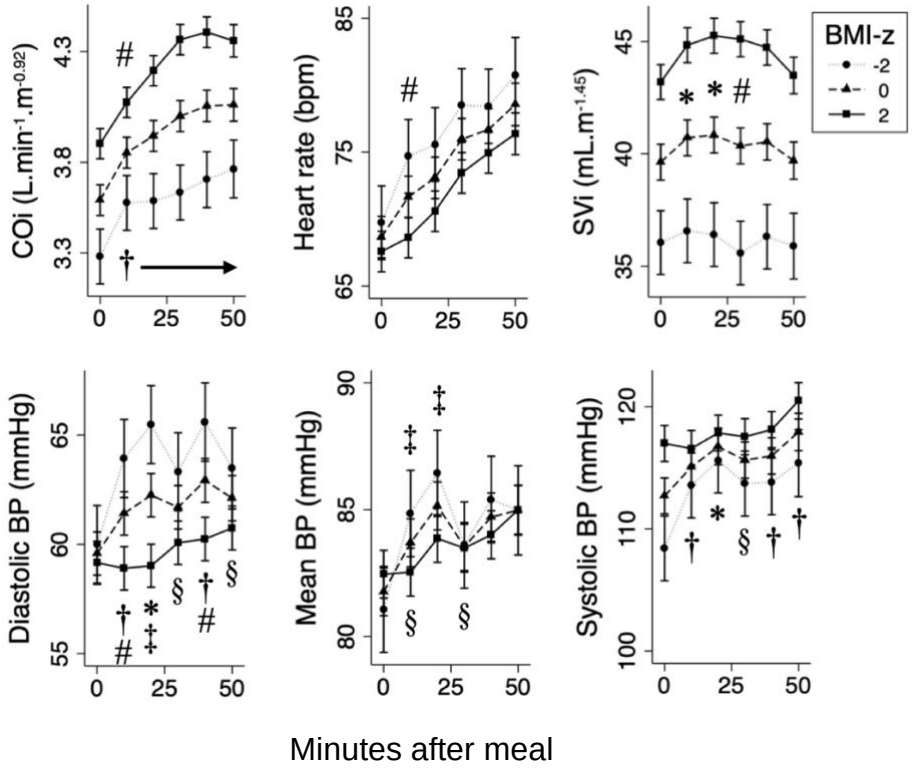

Figure 16. Marginal mean (± SE) postprandial responses in global haemodynamics in relation to adiposity.

Responses to the meal over time and the impact of BMI-z were assessed by repeated measures mixed models. **P*<0.05, §*P*≤0.01 and †*P*≤0.001 for changes in overall response with respect to baseline; #*P*<0.05 and ‡*P*≤0.01 for the impact of BMI-z on these responses. BMI-z = body mass index z-score; BP = blood pressure; CO = cardiac output; SV = stroke volume.

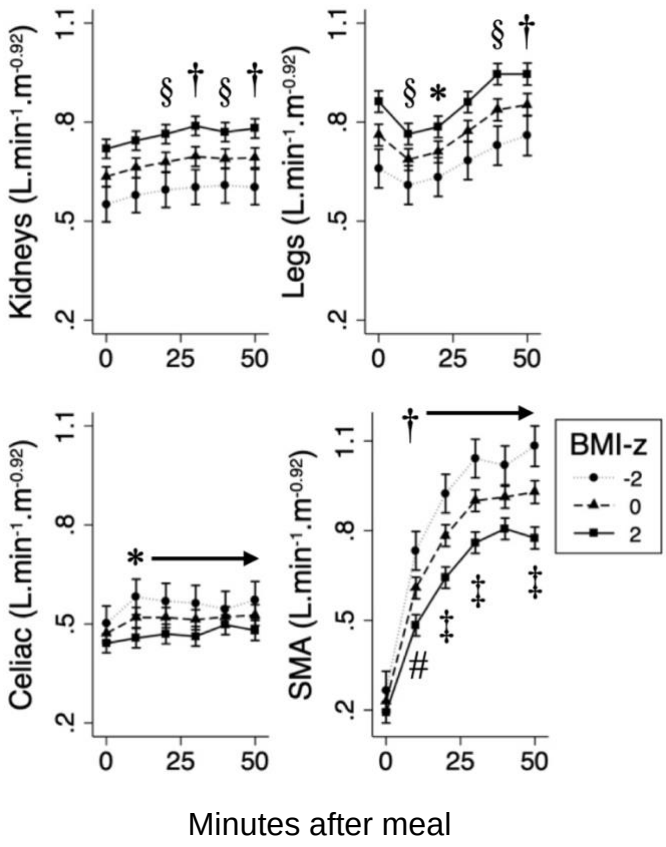

Figure 17. Marginal mean (± SE) postprandial regional blood flow responses in relation to adiposity.

Responses to the meal over time and the impact of BMI-z were assessed by repeated measures mixed models. *P<0.05, $^{§}P$≤0.01 and $^{†}P$≤0.001 for changes in overall response with respect to baseline; $^{\#}P$<0.05 and $^{‡}P$≤0.01 for the impact of BMI-z on these responses. BMI-z = body mass index z-score; SMA = superior mesenteric artery.

Unindexed and indexed SMA flow increased too (time-weighted mean unindexed ΔSMA flow 0.76 [SD 0.35] L·min^{-1}; P=4.2x10^{-31}) and by more, on average, than CO did (mean difference in responses 0.31 L·min^{-1}; P=5x10^{-5}), suggesting that, in addition to the CO rise, some flow redistribution from other regions occurred to support increased flow demand in the mesenteric vascular bed. The magnitude of this response was blunted by increased adiposity (P<0.05 at 10 min and P<0.01 at 20, 30 and 50 min for the continuous interaction of time and BMI z-score; ***Figure 17***). Both ΔSMA (B=-0.07 L·min^{-1}; P=0.003) and ΔSMAi were blunted in those with greater BMI z-score.

Blood flow to the kidneys and the celiac axis increased significantly from 10 min onwards. These changes persisted for the entire duration of the experiment and were not related to adiposity. Blood flow to the legs decreased initially and rose to levels greater than baseline at 40 and 50 min (***Figure 17***). This response was not influenced by BMI z-score either.

5.3.3. Associations of mesenteric vascular function with SBP and LV remodelling

Blunted ΔSMAi was associated with increased resting SBP (***Table 7***, Model 1; ***Figure 18***). Addition of BMI (Model 2) and resting HR (Model 3) did not explain this association. Moreover, blunted ΔSMAi was associated with a significantly increased risk of hypertension (log likelihood: -20.3; odds ratio: 0.01 [95% CI: $7x10^{-4}$, 0.89], *P*=0.045; R^2=0.11), but not eSBP, a prehypertensive category in children (*P*=0.33).

Blunted ΔSMAi was associated with increased risks of LVH (log likelihood: -5.4; odds ratio: 0.005 [95% CI: $1x10^{-3}$, 0.219], *P*=0.003; R^2=0.15) and concentric hypertrophy (log likelihood: -9.9; odds ratio: $5x10^{-5}$ [95% CI: $4x10^{-8}$, 0.061], *P*=0.001; R^2=0.31), but not eccentric hypertrophy (*P*=0.48). This was supported by an inverse linear association of ΔSMAi with LVMi (***Table 7***, Model 1; ***Figure 18***). A similar association was found between the unindexed variables. Addition of BMI (Model 2) and of resting SBP (Model 3) to the multiple regression did not fully explain the association. In further modelling, all associations remained significant after addition of age, Tanner score, and HOMA-IR (***Table 8***). Associations with LVMi were also independent of resting SVi and postprandial SBP response (time-weighted mean Δ).

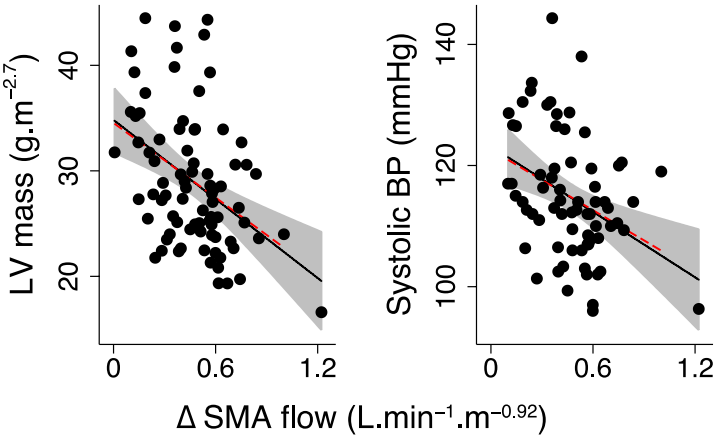

Figure 18. Inverse relationships of postprandial superior mesenteric artery flow response (ΔSMAi) with left ventricular (LV) mass index and resting systolic blood pressure (BP).

Graphs show the unadjusted models (r=-0.43, *P*=0.0001 for LV mass, and r=-0.32, *P*=0.006 for systolic BP). The associations were robust to adjustment for a range of potential confounders (***Table 7 & 8***) and to exclusion of the rightmost point on the graphs. Solid lines show linear regressions, dashed lines show effect of removing rightmost point, and 95% CIs are shown as grey bands. With permission from: (4)

Table 7. Associations of postprandial superior mesenteric artery blood flow response (∆SMAi) with systolic blood pressure (SBP) and left ventricular mass (LVM).

	Resting SBP (mmHg)				LVM ($g \cdot m^{-2.7}$ height)			
	B	**95% CI**	***P***	**R^2**	**B**	**95% CI**	***P***	**R^2**
Model 1								
∆SMAi	**-18.0**	**-28.5, -7.4**	**0.001**	**0.17**	**-12.7**	**-18.6, -6.8**	**$6x10^{-5}$**	**0.24**
Female	-3.8	-8.3, 0.8	0.10		-3.2	-5.8, -0.6	0.02	
Model 2								
∆SMAi	**-16.0**	**-26.8, -5.2**	**0.004**	**0.22**	**-8.7**	**-14.0, -3.4**	**0.002**	**0.45**
Female	-4.1	-8.6, 0.4	0.07		-3.1	-5.3, -0.9	0.007	
BMI	0.3	-0.0, 0.6	0.06		0.4	0.3, 0.6	$1x10^{-6}$	
Model 3								
∆SMAi	**-16.5**	**-27.7, -5.3**	**0.004**	**0.24**	**-7.8**	**-13.4, -2.1**	**0.008**	**0.56**
Female	-4.0	-8.5, 0.4	0.08		-3.9	-6.1, -1.6	0.001	
BMI	0.3	0.0, 0.6	0.04		0.5	0.4, 0.7	$2x10^{-8}$	
Resting HR	0.1	-0.1, 0.3	0.26		-	-	-	
Resting SBP	-	-	-		0.0	-0.1, 0.2	0.54	

Multiple linear regression analysis to assess the independent influence of potential determinants of LVM and resting SBP. Further models (***Table 8***) showed that these associations were robust to adjustment for age, Tanner score, stroke volume and HOMA-IR (for LVM). BMI = body mass index; HOMA-IR = homeostatic model assessment of insulin resistance; HR = heart rate. With permission from: (4)

Table 8. Associations of postprandial superior mesenteric arterial blood flow response (∆SMAi) with systolic blood pressure (SBP) and left ventricular mass (LVM).

	Resting SBP				LVM			
	B	**95% CI**	***P***	**R^2**	**B**	**95% CI**	***P***	**R^2**
Model 4								
∆SMAi	**-12.0**	**-23.9, -0.9**	**0.048**	**0.23**	**-5.4**	**-9.9, -1.0**	**0.018**	**0.77**
Female	-3.8	-8.8, 1.3	0.141		-2.4	-4.5, -0.4	0.022	
BMI	0.3	0.0, 0.7	0.078		0.6	0.4, 0.7	$1.3x10^{-10}$	
Resting HR	0.2	-0.0, 0.4	0.106		-	-	-	
Resting SBP	-	-	-		0.2	0.0, 0.4	0.117	
Age	0.6	-0.9, 2.0	0.415		0.2	-0.4, 0.7	0.567	
Tanner score	0.9	-2.1, 4.0	0.545		1.1	0.0, 2.3	0.050	
Stroke volume	0.2	-0.3, 0.6	0.436		0.4	0.3, 0.6	$1.8x10^{-6}$	
HOMA-IR	-	-	-		-0.3	0.0, 0.7	0.051	
∆SBP (AUC)	-	-	-		-0.2	-0.4, 0.1	0.176	

Multiple linear regression analysis to assess the independent influence of potential determinants of LVM and resting SBP. AUC = area under the curve; BMI = body mass index; HOMA-IR = homeostatic model assessment of insulin resistance; HR = heart rate. With permission from: (4)

5.4. Discussion

5.4.1. Overview

Abnormal (blunted) ∆SMA after ingestion of a high-calorie liquid meal was associated with concentric LVH, increased LVM, higher resting BP, and hypertension in adolescents. These findings were independent of factors known to influence LVM (age, sex, pubertal status, BMI, insulin resistance, SV and BP). Perhaps most importantly, the associations were not influenced by variation in progression through puberty and therefore are unlikely to be explained by altered sex hormone levels, which are known to influence LVM.

5.4.2. Comparison with existing literature

Although this study was not designed to elucidate any mechanism causally linking postprandial vascular dysfunction in the gut with LVH, some evidence was presented in adolescents supporting a mechanism already detailed in rodents. Sartor *et al.* showed that under fasting conditions, blood supply to the gut is inhibited centrally by sympathetic vasomotor outflow from the rostro-ventrolateral medulla. Food ingestion normally suppresses the activity of these efferents via vagal feedback to the brainstem, resulting in increased blood flow to the gut.(24, 133) This feedback mechanism is mediated predominantly locally by gastric release of leptin and cholecystokinin as well as, possibly, other factors. The paracrine effects of gastric leptin are distinct from its systemic effects, which include raised sympathetic nervous activity and central nervous regulation of appetite and energy homeostasis. In rodents, obesity and a diet rich in lipids and carbohydrates have been shown to blunt the local, paracrine effects of leptin.(25) This reduces its vasodilatory effects in the gut, whilst possibly preserving vasoconstrictive effects in the limbs and on the augmentation of CO.(24, 133) It has been suggested that increased afterload caused by raised splanchnic vascular resistance in this context could promote development of hypertension and LVH.(125)

In this experiment, it was shown that adolescent obesity was similarly associated with blunting of normal postprandial vasodilatory responses. A possible explanation for this is that myogenic autoregulation of the SMA could have attenuated mesenteric vasodilation in overweight/obese adolescents, as resting BP was somewhat higher in this group. However, data from animal studies suggest that, rather on the opposite, myogenic autoregulation of the mesenteric arteries is impaired in obese rats.(134) Therefore, this explanation is considered unlikely. Interestingly, blunted ΔSMA was associated with raised LVM independently of resting BP or postprandial BP responses, suggesting that the explanation for this association is probably more complex than suggested previously.(24, 133) For example, disordered neurohumoral signalling that affects both vascular function in the gut and cardiomyocyte growth could mediate this association. This study was not designed to investigate such

possibilities. The partial independence of its findings from the degree of adiposity is consistent with the observation that postprandial vascular dysfunction in high-fat fed rodents normalises with low-fat diet irrespective of weight loss and suggests a role for abnormal diet in the pathogenesis of postprandial vascular dysfunction.(133) The high-calorie meal used in this experiment was designed to replicate the worst excesses of a modern diet. Further study will be needed to determine how altering diet composition affects the postprandial response.

5.4.3. Clinical implications

Vascular dysregulation was more common in overweight/obese individuals. This supports existing advice to reduce high-calorie food intake in adolescents, and is evidence for a potential new pathway linking obesity and LVH in young people. Notably, high BMI in a cohort of Swedish adolescents has been shown to be a particularly strong risk for future HF, with hazard ratios approaching 10 for those with a BMI above 35.(121) Further investigation of the mechanism behind the findings of the present study could, therefore, yield new opportunities for prevention of the cardiac and vascular consequences of poor diet and obesity in the young.

Indeed, this study demonstrated that adolescents with a blunted postprandial mesenteric blood flow response tended to be overweight, and were more likely to be hypertensive and have LVH. These are known, major risk factors for the development of CVD. This study was not designed to determine why they were linked to abnormal postprandial vascular responses, but the associations did not depend on a range of factors known to drive their development, such as adiposity or insulin resistance. This raises the possibility of a previously unrecognised mechanism underlying the development of hypertension and LVH in young people. Exploration of this could yield new diagnostic tools and even, perhaps, lead to interventions in the earliest stages of CVD. For example, vascular responses to a high fat, high sugar meal could be used to identify increased cardiovascular risk in young people before other, more established risk factors, are diagnosed, allowing for earlier preventative measures.

Interestingly, blunted vasoreactivity was associated with increased LVM independently of SBP. Thus, a simple mechanism for the association, acting through increased BP and, therefore, raised LV afterload, is unlikely. Other possibilities, such as deranged neurohumoral signalling, could be responsible and deserve further investigation.

Blunted postprandial mesenteric blood flow responses were associated with concentric LVH, but not other patterns of LVH. Although the relationship between patterns of LVH and underlying pathology is not fully understood,(135) concentric LVH in animal models arises largely as a compensatory mechanism to normalise LV wall stress in response to pressure overload. This would be consistent with this study's finding that blunted ΔSMA was related to increased resting BP and hypertension. However, relationships of blunted ΔSMA with LVMi and concentric LVH were not fully explained by resting BP status. Therefore, the mechanism of concentric LVH development in this context may be due to factors other than only increased LV afterload. Irrespective of the mechanism, abnormal mesenteric vascular function is an independent biomarker for a phenotype prone to LVH and, possibly therefore, to CVD.

The insight that hypertension is to a large part caused by raised sympathetic nervous activity has led to a number of therapeutic strategies. Historically, severe hypertension was treated by surgical disruption of the sympathetic nervous system of all abdominal organs, including the gut (radical splanchnicectomy). This was an effective treatment but was abandoned in the 1950s due to high surgical mortality and frequent postural hypotension, as well as the development of new therapeutics.(136) Of note, BP reductions were greater than those usually seen with renal sympathetic denervation alone. For example, BP was lowered by between 27/15 and 61/43 mmHg in 80% of patients, 5 years following surgery.(137) Renewed interest in renal sympathetic nerve ablation occurred recently with the development of non-surgical techniques but similarly, this has proven to be ineffective.(138) The question of why extensive sympathectomy was more effective than renal denervation has not been addressed adequately. In addition to renal sympathetic supply, the

splanchnic nerves supply the gut and other abdominal viscera. Together, these comprise one of the largest and most dynamic vascular beds in the body, able to command up to half of CO when fully activated but drawing relatively little at rest.(3) The presented data offer a novel potential explanation for the substantial decline in BP seen after splanchnicectomy and suggest that sympathetic signalling of the gut may have a fundamental role in the development of hypertension.

5.4.4. Strengths and limitations

Definitions of left ventricular hypertrophy

Accurate definition of LVH on the basis of MRI measures in childhood is challenging. No published paediatric reference ranges are adjusted for a power of height, and existing references are based on small populations. This and widespread variations in imaging and image segmentation techniques mean that current published MRI LVM normal values in adolescents are not a reliable reference. To address this issue, and recognising that the sample of normal adolescents in this study was larger than many such reference populations, a normal range for LVM was defined in this cohort, and adjusted for age and sex in order to minimise their influence on the normal distribution. Because it was partly recruited from an obesity clinic, this normal range was defined in a subpopulation with a normally distributed BMI range, as proposed previously.(123)

Allometric scaling

One of the key challenges in studying the effects of adiposity on haemodynamics is allometric scaling. Conventional methods to normalise for body size (e.g., indexing for BSA) do not account for the effects of obesity, i.e. disproportionately larger increase in adipose body mass (i.e., metabolically less active tissue) than in lean body mass, on physiological measures. Previous research has addressed this problem and provided appropriate indices to normalise SV, CO and LVM for the effects of obesity, which were used in this study.(128, 129) Importantly, statistical analysis was repeated using BSA as conventional standardisation factor for blood flow to show that the effects of

obesity on mesenteric blood flow regulation persisted, indicating that allometric scaling did not explain the adiposity-related disparities in sympathoinhibitory responses.

5.4.5. Conclusions

I. Abnormal (blunted) postprandial regulation of splanchnic vascular tone can be observed in otherwise healthy teenagers.

II. Obesity is associated with an increased likelihood of such an abnormal response.

III. A blunted postprandial mesenteric blood flow increase is associated with abnormal LVM and raised BP, independently of known determinants of LVH and high BP.

Chapter 6. Cardiovascular responses to food ingestion in Fontan physiology

Abstract

In univentricular (Fontan) physiology, peripheral and splanchnic vascular tone may be raised to counteract reduced CO and elevated central venous pressure (CVP), and thus maintain vital organ perfusion. This could negatively affect the normal cardiovascular response to food ingestion, where mesenteric vasodilation and a concurrent rise in CO are central. The following experiment sought to elucidate this using rapid cardiovascular MRI.

Thirty fasting subjects (50% healthy volunteers) ingested a standardised meal. Responses over ~50 min in MAP, CO and blood flow in all major aortic branches were measured and regional vascular impedance (Z_0) calculated. Differences from baseline and between groups were assessed by repeated-measures mixed models. Compared to the control group, Fontan patients had greater fasting Z_0 of the legs and kidneys, resulting in greater systemic Z_0 and similar MAP. They further had similar blood flow to the digestive organs at baseline, despite larger variation in mesenteric resistance. Postprandially, blood flow to the legs decreased in the control group but not in patients. Increases in CO and superior mesenteric blood flow were similar in both groups but the celiac response was blunted in patients. No significant differences in MAP responses were observed.

In conclusion, alterations in vascular tone to counteract adverse haemodynamics and raised hepatic afterload may blunt vasoreactivity in the legs and the celiac axis in Fontan physiology. Further study is needed to determine whether blunted celiac or mesenteric vasoreactivity is linked to deteriorating haemodynamics and poor prognosis in Fontan patients.

6.1. Background

6.1.1. Univentricular heart disease

Univentricular heart disease is a subset of CHD where either of the 2 ventricles is structurally or functionally absent. This can be due to atresia or hypoplasia of any of the 4 valves, abnormal septation of the heart, AV septal defect, or combinations of any of these pathologies. As biventricular surgical repair is usually not possible, prognosis is extremely poor. While univentricular CHD is highly heterogeneous in morphology, it can be grossly divided into phenotypes with an underdeveloped RV, and such with an underdeveloped LV (as well as substantially rarer lesions with a single ventricle of indeterminate morphology, and those where 2 ventricles are developed sufficiently, but associated anomalies preclude biventricular surgical repair). Although its incidence is rare, improved surgical and medical management has extended the life expectancy of patients with univentricular CHD substantially over the last few decades, making them a growing population.(139-141)

6.1.2. The Fontan circulation

Overview

The total cavo-pulmonary connection (TCPC), or Fontan circulation, is the standard approach for the palliation of univentricular CHD and has improved the long-term survival of patients substantially.(141) As this population grows and ages, the complications of the univentricular circulation become more prevalent and more pronounced.(140) A better understanding of its physiology is therefore crucial. The following section will outline the concept of the Fontan circulation. As univentricular CHD is a morphologically heterogenous and oftentimes complex group of malformations, certain aspects of this summary may not fully apply to certain anatomical subgroups. This includes pathologies with abnormal situs (e.g., azygos continuity), or those with abnormal AV or ventriculo-arterial connections.

Management – Stage 1

The morphology of the preserved ventricle and the associated lesions determine the initial management and have impact on long-term outcome. In the initial phase, i.e. immediately after birth, all patients with univentricular CHD require shunting on 2 levels in order to survive. Firstly, a defect of the atrial septum is needed to allow mixing of pulmonary venous with systemic venous blood. This is frequently present natively but can also be created by interventional means if required (balloon atrioseptostomy). Secondly, a shunt between the systemic and the pulmonary arterial vascular bed is needed. If necessary, this is can be achieved by preventing the ductus arteriosus from closing during the neonatal period (e.g., by prostaglandin infusion or stent implantation).(139)

In tricuspid atresia, for instance, where the RV is functionally absent due an anomaly of the tricuspid valve, mixed blood is ejected into the aorta by the intact LV. From there, blood shunts into the lungs and subsequently mixes with systemic venous blood in the atria. In a different scenario, e.g., in hypoplastic left heart syndrome (HLHS), the preserved RV pumps mixed blood into the PA, from where part shunts into the aorta. In all scenarios, hypoxaemia and cyanosis are physiological hallmarks due to the parallel configuration of the pulmonary and the systemic circulation. While the described measures usually make initial survival possible irrespective of the underlying condition, the subsequent surgical strategy varies by anatomy.

The following management depends on the morphology of the preserved ventricle and the size and position of the great arteries. In lesions with a hypoplastic RV (e.g., tricuspid atresia), the LV and the aorta are usually developed normally. This allows for a normal systemic circulation, while the pulmonary circulation can be compromised, e.g., when the tricuspid valve and/or the RV and/or the pulmonary valve are hypoplastic, and no ventricular septal defect (VSD) exists. To overcome this, a shunt is usually sited between the systemic circulation (e.g., the subclavian artery) and the PA to allow for blood to be oxygenated. Antegrade blood flow into the PA may also be normal

(e.g., when an unrestrictive VSD exists and the pulmonary valve is unobstructed). In such cases, banding of the main PA is performed instead of siting an aortopulmonary shunt in order to throttle systolic PA pressure (PAP) to sub-systemic levels.(139)

In the inverse scenario (e.g., in HLHS), the RV and pulmonary trunk are normal, whereas the LV and the aorta are hypoplastic. As the systemic circulation is a high resistance circuit, an active pump is indispensable in order to produce sufficient perfusion pressure to maintain organ function. Therefore, the RV is repurposed into a systemic ventricle. This is achieved by the Norwood procedure, where the main PA is disconnected from the branch PAs and modelled into a ‘neo-aorta’ using prosthetic material as well as the hypoplastic native ascending aorta and the aortic arch. The disconnected PA are subsequently connected to the RV using a shunt (this is to avoid diastolic runoff into the lungs, which is more frequently observed with aortopulmonary shunts, and can cause hypotension).(139)

In either scenario, the atrial septum is usually excised surgically during the same procedure in order to allow for unrestricted shunting between the atria. This initial management is commonly referred to as ‘stage 1-palliation’.

Management – Stage 2

In these scenarios, a substantial proportion of blood is shunted between the systemic and the pulmonary circulation. This causes volume loading of the systemic ventricle, which leads to progressive dilation and deteriorating function. Additionally, in lesions with an absent LV, the remaining RV is by nature pressure-overloaded, as it is not developed to supply the systemic circulation. Therefore, unloading of the remaining, systemic ventricle is paramount to secure long-term survival, and to improve blood oxygen saturation.

Once pulmonary vascular resistance (PVR) has decreased (usually between 3 and 6 months of age), this is usually achieved by connecting the superior vena

cava directly to the PA and by taking down the RV-to-PA or the aortopulmonary shunt surgically. This is called Glenn procedure, or bidirectional cavo-pulmonary connection.(139)

Management – Stage 3

While the Glenn procedure improves volume-loading of the systemic ventricle, there is still mixing of deoxygenated blood recirculating from the inferior vena cava (IVC) with pulmonary venous blood. Because the lower body grows more in proportion to the upper body during the first years of life, hypoxaemia usually worsens as the child grows in length, and proportionally more deoxygenated blood returns from the lower body. Moreover, the systemic ventricle remains partially volume-loaded. Therefore, the IVC is connected to the pulmonary vascular bed in a third procedure. This completes the total cavo-pulmonary connection (TCPC), or Fontan circulation, named after one of the surgeons who described this technique initially as a concept to palliate patients with tricuspid atresia.(141)

While the surgical technique has undergone a series of modifications, the physiological concept remains unchanged: blood flows passively into the lungs (i.e., a low pressure-system), hence bypassing the functionally absent ventricle. By contrast, the remaining ventricle supplies the systemic circulation (i.e., a high pressure-system). The main driving forces for pulmonary blood flow are raised central venous pressure (CVP), negative inspiratory pressure, low end-diastolic pressure of the systemic ventricle, as well as gravity (for the upper body), and the skeletal muscle pump (for the lower body).(140)

Physiological consequences of the Fontan circulation

Although the TCPC ensures normal oxygen saturation, it comes at significant haemodynamic cost.(140) Firstly, the systemic and pulmonary vascular beds are added in series, and both contribute to the non-pulsatile component of systemic vascular impedance (Z_0; ***Figure 19***). This increases afterload and may partly explain the lower CO usually seen in these patients.(140, 142)

Secondly, in the absence of a sub-pulmonary ventricle, increased CVP becomes the main driving force for pulmonary blood flow (***Figure 19***). A crucial determining factor of pulmonary blood flow is therefore PVR, which has to be low in order for the Fontan circulation to function. However, PVR is frequently increased in this population, either as a late consequence of aorto-pulmonary shunt flow in early childhood (through vascular remodelling of the pulmonary arterioles), or due to hypoplasia of the PAs, which is often seen in patients with HLHS. Excessive elevation of CVP frequently results, with long-term consequences for virtually every organ.

As MAP is usually normal in these patients, elevated CVP results in reduced organ perfusion pressure. Consequently, vasoconstriction of the limbs and the splanchnic vascular bed has been suggested as a possible compensatory mechanism to ensure perfusion of vital organs.(143, 144) By contrast, autoregulation of the liver has been shown to counteract systemic (and thus, hepatic) venous congestion by inducing a shift from portal venous to hepatic arterial blood flow.(145, 146)

Another critical factor determining pulmonary blood flow in the Fontan circulation is diastolic pressure of the systemic ventricle. Diastolic dysfunction is a frequent complication in Fontan patients (e.g., due to chronic volume loading during the early stages, or due to concomitant aortic coarctation). Other factors that influence function of the Fontan circulation but are frequently abnormal in this population (e.g., due to frequent surgery) are:

- heart rhythm (e.g., poor ventricular filling due to AV-dissociation);
- AV-valve competency;
- respiratory function (i.e., poor perfusion resulting from poor ventilation);
- motility of the diaphragm (e.g., impaired vital capacity), and
- patency of the pulmonary veins.

Normal

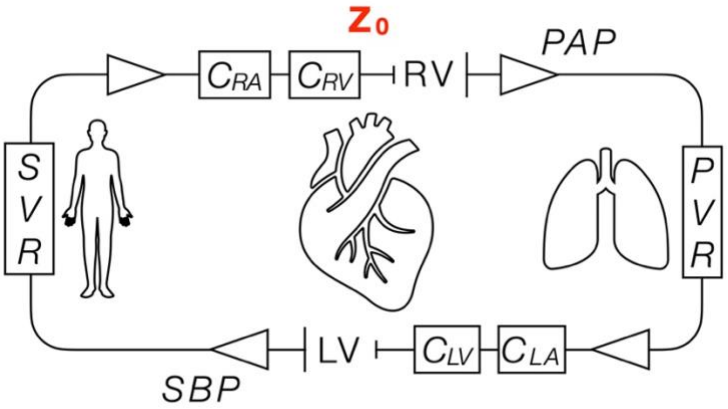

Fontan

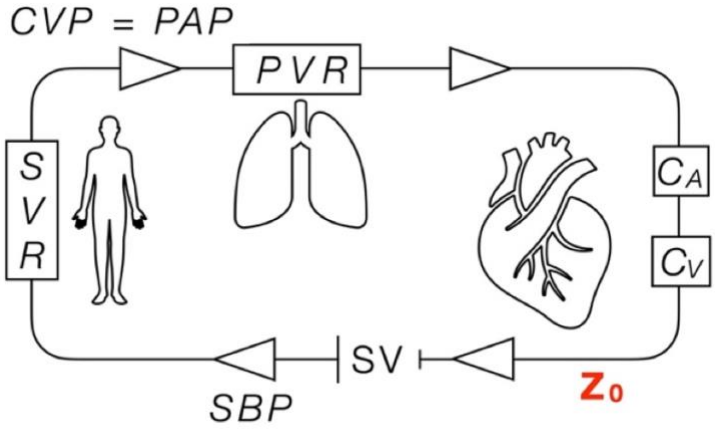

Figure 19. Diagrams of normal (biventricular) and of Fontan haemodynamics.
Due to the addition in series of the pulmonary vascular bed to the systemic circulation, systemic vascular impedance Z_0 reflects both, PVR and SVR in the Fontan circulation (as well as pressure in the pulmonary venous atrium). By contrast, Z_0 reflects mostly SVR in the normal circulation, given that RA pressure is normally negligible.
A = atrial; C = compliance; LA: left atrial; LV = left ventricular; PAP = pulmonary arterial pressure; PVR = pulmonary vascular resistance; RA = right atrial; RV = right ventricle; SBP = systolic blood pressure; SV = single ventricle; SVR = systemic vascular resistance; V = ventricular; Z_0 = vascular impedance.

Long-term complications

A number of long-term complications result from the Fontan physiology. Exercise capacity is typically reduced and declines progressively in this population.(147, 148) Progressive failure of the single, systemic ventricle over time, as well as impaired diastolic function are main contributing factors for this.(148) Skeletal muscle mass has also been shown to be decreased in this population. However, whether this is a consequence of physical inactivity, or a result of poor peripheral perfusion, has not yet been resolved.(144)

Chronic elevation of CVP has been linked to abnormal lymphatic drainage. This has been identified as the main mechanism for plastic bronchitis, one of the most common causes of death in this population, characterised by deposits of proteinaceous material in the bronchi. Systemic venous congestion and failure of the lymphatic system have also been identified as key mechanisms for protein-losing enteropathy (PLE), another major cause of attrition in this population.(142) However, this pathology is still poorly understood. In addition to chronic venous and lymphatic congestion (‘backward failure’), raised mesenteric vascular resistance has been proposed as possible mechanism (‘forward failure’). Abnormal glycosylation, and inflammation have also been discussed as putative contributing factors.(149)

6.1.3. Purpose of the study

To test the hypothesis that in Fontan patients, the normal cardiovascular responses to food ingestion are attenuated due to limited ability to increase CO, or by overriding mesenteric vasoconstriction.

6.1.4. Publication

Findings from this chapter were published as original article in the *American Journal of Physiology: Heart and Circulatory Physiology*.(5)

6.2. Methods

6.2.1. Subjects

Subjects were enrolled between November 2016 and March 2018. Fontan patients were recruited from a cardiac outpatient clinic (Bart's Heart Centre, London, UK). Local hospital staff volunteered as healthy controls.

6.2.2. Study protocol

The study protocol was carried out as described in 3.1. Oxygen saturation was measured by pulse-oximetry in patients. The size of the study meal and all of its constituents was reduced by ~40% for this study (energy 925 kcal, total fluid volume ~200 mL). This was considered sufficient to demonstrate cardiovascular vascular changes, while improving the acceptability of the meal in adult subjects.

6.2.3. Imaging

Aortic blood flow was acquired at sinus level and proximal to the iliac bifurcation, and regional blood flow was acquired for the common carotid and vertebral arteries, the celiac artery, the SMA, and each renal artery, as described in 3.2. Due to the complex and heterogenous anatomies present in this population, ventricular mass and function were not measured.

6.2.4. Statistics

Data are presented as mean (SD) and were compared by *t*-test if normally distributed, or presented as median (IQR) and compared by Mann-Whitney-U test otherwise (except X^2 for sex). Reported CO, regional blood flow and SV were all indexed for BSA. In this study, the non-pulsatile (at 0 Hz) component of vascular input impedance (Z_0) was used, rather than resistance, as in the Fontan population, systemic pressure-flow relationships also included pulmonary vascular resistance (PVR). Nevertheless, calculation of Z_0 is similar to calculation of resistance.(150) Global vascular impedance index was calculated as MAP divided by indexed CO. Regional vascular Z_0 was obtained by dividing MAP by indexed regional blood flow. In regions supplied by more

than one artery (e.g., the head), Z_0 was calculated from the sum of all flow data measured in the supplying vessels. This assumes that MAP in major vessels was the same as brachial MAP, which is in keeping with previous invasive studies that compared MAP in the aorta with MAP in the radial, brachial and femoral arteries.(151) Repeated measures mixed models to assess quantitative changes in physiological data over time (as described in 3.5.) included presence of Fontan circulation, sex and BMI as covariates.

6.3. Results

6.3.1. Study population and resting (fasting) physiology

In the patient group, 12 (80%) had undergone total cavo-pulmonary connection with an extracardiac conduit, with the remainder having received the classic (atrio-pulmonary) Fontan procedure. Oxygen saturation level was 94% (IQR: 93-95%) in the Fontan group.

At baseline, there was no statistically significant difference in MAP between groups. However, Fontan patients had significantly higher systemic Z_0. Although SVi was significantly lower in Fontan subjects, their resting HR was significantly higher, resulting in only a trend towards lower COi compared to controls (***Table 7***).

Fontan patients had significantly greater baseline regional Z_0 in the kidneys (~1.3x) and legs (~1.7x), compared to controls. This resulted in a significantly lower proportion of blood flow distribution to the legs, but no statistically significant difference in renal perfusion (***Table 9***). In all other territories, relative blood flow and vascular Z_0 showed no statistically significant difference between groups. Three patients took diuretics and/or angiotensin converting enzyme inhibitors. Adjustment for such therapy had no significant impact on the regression analysis.

Table 9. Baseline (fasting) physiology and population data.

	Control (n=15)	Fontan (n=15)	*P*-value
Age (years)	32.1 (29.1, 38.6)	27.6 (21.8, 34.6)	.059
Female	7 (46.7%)	5 (33.3%)	.456
BSA (m^2)	1.76 (1.64, 1.96)	1.79 (1.68, 1.93)	.885
COi ($L \cdot min^{-1} \cdot m^{-2}$)	2.8 ± 0.4	2.6 ± 0.6	.067
Heart rate ($beats \cdot m^{-1}$)	62.8 (56.2, 67.6)	73.3 (64.7, 80.5)	.007
SVi ($mL \cdot min^{-1} \cdot m^{-2}$)	44.1 (40.1, 51.4)	35.7 (28.3, 41.3)	.008
MAP (mmHg)	85 ± 6	86 ± 7	.695
Systemic Z_0 ($WU \cdot m^2$)	30.3 ± 4.5	35.2 ± 10.1	.048
Regional blood flow at baseline ($L \cdot min^{-1} \cdot m^{-2}$)			
Head	0.59 (0.51, 0.71)	0.52 (0.35, 0.75)	.458
Legs	0.67 (0.56, 0.76)	0.40 (0.25, 0.54)	<.001
Celiac	0.45 (0.40, 0.56)	0.38 (0.24, 0.61)	.800
SMA	0.15 (0.11, 0.20)	0.15 (0.06, 0.28)	.548
Kidneys	0.43 (0.36, 0.50)	0.56 (0.49, 0.65)	.008
Distribution of blood flow at baseline (% of CO)			
Head	19.2 (18.1, 24.7)	21.4 (15.8, 27.7)	1.000
Legs	23.1 (19.7, 25.7)	16.2 (9.9, 19.2)	.029
Celiac	13.9 (9.7, 20.6)	17.0 (16.2, 17.7)	.662
SMA	5.2 (4.5, 7.5)	5.4 (1.9, 10.0)	.694
Kidneys	19.7 (17.5, 24.5)	17.5 (11.7, 23.7)	.206
Vascular impedance (Z_0) by compartment ($WU \cdot m^2$)			
Head	145 (125, 168)	154 (108, 251)	.432
Legs	130 (110, 147)	223 (148, 363)	<.001
Celiac	224 (143, 358)	177 (167, 212)	.836
SMA	549 (433, 737)	658 (324, 1,607)	.576
Kidneys	154 (138, 178)	195 (168, 216)	.008

BSA = body surface area; CO = cardiac output; MAP = mean arterial pressure; SMA= superior mesenteric artery; SV = stroke volume; WU = Wood unit. Modified with permission from: (5)

6.3.2. Postprandial global haemodynamic responses

All subjects completed the protocol without adverse events. Following ingestion of the meal, systemic Z_0 dropped significantly after 20 min with no statistically significant difference between groups. In both groups, systemic Z_0 started to normalise after 50 min with no significant difference compared to baseline. Correspondingly, there was a rise in COi with a peak observed at 40 min. This response was not statistically different between groups and attributable to an increment in HR in both. SVi and MAP did not change significantly in either group after ingestion of meal (***Figure 20***).

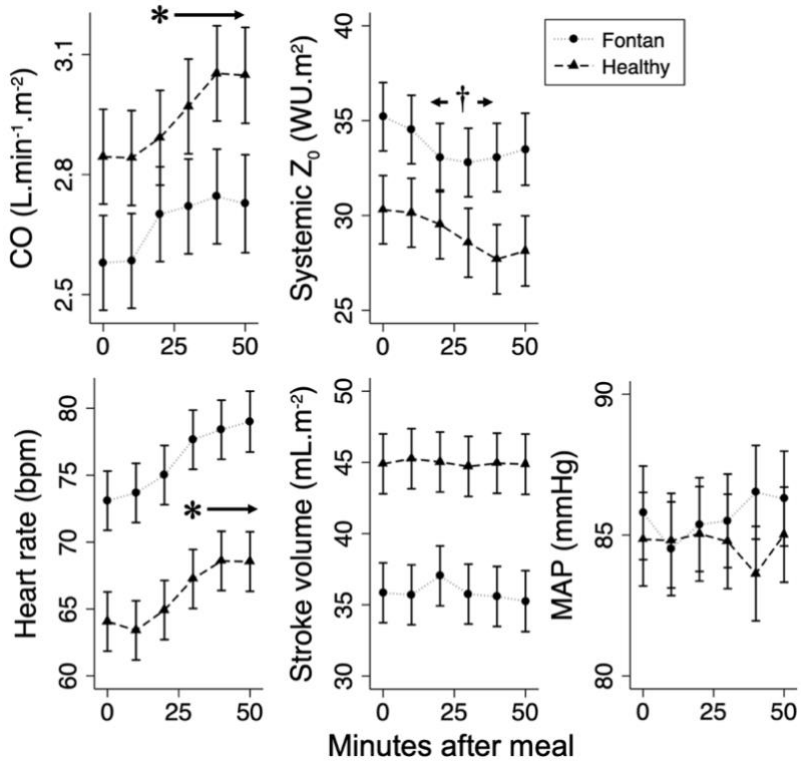

Figure 20. Global haemodynamic response (mean ±SE).
Responses to the meal over time and the impact of the Fontan circulation were assessed by repeated measures mixed models. *P<0.05 and †P≤0.001 for changes in overall response with respect to baseline. Adjustment for age, sex and body mass index had no significant effect on the response. CO = cardiac output; MAP = mean arterial pressure; WU = Wood unit; Z_0 = vascular impedance. With permission from: (5)

6.3.3. Postprandial changes in regional blood flow and vascular impedance

Superior mesenteric vascular Z_0 decreased significantly within 10 min and further decreased until the end of the experiment in both groups (***Figure 21***). This was associated with a similar increase in SMAi blood flow in both groups (***Figure 22***). It should be noted that the increase in SMAi blood flow was greater than the increase in COi, indicating that blood flow was redistributed from other compartments.

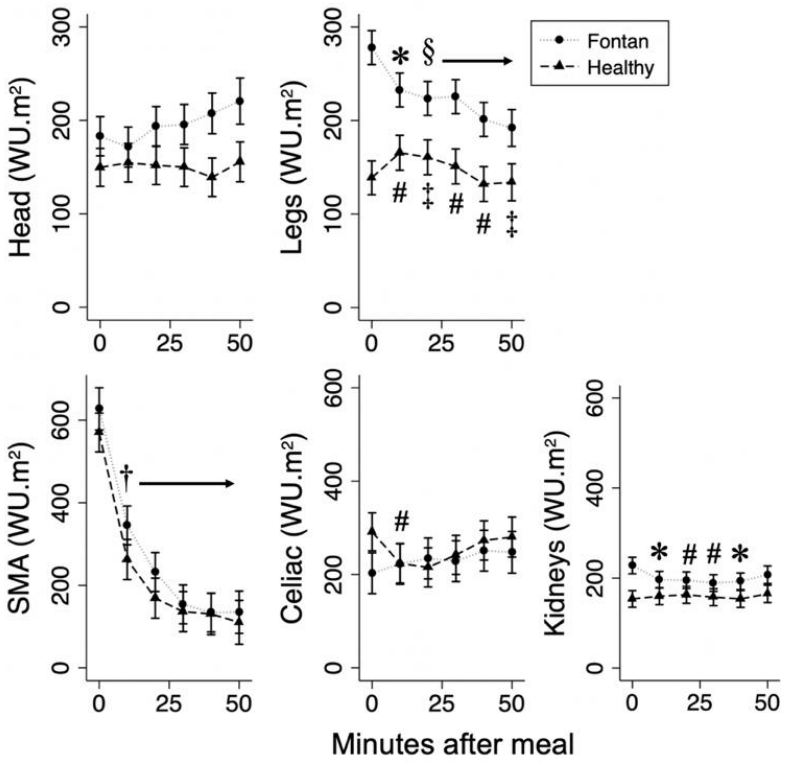

Figure 21. Changes in indexed regional vascular impedance (Z_0; mean ±SE). Responses to the meal over time and the impact of the Fontan circulation were assessed by repeated measures mixed models. Three outliers with excessive baseline SMA resistance were excluded in the Fontan group. **P*<0.05, $^{\S}P \leq 0.01$ and $^{\dagger}P<0.001$ for changes in overall response with respect to baseline; $^{\#}P<0.05$ and $^{\ddagger}P \leq 0.01$ for differences in responses between groups. Adjustment for age, sex and body mass index had no significant effect on the response. SMA = superior mesenteric artery; WU = Wood units. With permission from: (5)

In the celiac artery, there was a decrease in regional Z_0 at 10 min in the control group associated with an increase in blood flow (***Figure 21***). This response was not seen in the Fontan group. After 40 min, celiac blood flow was lower than baseline in both groups (***Figure 22***).

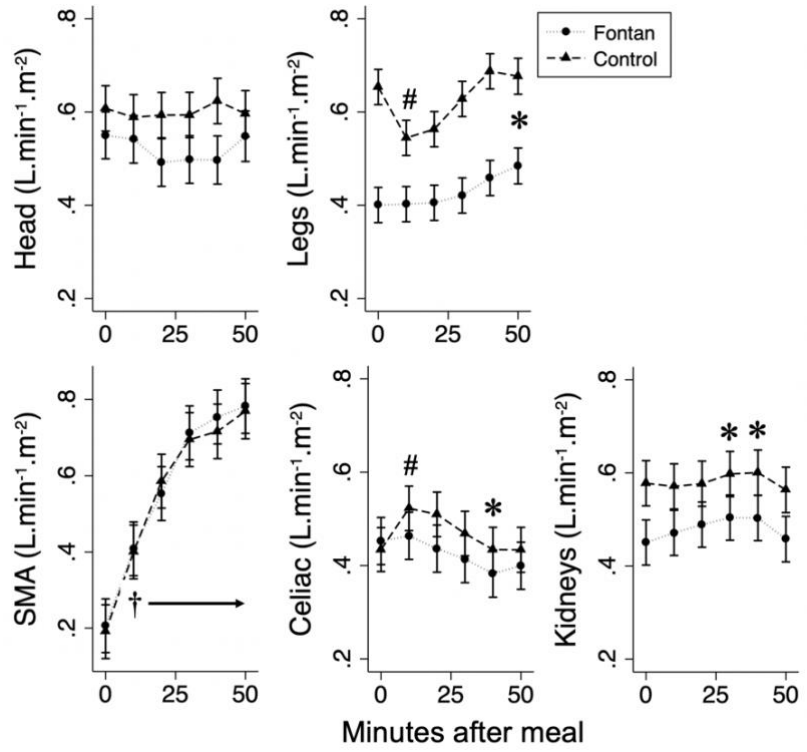

Figure 22. Regional indexed blood flow responses (mean ±SE).
Responses to the meal over time and the impact of the Fontan circulation were assessed by repeated measures mixed models. **P*<0.05 and †*P*<0.001 for changes in overall response with respect to baseline; #*P*<0.05 for differences in responses between groups. Adjustment for age, sex and body mass index had no significant effect on the response. SMA = superior mesenteric artery. With permission from: (5)

Haemodynamic responses in the lower limbs differed significantly between groups. In the Fontan group, lower limb Z_0 had decreased significantly from 10 min onwards (***Figure 21***). As a result, blood flow was significantly higher than baseline by 50 min (***Figure 22***). By contrast, lower limb Z_0 increased initially in

the control group, leading to a transient drop in blood flow (***Figure 21*** *&* ***22***). In this group, lower limb Z_0 and blood flow returned to baseline levels by the end of the experiment.

There was also a small but significant decrease in renal Z_0 and an increase in renal blood flow in both groups after meal ingestion (***Figure 21*** *&* ***22***). In the cranial vessels, no significant change in Z_0 or blood flow was seen.

6.3.4. Responses in individual Fontan patients

The responses of individual Fontan patients are shown in ***Figure 23.*** Due to wide variation between individual responses, only limited conclusions are possible. SMA flow increased in all patients, but the magnitude of this rise varied widely. Patients with a history of PLE tended to have lower SMA blood flow at baseline and a slower postprandial increase. However, this pattern was also seen in some subjects without history of PLE. The magnitude of the SMA flow increase was not lower in patients with a history of PLE than in those without.

Another common response was an increase in renal flow, but this was not seen as consistently. By contrast, the responses in celiac blood flow were highly heterogenous and did not seem to follow any pattern.

A noteworthy finding was the presence of 2 patterns of responses in leg blood flow: while subjects with lower flow at baseline tended to exhibit a gradual increase, patients with greater resting flow were more likely to show an initial decrease, followed by a decrease later in the experiment to baseline levels or above.

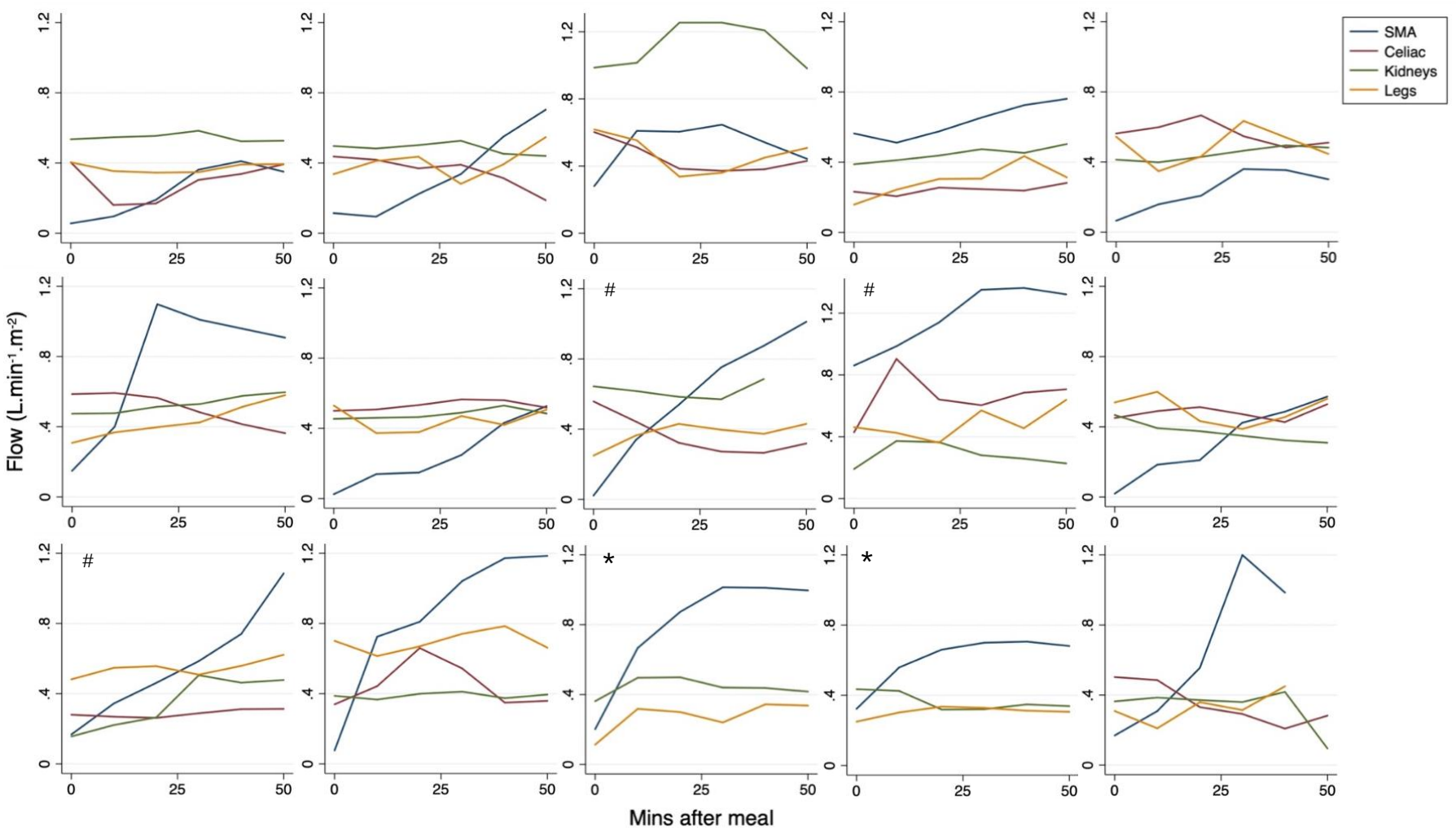

Figure 23. Cardiovascular responses in individual Fontan patients (truncated at 50 min).

*Abnormal situs and no typical celiac artery to measure flow from; #history of protein-losing enteropathy. SMA = superior mesenteric artery.

6.4. Discussion

6.4.1. Overview

This study employed the protocol validated in the previous chapters to investigate the cardiovascular responses to a meal in Fontan patients compared to a control group. The main findings were that Fontan patients had (i) increased baseline systemic, renal and lower limb Z_0, and (ii) similar global haemodynamic responses, but blunted celiac and lower limb vascular responses to food ingestion.

6.4.2. Comparison with existing literature

At baseline, systemic Z_0 in patients was greater than in the control group. This was expected, as in Fontan physiology, Z_0 includes PVR as well as SVR due to their addition in series. This is in contrast to normal subjects in whom $Z_0 \approx$ SVR (assuming low RAP). As systemic Z_0 is one of the primary components of cardiac afterload, these data partly explain the reduced SV seen in Fontan patients. Although reduced SV was partially compensated for by an increase in HR, there was a trend for lower CO in Fontan patients.

The present findings suggest that this may be compensated for by regional increases in vascular resistance, in keeping with previous research.(143, 144) However, this must be interpreted in the context of the fact that this experiment measured regional vascular impedance (Z_0), rather than vascular resistance. Similar to global systemic Z_0, regional Z_0 also includes a component of PVR in the Fontan circulation. It can be shown that in Fontan patients, regional Z_0 approximates to regional vascular resistance scaled by [(SVR+PVR)/SVR]. Using data from normal controls in this study as reference, this ratio could also be estimated as $Z_{0\,(Fontan)}/Z_{0\,(Control)}$ (i.e., 35.2/30.3 ≈ 1.16). Normalisation of regional Fontan Z_0 measures for this factor may allow for more meaningful comparison with corresponding measures from normal subjects (***Table 10***). This shows that after normalisation, lower limb Z_0 remains elevated in Fontan patients, supporting vasoconstriction of the legs. This is in keeping with

previous research and may reflect a mechanism to prioritise blood flow to more important vascular beds.(143) Other authors found links between diminished muscle mass of the legs and poor perfusion of the extremities, possibly as a consequence of physical inactivity.(144) While the direction of the causal link between muscle mass and limb perfusion, if any, has yet to be fully determined, it is possible that poorer vascularity of the legs due to sarcopenia, possibly caused by lack of exercise, explained the poor perfusion of the lower extremity in the present population.

Table 10. Normalised Fontan vascular impedance versus control subjects.

	Control (n=15)	Fontan (n=15)	*P*-value
Head	145 (125, 168)	132 (93, 216)	.432
Legs	130 (110, 147)	191 (127, 312)	<.001
Celiac	224 (143, 358)	152 (144, 183)	.836
SMA	549 (433, 737)	566 (279, 1,384)	.576
Kidneys	154 (138, 178)	168 (145, 186)	.008

Fasting regional vascular resistance ($WU \cdot m^2$) was approximated in Fontan patients by dividing MRI-measurements of Z_0 by 1.16 (obtained by $Z_{0\ (Fontan)}/Z_{0\ (Control)}$). This was done in order to normalise for pulmonary vascular resistance, which is part of Z_0 in Fontan patients. Data are presented as median (IQR). SMA = superior mesenteric artery; WU = Wood unit. With permission from: (5)

Similar to the legs, the raised Z_0 demonstrated in the renal compartment could be explained by vasoconstriction secondary to neurohumoral activation, as seen in other states with low CO, such as heart failure.(144) However, the normalised renal Z_0 (***Table 10***) was only slightly higher in Fontan patients, suggesting that this finding may also be partly explained by raised CVP in this group. By contrast, findings from this experiment suggest vasodilation of the celiac axis in Fontan patients. This may be due to a decrease in hepatic arterial resistance, which has been described as a possible mechanism to counteract hepatic congestion in the Fontan circulation.(145, 146, 152) Dynamic regulation

of regional vascular resistance is a central element of postprandial physiology.(3, 4) Therefore, this study tested vasoreactivity in Fontan patients with a meal.

Globally, no significant differences were found in the haemodynamic response to food ingestion, with a similar increase in CO and decrease in systemic Z_0 observed in both groups. By contrast, regional responses differed significantly. In the control group, there was an early increase in lower limb Z_0 and an associated fall in lower limb blood flow, with a slow recovery back to baseline. This suggests redistribution of blood flow from the legs to the gut, as described previously.(7) Conversely, in Fontan patients, lower limb Z_0 fell in response to the meal, leading to a modest but steady increase in lower limb blood flow. Interestingly, this response was seen predominantly in patients with lower blood flow at baseline, whereas patients with greater fasting blood flow showed a response that was more similar to that of the control group.

This appears to align with previous reports showing a biphasic vascular response of the legs in humans.(7, 153) In the normal population, early postprandial vasoconstriction of the limbs is driven by increased sympathetic activity, whereas late vasodilation has been linked to humoral responses, such as insulin secretion.(153-155) In the present experiment, Fontan patients already showed signs of vasoconstriction of the legs at baseline and therefore, may have been unable to increase sympathetic vasoconstriction any further. Analysis of the individual responses in the patient group supports this interpretation. Blunted responsiveness to vasoconstrictive signalling could have unmasked the effect of humoral vasodilators released in response to a meal. Several studies have shown that gut-released hormones are potent peripheral vasodilators and, without a counteracting increase in sympathetic tone, cause a significant drop in vascular resistance, even in non-digestive territories.(125, 156) This appears to be one of the causes of postprandial hypotension in patients with autonomic dysfunction.(82, 154, 155) It is possible that a similar mechanism explains the presented findings and could increase the risk of postprandial hypotension in this population, especially as they age.(157) This

may be particularly true in more realistic situations where subjects are not in supine position.

Further evidence of an abnormal vascular response to food ingestion was seen in the celiac axis, where Fontan patients did not show the early postprandial fall in celiac Z_0 (and the associated increase in blood flow) seen in the control group. As noted previously, the presented data suggest that the celiac vascular bed may already be vasodilated in Fontan patients at baseline. This may explain the lack of a further decrease in celiac Z_0 in this group. It has been shown previously that fasting celiac resistance predicts future PLE.(158) Future research could address whether abnormal celiac vasoreactivity provides additional prognostic information compared to resting celiac Z_0 alone.

Interestingly, mesenteric vascular responses were preserved in this Fontan population, contrasting previous ultrasound-based studies showing greater vascular resistance under fasting conditions.(159, 160) This finding could be explained by the relatively well-compensated clinical condition and young age of this study's population, compared to previous experiments, which focused on patients with PLE. Furthermore, previous studies typically assessed fasting physiology only, and were limited by their use of Doppler ultrasound which does not provide reliable or absolute measures of blood flow or vascular resistance. Nevertheless, decreased mesenteric blood flow has been proposed as a key mechanism causing PLE, one of the most serious long-term complications of the Fontan palliation.(142, 149) Such derangement has been suggested to promote leakage of chyle into the intestinal lumen via reduced perfusion of the intestinal mucosal layer. While the abnormalities in blood flow demonstrated in this chapter may not be clinically relevant, its findings could help generate new hypotheses for future research and perhaps support the development of new markers for clinical practice. Further longitudinal studies of larger populations of Fontan patients are needed to determine whether abnormal mesenteric vascular resistances and/or vasoreactivity may be linked to long-term complications, such as PLE, in a subset of patients.

6.4.3. Limitations

An important point to note is that the observed increase in SMA blood flow was greater than explained by the increase in CO and the decrease in leg perfusion alone. This suggests redistribution of blood flow from vascular beds not assessed in this protocol, such as the arms, the inferior mesenteric artery, as well as bronchial arteries and aorto-pulmonary collaterals in Fontan patients. Future research should include these regions to assess their role in the Fontan circulation.

All subjects underwent MRI in supine position. This could have influenced cardiac loading conditions. As this study was non-invasive in design, central venous (Fontan) pressure was not measured and therefore, vascular resistance *per se* not assessed. However, literature research showed no evidence suggesting that CVP, PAP or pulmonary capillary wedge pressure would change following ingestion of a meal. Therefore, Z_0 was assessed as an estimate of vascular function in this group. Furthermore, it is unlikely that the brief time (1-2 min) that the subjects sat up to ingest the meal affected the results of this experiment as imaging was resumed ~7-10 min after ingestion. It is likely that, by this time, the acute effects of the brief period of sitting should have mostly subsided.

The formula used to calculate Z_0 relied on the assumption that MAP is constant throughout the examined body compartments. While efforts were undertaken to rule out any vascular abnormalities that could have caused regional variations in MAP (e.g., kinking or stenosis), such lesions could, in theory, have confounded findings if undetected. While abnormal vascular tone was demonstrated for some compartments, this study may have been underpowered to detect weaker signals in others.

6.4.4. Conclusions

I. Under fasting conditions, Fontan patients showed vasoconstriction of the legs and kidneys, as well as possible vasodilation of the celiac axis.

II. Consequently, there was blunted postprandial vasoreactivity of the legs and the celiac axis in Fontan patients, compared to normal controls.

III. By contrast, both, fasting and postprandial mesenteric vascular tone was similar between groups.

Chapter 7. Discussion and future perspective

7.1. Summary of findings

Using a newly developed dynamic MRI protocol, it was shown that the ingestion of food led to a pronounced drop in mesenteric vascular resistance, and that this was compensated for primarily by a rise in CO, with no significant redistribution occurring from other compartments.

In order to investigate a link between impaired mesenteric vasoreactivity and indicators of cardiovascular risk previously described in animals, the proposed protocol was conducted in normal weight and overweight adolescents. Irrespective of body weight, blunted postprandial mesenteric vasoreactivity was associated with raised SBP and greater LVM. While overweight/obesity increased the likelihood of such an abnormal response, this association was independent of other factors known to influence these variables, such as pubertal stage, obesity, insulin resistance, and resting BP.

Abnormal vascular resistance of the limbs and the intestine has been described in Fontan-palliated patients with univentricular CHD, possibly in order to maintain organ perfusion in the presence of low CO and chronic venous congestion. It was hypothesised that this mechanism could interfere with the described cardiovascular responses to feeding. Using the established protocol, vasoconstriction of the legs and kidneys, as well as possible evidence of vasodilation of the celiac axis were found in fasting Fontan patients compared to controls. While both, their fasting and their postprandial mesenteric resistance were similar to normal volunteers, Fontan patients had abnormal responses of the celiac axis and the lower limbs.

The presented research was the first to conduct an oral challenge in an MRI environment to study cardiovascular physiology comprehensively and dynamically in humans. This approach was demonstrated to be safe and overall well-tolerated.

7.2. Discussion of results

7.2.1. Comparison of findings between chapters

In order to allow for meaningful comparison between the vascular responses of adolescents and those of adults, resistance was recalculated in adolescents using BSA for indexation (***Figure 24***). Fasting resistance in the SMA (570 ± 233 *vs.* 618 ± 505 WU.m^2, *P*=0.73), the legs (140 ± 46 *vs.* 125 ± 45 WU.m^2, *P*=0.26), the celiac artery (291 ± 129 *vs.* 272 ± 199 WU.m^2, *P*=0.74), and the kidneys (154 ± 33 *vs.* 153 ± 62 WU.m^2, *P*=0.96) did not differ significantly between adults and adolescents, and neither did mean BP (82 ± 6 *vs.* 85 ± 6 mmHg, *P*=0.12).

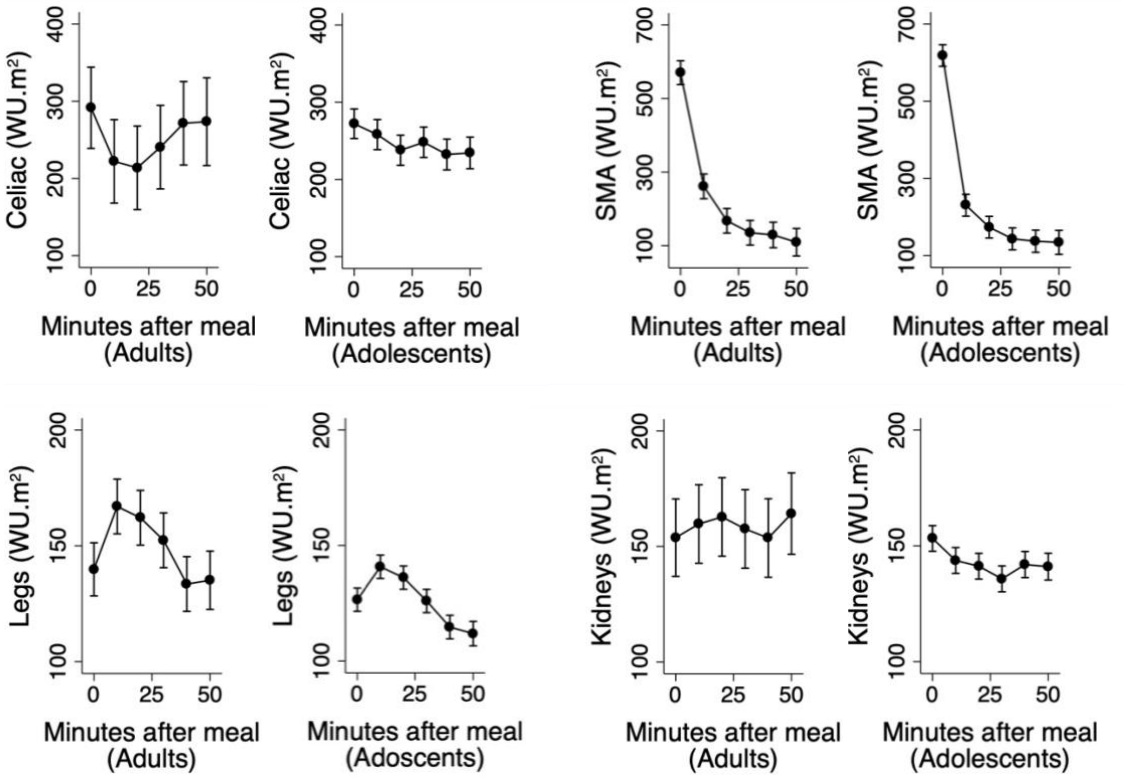

Figure 24. Comparison of vascular responses in 4 compartments in adults *vs.* in adolescents.

Postprandial responses in SMA blood flow were comparable (3- to 4-fold decrease from baseline) between all 3 populations (incl. Fontan patients), despite the lower calorie load used in the Fontan experiment. This raises the possibility that the type of nutrients and the consistency of the meal may be

more important to the magnitude of mesenteric blood flow increases than the total calorie load.

CO increases were also comparable between experiments (~25% increase from baseline). This was driven almost exclusively by an increase in HR in all study populations – adults, adolescents, and Fontan patients. Interestingly, this increase was observed somewhat later in control subjects in the Fontan study (Chapter 6. Cardiovascular responses to food ingestion in Fontan physiology) than in the others. The greater calorie load administered in the first 2 experiments may have triggered a greater sympathetic response, and thus, an earlier rise in CO compared to the last experiment.

A finding that was consistent across experiments was that resistance in the cranial vessels did not change significantly after the meal. By contrast, an important and seemingly inconsistent finding that deserves attention is that in adolescents (Chapter 5) and in normal controls in the Fontan study (Chapter 6), resistance in the legs rose postprandially, whereas in subjects scanned for the first experiment (Chapter 4), it did not. Similarly, in the celiac artery, an early drop in resistance was observed in normal controls in the Fontan study, followed by an increase to levels somewhat below baseline, whereas, in adolescents, a steady decrease was seen, and in adults in the first study no significant changes were recorded at all (***Figure 24***). A number of possible explanations for this are proposed.

As can be seen in ***Figure 21***, the magnitude of vasoconstriction in the legs is relatively small. It is likely that the greater number of flow acquisitions in the Fontan study (mean N of measurements: 7.6; range 5-9) compared to the first study (mean N of measurements: 5.7; range 4-6) may have increased the statistical power of the repeated-measures mixed models used in the later experiment, and therefore, it showed statistically significant changes where this was not previously possible. Moreover, as the conduction of the protocol became more well-established (and efficient) over the course of this PhD, the time required to re-plan imaging planes following ingestion of the meal

decreased. Also, the relatively smaller meal used in the Fontan experiment required shorter time to consume (≤1 min) than in the others (~2 min). Thus, although efforts were undertaken in all studies to acquire postprandial data as quickly as possible after the meal, the first postprandial flow data for the legs and the celiac artery were acquired ~4 min earlier, on average, in the Fontan study than they were in the earlier experiments. Therefore, it is possible that in the Fontan study, responses in the legs and celiac axis were recorded correctly in healthy subjects, whereas they were missed in the first experiment. This is supported by a systematic literature review on splanchnic blood flow, which found that early timing of postprandial blood flow measurement was crucial in order to detect postprandial increases in celiac blood flow accurately.(41) Similar issues may explain the inconsistent findings in the previous literature, where some studies reported changes in the legs, whereas others did not.(7, 74)

Renal vascular resistance also decreased postprandially in subjects in the first 2 studies, whereas in the Fontan study it did not change significantly in normal controls. As discussed in 4.4.2. it is possible that the small but continuous surge in renal blood flow was the result of metabolites that augment renal blood flow. As the meal used in the Fontan study was lower in both, lipids and carbohydrates, it is possible that it was insufficient to produce the same response in renal blood flow as in the previous experiment. This is particularly likely in view of the fact that the overall effect on renal blood flow was small, despite the substantial nutrient load ingested by subjects in the first experiment. The factors possibly explaining the discrepancies in the lower limb and celiac responses may have also contributed to this minor inconsistency.

7.2.2. Redistribution of blood flow

An interesting finding that was consistent across studies was that SMA blood flow increased to greater extent than was explained by the increase in CO alone. This discrepancy was not explained sufficiently by the decrease in lower limb blood flow (i.e., redistribution of blood flow) observed in subjects in the Fontan study. Regions that were not assessed as part of this thesis include the

inferior mesenteric artery, the arms, as well as cutaneous and thoracic vessels. Indeed, previous studies have shown that blood flow to the arms and the distal colon may decrease during the early postprandial state, supporting the hypothesis that redistribution from these compartments may account for the observed excess increase in SMA blood flow after the meal.(74, 154, 161) Of interest, one particular study demonstrated that subjects with a history of postprandial hypotension or autonomic dysregulation had diminished redistribution of forearm blood flow after a meal, and that this was associated with failure to maintain BP postprandially.(154) This suggests that postprandial brachial vasoreactivity may deserve further attention as a potential biomarker in future research on cardiovascular stress responses.

7.2.3. Comparison of findings with previous literature

Splanchnic blood flow in the normal population

In healthy volunteers it was firstly shown that the ingestion of food triggered a pronounced drop in mesenteric vascular resistance, and that this was compensated for primarily by a rise in CO, with no significant redistribution occurring from other compartments (Chapter 4. Cardiovascular responses to food ingestion in humans).

Only few MRI studies on splanchnic blood flow exist. One measured fasting regional blood flow to all major organs comprehensively in a cohort of 39 healthy children and adults.(71) Mean fasting blood flow in the SMA (0.23 $L.min^{-1}.m^{-2}$) and the celiac artery (0.54 $L.min^{-1}.m^{-2}$) were slightly higher than the data reported in the first 2 experiments of this PhD (0.15 to 0.19 $L.min^{-1}.m^{-2}$, and 0.35 to 0.41 $L.min^{-1}.m^{-2}$, respectively). It is possible that their approach to acquire flow data in free breathing may have led to these comparatively higher measurements.(58) A noteworthy observation is that healthy adult volunteers in the first experiment showed lower minimum observed values for the SMA and the celiac artery than reported by Muthusami *et al*. It is possible that the greater prevalence of overweight/obese people (mean BMI: 24.6 *vs.* 22.6) may have led to these lower BSA-indexed figures.

An older study measured postprandial responses of the SMA and the cranial vessels after an OGTT.(162) The magnitude of the increase in mesenteric blood flow from baseline was comparable to that observed in the first experiment, and similarly to this thesis, no changes in cranial blood flow were observed. As the authors did not index flow data for BSA, no meaningful comparison of data is possible. Moreover, they scanned with reduced spatial resolution in order to accelerate imaging and thus, acquired data with lower accuracy. Further, their experiment did not include blood flow measurement of the celiac axis, the legs and the kidneys, and was, therefore, not a complete assessment of haemodynamics.

On the other hand, numerous studies examined splanchnic blood flow using ultrasound.(7, 17, 37-40) A comprehensive and comparative overview of studies on fasting and postprandial splanchnic blood flow was published by Someya *et al*.(41) It should be noted that these studies typically did not report flow data indexed for BSA and therefore, no meaningful comparison of findings between studies is possible. The variance in splanchnic flow data tended to be smaller than reported in this thesis. However, sample sizes of previous studies were also considerably smaller than those in this thesis (typically in the range of 6-12 subjects). Furthermore, most previous studies used meals of much smaller calorie load and, therefore, produced smaller increase in mesenteric blood flow. An interesting observation in their systematic review was that some studies reported postprandial increases in celiac blood flow, whereas others did not. The authors concluded that this was due to the fact that celiac blood flow increases very early (1-5 min) and only transiently after the initiation of feeding, and that this response could, therefore, be missed easily. As stated earlier, efforts were undertaken, throughout this PhD, to acquire first blood flow data after the study meal as quickly as possible in all studies. Nevertheless, initial flow data after ingestion of the meal were acquired several minutes earlier in the Fontan study than in the others. Therefore, and in keeping with the thorough literature review conducted by Someya *et al.*, the earlier timing of flow acquisition likely explains why the first experiment in this PhD did not detect any increases in celiac blood flow, whereas the other 2 did.(41)

Splanchnic blood flow in the Fontan population

In Fontan patients, vasoconstriction of the legs and kidneys, as well as possible evidence of vasodilation of the celiac axis were found in the fasting state, as compared to controls. While both, their fasting and their postprandial mesenteric resistance were similar to normal volunteers, Fontan patients had abnormal responses of the celiac axis and the lower limbs (Chapter 6. Cardiovascular responses to food ingestion in Fontan physiology).

Two studies investigated splanchnic blood flow by MRI.(163, 164) In a retrospective study, Abbasi Bavil *et al.* characterised the mesenteric and portal circulation and investigated links between abnormal organ blood flow and morphological evidence of Fontan-associated liver disease.(164) The authors found that patients with morphological evidence of liver disease had a 41% reduction in SMA blood flow, as well as corresponding reductions in portal venous and hepatic venous blood flow.

Caro-Dominguez *et al.* came to similar conclusions and reported lower fasting celiac, lower limb, renal and mesenteric blood flow in paediatric Fontan patients, compared to normal controls.(163) This group also presented postprandial data acquired at a single timepoint 20 to 30 min following ingestion of a standardised meal. The authors found a smaller postprandial increase in CO, as well as in renal and mesenteric, but not in celiac or lower limb, blood flow. However, their study was limited by a number of factors. Firstly, it was retrospective in design. Secondly, MRI was performed under general anaesthesia in part of their cohort. This may have likely affected fasting haemodynamics. Thirdly, postprandial data were only acquired at a single timepoint. This may have caused investigators to miss some of the vascular responses if they did not occur at the same time in both groups, and hence, to misinterpret their findings. Lastly, the study comprised a significant proportion of patients with fenestrated Fontan circulation, which influenced their results. However, the authors did conduct subgroup analysis to account for this.

In both studies, mean SMA blood flow was overall higher than in the Fontan study in this thesis (SMA 0.22 and 0.27 *vs.* 0.15 $L.min^{-1}.m^{-2}$, respectively). As elucidated above, this is likely due to the effects of breath holding, which are likely even greater in patients with Fontan circulation. It should be noted that the variance of SMA flow data in the 2 studies (SD: 0.11 and 0.18) was similar to that in the Fontan study (IQR: 0.06 to 0.28), suggesting that flow was measured with comparable accuracy.

A limited number of studies assessed splanchnic blood flow in Fontan patients by ultrasound.(149, 158-160) A common shortcoming of these studies is that they typically only reported indirect measures of splanchnic blood flow and resistance, such as flow velocity, or resistance index. Only one study reported quantitative measures of flow.(149) Mean SMA blood flow was somewhat higher than that of patients in this PhD (0.33 to 0.35 *vs.* 0.15 $L.min^{-1}.m^{-2}$). However, data variance was also substantially greater using ultrasound (SD: 0.27 $L.min^{-1}.m^{-2}$ in the PLE group). While most of these studies showed evidence of greater splanchnic vascular resistance in Fontan patients, there were important limitations such as lack of control for prandial status,(160) or lack of a control group.(149, 158, 160) One study found that raised celiac but not mesenteric resistance was linked to poor outcome, conflicting a number of other studies.(158) Taken together, these data do support that abnormal splanchnic resistance may be a common feature in the Fontan population that may be associated with poor outcome. However, shortcomings in study design and data quality underscore the importance of conducting controlled prospective experiments using a more robust imaging method in this population.

Mesenteric vasoreactivity, obesity and cardiovascular risk

In adolescents (Chapter 5), it was shown that blunted postprandial vasoreactivity of the intestine was linked to higher BP and greater LVM in adolescents. Obese subjects were more likely to have blunted mesenteric vasoreactivity, but this finding was independent of obesity. While the underlying mechanisms can currently only be speculated about, some evidence exists to aid the interpretation of these findings and to direct future research.

Santisteban *et al.* conducted a series of experiments in rats and showed that spontaneously hypertensive animals, as well as rats with drug-induced hypertension, had reduced intestinal blood flow and increased permeability of the mucosa of the small intestine and of the proximal colon.(165) This was also linked to abnormal histopathology of the intestinal lining, as well as to raised pro-inflammatory markers, possibly as a result of the former. The observed changes in gut permeability were not found in prehypertensive and young rats, suggesting that these alterations were determined by BP status and were potentially reversible. In support of this, treatment with an antihypertensive drug partially reversed both, raised permeability and sympathetic nervous activity of the gut. Hypertension was also linked to dysbiosis of the intestine, but the authors did not examine whether these changes were reversible through antihypertensive treatment. Evidence was also found of augmented neuronal interplay between the gut and the brain in hypertensive animals.

The authors interpreted these findings as evidence that pro-hypertensive signals may be received from the brain and relayed to the intestine through central nervous pathways to promote sympathetic nervous activity and noradrenaline release. This would further cause the observed alterations in gut permeability, which would in turn promote inflammatory activity and dysbiosis, and subsequently, the development of hypertension. These pro-hypertensive signals in the gut are believed to be mediated by an unhealthy diet and are likely independent of adiposity, as others have shown.(24) However, the authors did not investigate the effects of changes in diet or adiposity on these findings, or whether raised sympathetic activity precedes or accompanies the observed changes in the gut. Another key question that was not addressed is whether changes in the gut microbiome are reversible through antihypertensive treatment, or inversely, whether an intervention on gut microbiome level could lower BP by reducing pro-inflammatory activity.

Nevertheless, taken together, these findings strongly suggest that hypertension and systemic inflammation, 2 key promotors of atherosclerosis, are driven by

sympathetic nervous cross-talk between the gut and the brain, mediated by diminished mesenteric perfusion and consequently, by intestinal dysbiosis.(166) This raised sympathetic nervous activity may also explain the link between blunted mesenteric vasoreactivity and LVH demonstrated in this PhD.(115) The findings from this thesis add further evidence to this model and highlight potential objectives for future research.

7.3. Future work and clinical applications

7.3.1. Postprandial vasoreactivity testing in clinical use

Cardiovascular stress tests are often used to diagnose cardiovascular disorders, such as autonomic dysregulation. The study protocol developed and validated in this thesis may be useful in the clinical assessment of disorders where cardiovascular responsivity to postprandial stress is blunted.

Falls and hypotension in elderly patients

A potential clinical application for the proposed protocol could be the assessment and management of elderly patients with falls. Falls in the elderly are a common issue with oftentimes severe outcome.(167) Meals are thought to increase susceptibility to falls as people age. The likely cause for this is a blunted postprandial increase in CO, which results in insufficient compensation for mesenteric vasodilation after a meal. This can lead to a drop in BP and thus, in cerebral perfusion.(168) Probable causes for these phenomena include, firstly, diminished target organ responsiveness to autonomic signals, leading to a weakened increase in HR (and thus, in CO) and in peripheral vascular tone, and secondly, diminished vagal withdrawal due to lower baseline parasympathetic activity at baseline in older people.(154, 155)

In this context, one study demonstrated that carbohydrate-rich meals and lipid-rich meals triggered different cardiovascular responses in elderly subjects. It was shown that the former depressed SBP postprandially, whereas the latter did not affect it significantly.(169) Attenuation of the normal vasoconstrictive response of the limbs could be responsible for this. In keeping, it was shown

elsewhere that postprandial epinephrine responses were preserved after a lipid-rich meal, but attenuated after a carbohydrate-rich one.(170) This raises the possibility that food rich in carbohydrates may convey greater risk of hypotension and falls in some individuals, but this remains to be confirmed by prospective studies.

While the significance of these observations in real-life scenarios has yet to be established, some older literature suggests that subjects with a history of falls, syncope or postprandial hypotension may indeed have blunted cardiovascular responses to a meal.(154, 155, 161) The protocol developed in this PhD could be used to assess the individual risk of postprandial hypotension by comparing the cardiovascular effects of meals of different compositions. This could support individual dietary recommendations to prevent falls, or serve as a tool to monitor responses to interventions, such as exercise.(171) Additional research is required to test and validate the protocol in these clinical applications.

Postprandial mesenteric vasoreactivity in neurological disease

Gastrointestinal symptoms such as constipation or delayed gastric emptying are common in patients with Parkinson's disease, and are thought to reflect neurodegenerative processes that may precede motor symptoms by a considerable amount of time. A very recent study measured blood flow responses in the SMA following ingestion of a standardised meal in patients with Parkinson's disease and in normal controls.(172) Patients showed an attenuated increase in SMA blood flow as well as a weaker glycaemic response compared to controls. The authors concluded that impaired gastrointestinal motility, as well as deficiencies in neuroendocrine signalling could impair postprandial vasoreactivity in this population. Therefore, the proposed protocol could be used to screen for neurodegenerative disease in asymptomatic patients at risk, or to resolve the role of the digestive system in other neurological disorders typically associated with gastrointestinal symptoms, such as migraine, tumours, or epilepsy.

7.3.2. Mesenteric vasoreactivity, obesity and cardiovascular risk

The nature of the associations between obesity and abnormal intestinal vasoreactivity, as well as those of blunted postprandial vasoreactivity with raised BP and LVH, and their direction, if causal, have yet to be established. However, the findings demonstrated in this PhD support those of mechanistic studies in animals,(165) highlighting the need for further human studies.

A possible approach to detangle the complex association between adiposity, BP, LVM, and intestinal permeability and vasoreactivity is to target specific associations in controlled interventional studies. For example, an interventional study randomising obese subjects to an intervention (e.g., diet or exercise) or to placebo, and comparing their outcomes to those of fit and of sedentary normal weight subjects, could elucidate whether blunted mesenteric vasoreactivity is reversible, whether it can be improved through intervention, and whether any improvement is due to a change in body mass or due to other factors. Such a study in 200 adolescents is currently ongoing at University of Oxford (OxSOCRATES).

Subsequent longitudinal studies will be required to monitor if this intervention has measurable impact on cardiovascular measures, such as BP or LVM. Other factors that may mediate these associations, such as the gut microbiome, should be assessed during follow-up to better understand their role or causality. As this PhD demonstrated that LVH emerges to a significant degree even in otherwise healthy adolescent populations, the timeframe for such follow-up studies is considered achievable.

In addition, confounding factors that affect both, BP and cardiomyocyte growth, could be identified in order to explain the associations demonstrated. Such factors may include genetic markers, neurohumoral mechanisms, or alterations in the gut microbiome, all of which have known or suspected links with BP regulation, or myocardial architecture and growth. Interventional studies, such as microbiome transplantation, could address specific mechanisms and resolve their role in the associations described in this thesis.

7.3.3. Applications in the Fontan circulation

Mesenteric vasoreactivity and ventricular hypertrophy

As diastolic function of the systemic ventricle is one of the main determinants of pulmonary blood flow in the Fontan circulation, hypertrophy of the systemic ventricle (e.g., due to residual aortic coarctation) is an important risk factor for poor haemodynamics and outcome. Whether blunted mesenteric vasoreactivity is also associated with ventricular hypertrophy in the Fontan population was not assessed in this thesis. Heterogeneity of the ventricular anatomies of Fontan patients makes, both, accurate measurement and meaningful statistical analysis of ventricular mass in such a relatively small cohort challenging. Contrary to normal subjects, high resolution cine imaging in multiple anatomical planes would have been necessary to allow for accurate assessment of ventricular mass in this population. This would have extended the duration of the protocol critically, and thus likely reduced the time available for the dynamic whole-body blood flow study. Further study is needed to investigate links between mesenteric vasoreactivity and ventricular mass in the Fontan population.

Causes for intestinal protein loss

Although some evidence exists in Fontan patients linking abnormal splanchnic vascular tone to PLE, the underlying pathophysiology of this oftentimes detrimental long-term complication is still poorly understood. Moreover, the literature linking fasting mesenteric vascular resistance to intestinal protein loss has been inconsistent. Longitudinal studies are needed to show whether testing postprandial mesenteric vasoreactivity could help identify subjects at risk of PLE before abnormalities in resting vascular tone can be detected. The direction of this association, if causal, may stimulate the development of new treatment strategies to improve intestinal perfusion. For example, GLP-2 and its analogues (e.g., teduglutide) are potent mesenteric vasodilators.(173) They could, therefore, be explored as a strategy to improve mesenteric blood flow in order to potentially prevent PLE in Fontan patients. However, the possible role of mesenteric vasoconstriction in optimising organ perfusion must be considered when testing this, as pharmacologically mediated mesenteric

vasodilation could negate its stabilising effects and compromise organ perfusion in patients with poor CO.

Peripheral vasoconstriction and muscle mass

Fontan patients have been shown to have diminished peripheral muscle mass, particularly of the legs.(144) Although the underlying causes for this association have yet to be fully understood, several mechanisms are conceivable. Reduced exercise capacity and self-restraint in this population may cause muscle mass to decline. Chronic vasoconstriction of the legs to compensate for poor organ perfusion may also entail loss of muscle.(144) Venous remodelling to counteract venous pooling in the legs and to improve systemic venous return has also been suggested to contribute to this.(143) Intestinal malabsorption, or even loss, of dietary protein due to intestinal congestion may further aggravate sarcopenia.

Future research should address the direction of these associations, if causally linked. For example, Fontan patients could be randomised to 2 types of exercise intervention – either muscle build-up or endurance exercise – and changes in lower limb muscle mass and in blood flow could be assessed as outcome parameters. This could narrow down possible causes for sarcopenia in this population. If successful, improved blood flow to the legs due to greater muscle mass could improve cardiovascular responses to stress by enabling more redistribution of blood flow to support CO augmentation. A different intervention strategy (or an additional arm in the hypothetical study above) could aim at improving peripheral blood flow through pharmacological measures, although effects on BP (via peripheral vasodilation) could likely be limiting factors for this approach.

7.4. Evolution, challenges and limitations of the protocol

7.4.1. Protocol development and challenges

Study meal

The study meal was designed to expose subjects to a great calorie load, while being compatible with an MRI environment and being quick and easy to ingest in order not to miss early postprandial responses. Protein load was kept low due to possible effects of protein intake on vascular responses(174) and in order to not unnecessarily increase osmotic load, which may have affected tolerability. Maltose syrup was used instead of glucose as it is less sweet and thus, less likely to cause nausea and vomiting, which would pose a risk in an MRI scanner. The resulting liquid meal was overall well-tolerated: of the 132 subjects exposed to the meal in total throughout the different experiments in this thesis, 2 vomited during the MRI scan, and another 2 reported late vomiting, several hours later (3% adverse events in total). This was despite the enormous nutrient and calorie load administered, and despite the fact that subjects were only allowed little time for consumption before returning to supine position for an extended period.

Image planning

A challenge of the study protocol that deserves mention was image planning. While the initial planning of the imaging planes could be done conventionally and without any unusual challenges, defining the imaging planes for flow acquisition after ingestion of the study meal was a potential limitation, as it could delay acquisition of postprandial data. In order to obviate the need for re-planning due to patient movement caused by ingestion of the meal, initial test runs used a vacuum mattress, which was moulded to the subject's contours and would force them to lie down in the same position after ingestion of the meal, as they had been in before. However, this approach was flawed by the fact that the internal organs (and, therefore, the supplying vessels) shifted due to displacement caused by the stomach, which was now filled by the study meal. Moreover, the vacuum mattress could not be fitted sufficiently to larger subjects. Therefore, this solution was soon abandoned, and planes for postprandial

imaging were planned conventionally by 3D b-SSFP, but with slightly reduced spatial resolution in order to accelerate scanning times. This allowed postprandial data to be acquired within an acceptable timeframe.

Measurement of cranial blood flow

Similar to the other experiments, the original protocol for the adolescent study foresaw measurement of blood flow to the head using a neck coil. However, after 2 patients vomited during the scan in the earlier stages of the study, it was decided to forego measurement of cranial blood flow and to remove the neck coil in order to allow subjects to turn their heads to the side in case of vomiting (it should be noted that no further cases of vomiting occurred). Thus, cranial blood flow data are unavailable for that experiment. For the Fontan study, measurement of cranial blood flow was reimplemented, as the meal was smaller in size and thus, the likelihood of vomiting was deemed low.

Parameters of vascular function

An important thing to note is that, in the Fontan study, vascular resistance was not measured *per se*, as this would have necessitated invasive measurement of PAP in order to isolate the PVR component of Z_0 from vascular resistance. As participation in the study was voluntary, invasive measurement of PVR was not an option. Therefore, efforts were undertaken to adjust Z_0 for a factor estimated to correspond to PVR on a group level. Nevertheless, individual subjects may still show abnormalities in vascular resistance that are explained to greater degree by PVR than this approach was able to show. Therefore, invasive measurement of PAP remains without alternative in order to describe abnormalities in resistance in the individual patient with clinical issues.

In normal physiology, where the systemic veins drain into the RA, and not into the PA, such adjustment is not needed, as RAP is normally negligible and, therefore, does not contribute significantly to systemic Z_0. The term, ‘resistance’, is, therefore, used synonymously with ‘impedance’ in normal subjects in clinical practice. Thus, vascular data from people with normal cardiac anatomy are comparable between chapters in this PhD, provided that

allometric scaling matches. This may not be possible with the adolescent study, where vascular data had to be adjusted specifically for factors used to correct for obesity. These adjustments are preferred over BSA as the normal allometric scaling relationships between cardiovascular measures and BSA break down in obesity, resulting in over-adjustment for the excess BSA of obese people.(128)

7.4.2. Limitations

Investigator blinding

One potential limitation was that imaging data were analysed by an investigator who was not blinded to patient history or weight status. However, in Fontan patients, abnormal anatomy of the heart and the abdominal vasculature, and/or sternal wires or other devices can often be seen in flow images. Similarly, body fat and frame can usually be derived from flow and cine images. These factors would have likely functionally unblinded the investigator in a significant proportion of examinations. Therefore, the feasibility and impact of blinding on image analysis are questionable.

Validation of imaging methods in specific organs

Agreement between respiratory triggered, cardiac gated PCMR and RAGS PCMR was not assessed specifically for the SMA. However, Steeden *et al.* demonstrated good agreement between the 2 methods for the renal arteries.(47) The renal arteries are, on average, substantially smaller than the SMA (~50% smaller cross-sectional area assuming a diameter of 5.2 *vs.* 7.3 mm)(175) and are, therefore, covered by a greater proportion of pixels at the edge of the lumen, where flow is underestimated (see 2.4.2.). Consequently, it can be assumed that RAGS PCMR should be no less accurate for SMA imaging than for the renal arteries. Furthermore, the RAGS PCMR sequence used in this study detected even small changes in blood flow in the smallest vessels (i.e. the renal arteries) with high statistical significance (e.g., ***Figure 17***). This strongly supports that this technique is highly reliable for blood flow measurement in the splanchnic vasculature.

Effects of breath holding

The review of previous literature in 7.2.1. suggests that the technique used in this thesis for the measurement of regional (and particularly splanchnic) blood flow may have underestimated flow somewhat due to the necessity for breath holding. However, conventional free-breathing techniques necessitate longer image acquisition times and are, therefore, not suitable to study postprandial blood flow responses in a dynamic fashion. Future development could overcome this by designing MRI sequences that allow flow acquisition by averaged imaging during free breathing.

7.5. Conclusion

Postprandial cardiovascular physiology in humans can be studied safely and in a dynamic fashion using MRI. The proposed study protocol may reduce or even obviate the need for animal trials for *in vivo* cardiovascular studies, and may serve as basis to investigate the role of postprandial vasoreactivity in various clinical settings and populations. Additional research is needed to resolve the involvement of the gut in the development of CVD, and to determine the potential role of mesenteric vasoreactivity as prognostic marker in the Fontan population.

vii. Appendix: Academic output during this PhD

Journal articles

Hauser JA, Muthurangu V, Pandya B, Michel-Behnke I, Taylor AM, Demyanets S. Postprandial variability of novel heart failure biomarkers in Fontan patients compared to healthy volunteers. *Int J Cardiol Congenital Heart Disease* 2021 May; 3, 100127

Hauser JA, Jones A, Pandya B, Taylor AM, Muthurangu V. Comprehensive MRI assessment of the cardiovascular responses to food ingestion in Fontan physiology. *Am J Physiol Heart Circ Physiol*. 2020,319(4):H808-13.

Hauser JA, Muthurangu V, Sattar N, Taylor AM, Jones A. Postprandial Vascular Dysfunction Is Associated With Raised Blood Pressure and Adverse Left Ventricular Remodeling in Adolescent Adiposity. *Circ Cardiovasc Imaging*. 2019;12(11):e009172.

Schneider M, Beichl M, Nietsche C, Beitzke D, Porenta G, Beran G, et al. Systematic Evaluation of Systemic Right Ventricular Function. *J Clin Med*. 2019;9(1).

Cheang MH, Barber, NJ, Khushnood A, Hauser JA, Kowalik G, Steeden J, Quail M, Tullis K, Hothi D, Muthurangu V. A comprehensive characterization of myocardial and vascular phenotype in pediatric chronic kidney disease using cardiovascular magnetic resonance imaging. *J Cardiovasc Magn Reson*. 2018;20(1):24.

Hauser JA, Taylor AM, Pandya B. How to Image the Adult Patient With Fontan Circulation. *Circ Cardiovasc Imaging*. 2017;10(5).

Hauser JA, Demyanets S, Rusai K, Goritschan C, Weber M, Panesar D, et al. Diagnostic performance and reference values of novel biomarkers of paediatric heart failure. *Heart*. 2016;102(20):1633-9.

Hauser JA, Muthurangu V, Steeden JA, Taylor AM, Jones A. Comprehensive assessment of the global and regional vascular responses to food ingestion in humans using novel rapid MRI. *Am J Physiol Regul Integr Comp Physiol*. 2016;310(6):R541-5.

Book chapters

Pacemaker Therapy (Chapter). International Society for Heart and Lung Transplantation (ISHLT) Guidelines for the Management of Paediatric Heart Failure. *ISHLT Monograph Series*. 2014, Vol. 8.

Prizes

American Heart Association Cardiovascular Disease in the Young (CVDY) Council – Early Career Award 2017 (Finalist)

viii. References

1. Kearney MT, Cowley AJ, Macdonald IA. The cardiovascular responses to feeding in man. Exp Physiol. 1995;80(5):683-700.

2. Lefebvre PJ, Scheen AJ. The postprandial state and risk of cardiovascular disease. Diabet Med. 1998;15 Suppl 4:S63-8.

3. Hauser JA, Muthurangu V, Steeden JA, Taylor AM, Jones A. Comprehensive assessment of the global and regional vascular responses to food ingestion in humans using novel rapid MRI. Am J Physiol Regul Integr Comp Physiol. 2016;310(6):R541-5.

4. Hauser JA, Muthurangu V, Sattar N, Taylor AM, Jones A. Postprandial Vascular Dysfunction Is Associated With Raised Blood Pressure and Adverse Left Ventricular Remodeling in Adolescent Adiposity. Circ Cardiovasc Imaging. 2019;12(11):e009172.

5. Hauser JA, Jones A, Pandya B, Taylor AM, Muthurangu V. Comprehensive MRI assessment of the cardiovascular responses to food ingestion in Fontan physiology. Am J Physiol Heart Circ Physiol. 2020;319(4):H808-H13.

6. Tse TF, Clutter WE, Shah SD, Miller JP, Cryer PE. Neuroendocrine responses to glucose ingestion in man. Specificity, temporal relationships, and quantitative aspects. J Clin Invest. 1983;72(1):270-7.

7. Sidery MB, Macdonald IA, Cowley AJ, Fullwood LJ. Cardiovascular responses to high-fat and high-carbohydrate meals in young subjects. Am J Physiol. 1991;261(5 Pt 2):H1430-6.

8. Monnier L, Colette C. Target for glycemic control: concentrating on glucose. Diabetes Care. 2009;32 Suppl 2:S199-204.

9. Vaz M, Turner A, Kingwell B, Chin J, Koff E, Cox H, et al. Postprandial sympatho-adrenal activity: its relation to metabolic and cardiovascular events and to changes in meal frequency. Clin Sci (Lond). 1995;89(4):349-57.

10. Sharrett AR, Heiss G, Chambless LE, Boerwinkle E, Coady SA, Folsom AR, et al. Metabolic and lifestyle determinants of postprandial lipemia differ from those of fasting triglycerides: The Atherosclerosis Risk In Communities (ARIC) study. Arterioscler Thromb Vasc Biol. 2001;21(2):275-81.

11. Masuda D, Yamashita S. Postprandial Hyperlipidemia and Remnant Lipoproteins. J Atheroscler Thromb. 2017;24(2):95-109.

12. Bartoli E, Fra GP, Carnevale Schianca GP. The oral glucose tolerance test (OGTT) revisited. Eur J Intern Med. 2011;22(1):8-12.

13. de Vries MA, Klop B, Janssen HW, Njo TL, Westerman EM, Castro Cabezas M. Postprandial inflammation: targeting glucose and lipids. Adv Exp Med Biol. 2014;824:161-70.

14. Lairon D, Lopez-Miranda J, Williams C. Methodology for studying postprandial lipid metabolism. Eur J Clin Nutr. 2007;61(10):1145-61.

15. Tamburrelli C, Gianfagna F, D'Imperio M, De Curtis A, Rotilio D, Iacoviello L, et al. Postprandial cell inflammatory response to a standardised fatty meal in subjects at different degree of cardiovascular risk. Thromb Haemost. 2012;107(3):530-7.

16. Matheson PJ, Wilson MA, Garrison RN. Regulation of intestinal blood flow. J Surg Res. 2000;93(1):182-96.

17. Qamar MI, Read AE. Effects of ingestion of carbohydrate, fat, protein, and water on the mesenteric blood flow in man. Scand J Gastroenterol. 1988;23(1):26-30.

18. Iwao T, Oho K, Nakano R, Yamawaki M, Sakai T, Sato M, et al. Effect of meal induced splanchnic arterial vasodilatation on renal arterial haemodynamics in normal subjects and patients with cirrhosis. Gut. 1998;43(6):843-8.

19. Vatner SF, Franklin D, Van Citters RL. Coronary and visceral vasoactivity associated with eating and digestion in the conscious dog. Am J Physiol. 1970;219(5):1380-5.

20. Avasthi PS, Greene ER, Voyles WF. Noninvasive Doppler assessment of human postprandial renal blood flow and cardiac output. Am J Physiol. 1987;252(6 Pt 2):F1167-74.

21. Trahair LG, Horowitz M, Hausken T, Feinle-Bisset C, Rayner CK, Jones KL. Effects of exogenous glucagon-like peptide-1 on the blood pressure, heart rate, mesenteric blood flow, and glycemic responses to intraduodenal glucose in healthy older subjects. J Clin Endocrinol Metab. 2014;99(12):E2628-34.

22. Namkung J, Kim H, Park S. Peripheral Serotonin: a New Player in Systemic Energy Homeostasis. Mol Cells. 2015;38(12):1023-8.

23. Jensen LJ, Nielsen MS, Salomonsson M, Sorensen CM. T-type Ca(2+) channels and autoregulation of local blood flow. Channels (Austin). 2017;11(3):183-95.

24. Sartor DM. Sympathoinhibitory signals from the gut and obesity-related hypertension. Clin Auton Res. 2013;23(1):33-9.

25. How JM, Pumpa TJ, Sartor DM. The circulatory and renal sympathoinhibitory effects of gastric leptin are altered by a high fat diet and obesity. Auton Neurosci. 2013;177(2):95-100.

26. How JM, Wardak SA, Ameer SI, Davey RA, Sartor DM. Blunted sympathoinhibitory responses in obesity-related hypertension are due to aberrant central but not peripheral signalling mechanisms. J Physiol. 2014;592(7):1705-20.

27. Gallavan RH, Jr., Chou CC. Possible mechanisms for the initiation and maintenance of postprandial intestinal hyperemia. Am J Physiol. 1985;249(3 Pt 1):G301-8.

28. Hansen LB. GLP-2 and mesenteric blood flow. Dan Med J. 2013;60(5):B4634.

29. Sidery MB, Macdonald IA. The effect of meal size on the cardiovascular responses to food ingestion. Br J Nutr. 1994;71(6):835-48.

30. Hoost U, Kelbaek H, Rasmusen H, Court-Payen M, Christensen NJ, Pedersen-Bjergaard U, et al. Haemodynamic effects of eating: the role of meal composition. Clin Sci (Lond). 1996;90(4):269-76.

31. Ferreira-Filho SR, Ferreira AC, Oliveira PC, Moreira JF, Ribeiro EC, Oliveira AM, et al. Systemic hemodynamic changes in elderly hypertensive patients after ingesting foods with lipid, protein, and carbohydrate contents. J Clin Hypertens (Greenwich). 2009;11(5):271-6.

32. Gliemann L, Mortensen SP, Hellsten Y. Methods for the determination of skeletal muscle blood flow: development, strengths and limitations. Eur J Appl Physiol. 2018;118(6):1081-94.

33. Kuipers JR, Sidi D, Heymann MA, Rudolph AM. Comparison of methods of measuring cardiac output in newborn lambs. Pediatr Res. 1982;16(8):594-8.

34. Corbally MT, Brennan MF. Noninvasive measurement of regional blood flow in man. Am J Surg. 1990;160(3):313-21.

35. Takagi T, Naruse S, Shionoya S. Postprandial celiac and superior mesenteric blood flows in conscious dogs. Am J Physiol. 1988;255(4 Pt 1):G522-8.

36. Vatner SF, Franklin D, Van Citters RL. Mesenteric vasoactivity associated with eating and digestion in the conscious dog. Am J Physiol. 1970;219(1):170-4.

37. Parker DR, Carlisle K, Cowan FJ, Corrall RJ, Read AE. Postprandial mesenteric blood flow in humans: relationship to endogenous gastrointestinal hormone secretion and energy content of food. Eur J Gastroenterol Hepatol. 1995;7(5):435-40.

38. Moneta GL, Taylor DC, Helton WS, Mulholland MW, Strandness DE, Jr. Duplex ultrasound measurement of postprandial intestinal blood flow: effect of meal composition. Gastroenterology. 1988;95(5):1294-301.

39. Cooper AM, Braatvedt GD, Qamar MI, Brown H, Thomas DM, Halliwell M, et al. Fasting and post-prandial splanchnic blood flow is reduced by a somatostatin analogue (octreotide) in man. Clin Sci (Lond). 1991;81(2):169-75.

40. Qamar MI, Read AE. Effects of exercise on mesenteric blood flow in man. Gut. 1987;28(5):583-7.

41. Someya N, Endo MY, Fukuba Y, Hayashi N. Blood flow responses in celiac and superior mesenteric arteries in the initial phase of digestion. Am J Physiol Regul Integr Comp Physiol. 2008;294(6):R1790-6.

42. Pees C, Glagau E, Hauser J, Michel-Behnke I. Reference values of aortic flow velocity integral in 1193 healthy infants, children, and adolescents to quickly estimate cardiac stroke volume. Pediatr Cardiol. 2013;34(5):1194-200.

43. Schuster AH, Nanda NC. Doppler echocardiographic measurement of cardiac output: comparison with a non-golden standard. Am J Cardiol. 1984;53(1):257-9.

44. Nayak KS, Nielsen JF, Bernstein MA, Markl M, P DG, R MB, et al. Cardiovascular magnetic resonance phase contrast imaging. J Cardiovasc Magn Reson. 2015;17:71.

45. Gatehouse PD, Keegan J, Crowe LA, Masood S, Mohiaddin RH, Kreitner KF, et al. Applications of phase-contrast flow and velocity imaging in cardiovascular MRI. Eur Radiol. 2005;15(10):2172-84.

46. Lotz J, Meier C, Leppert A, Galanski M. Cardiovascular flow measurement with phase-contrast MR imaging: basic facts and implementation. Radiographics. 2002;22(3):651-71.

47. Steeden JA, Muthurangu V. Investigating the limitations of single breath-hold renal artery blood flow measurements using spiral phase contrast MR with R-R interval averaging. J Magn Reson Imaging. 2015;41(4):1143-9.

48. Barber NJ, Ako EO, Kowalik GT, Cheang MH, Pandya B, Steeden JA, et al. Magnetic Resonance-Augmented Cardiopulmonary Exercise Testing: Comprehensively Assessing Exercise Intolerance in Children With Cardiovascular Disease. Circ Cardiovasc Imaging. 2016;9(12).

49. Jones A, McMillan MR, Jones RW, Kowalik GT, Steeden JA, Deanfield JE, et al. Adiposity is associated with blunted cardiovascular, neuroendocrine and cognitive responses to acute mental stress. PLoS One. 2012;7(6):e39143.

50. Bogaert J, Dymarkowski S, Taylor AM, Muthurangu V, SpringerLink. Clinical Cardiac MRI. Berlin, Heidelberg: Springer Berlin Heidelberg : Imprint: Springer; 2012. 1 online resource (707) p.

51. Ridgway JP. Cardiovascular magnetic resonance physics for clinicians: part I. J Cardiovasc Magn Reson. 2010;12:71.

52. Lipton ML, Kanal E, SpringerLink. Totally accessible MRI : a user's guide to principles, technology, and applications. New York
New York, NY: Springer
Springer New York; 2008. 1 online resource (xxi, 313 pages) : illustrations p.

53. Biglands JD, Radjenovic A, Ridgway JP. Cardiovascular magnetic resonance physics for clinicians: Part II. J Cardiovasc Magn Reson. 2012;14:66.

54. Fratz S, Chung T, Greil GF, Samyn MM, Taylor AM, Valsangiacomo Buechel ER, et al. Guidelines and protocols for cardiovascular magnetic resonance in children and adults with congenital heart disease: SCMR expert consensus group on congenital heart disease. J Cardiovasc Magn Reson. 2013;15:51.

55. Muthurangu V, Lurz P, Critchely JD, Deanfield JE, Taylor AM, Hansen MS. Real-time assessment of right and left ventricular volumes and function in patients with congenital heart disease by using high spatiotemporal resolution radial k-t SENSE. Radiology. 2008;248(3):782-91.

56. Steeden JA, Atkinson D, Hansen MS, Taylor AM, Muthurangu V. Rapid flow assessment of congenital heart disease with high-spatiotemporal-resolution gated spiral phase-contrast MR imaging. Radiology. 2011;260(1):79-87.

57. Tsao J, Kozerke S, Boesiger P, Pruessmann KP. Optimizing spatiotemporal sampling for k-t BLAST and k-t SENSE: application to high-resolution real-time cardiac steady-state free precession. Magn Reson Med. 2005;53(6):1372-82.

58. Sakuma H, Kawada N, Kubo H, Nishide Y, Takano K, Kato N, et al. Effect of breath holding on blood flow measurement using fast velocity encoded cine MRI. Magn Reson Med. 2001;45(2):346-8.

59. Park JB, Santos JM, Hargreaves BA, Nayak KS, Sommer G, Hu BS, et al. Rapid measurement of renal artery blood flow with ungated spiral phase-contrast MRI. J Magn Reson Imaging. 2005;21(5):590-5.

60. Park JB, Olcott EW, Nishimura DG. Rapid measurement of time-averaged blood flow using ungated spiral phase-contrast. Magn Reson Med. 2003;49(2):322-8.

61. Shannon CE. Communication in the presence of noise. Proceedings of the Institute of Radio Engineers. 1949;37(1):10-21.

62. Quail MA, Steeden JA, Knight D, Segers P, Taylor AM, Muthurangu V. Development and validation of a novel method to derive central aortic systolic pressure from the MR aortic distension curve. J Magn Reson Imaging. 2014;40(5):1064-70.

63. Heseltine D, Dakkak M, Woodhouse K, Macdonald IA, Potter JF. The effect of caffeine on postprandial hypotension in the elderly. J Am Geriatr Soc. 1991;39(2):160-4.

64. Malin SK, Rynders CA, Weltman JY, Jackson Roberts L, 2nd, Barrett EJ, Weltman A. Endothelial function following glucose ingestion in adults with prediabetes: Role of exercise intensity. Obesity (Silver Spring). 2016;24(7):1515-21.

65. Unal B, Bilgili MY, Yilmaz S, Caglayan O, Kara S. Smoking prevents the expected postprandial increase in intestinal blood flow: a Doppler sonographic study. J Ultrasound Med. 2004;23(5):647-53.

66. Pullicin AJ, Penner MH, Lim J. The Sweet Taste of Acarbose and Maltotriose: Relative Detection and Underlying Mechanism. Chem Senses. 2019;44(2):123-8.

67. Molarius A, Seidell JC, Sans S, Tuomilehto J, Kuulasmaa K. Waist and hip circumferences, and waist-hip ratio in 19 populations of the WHO MONICA Project. Int J Obes Relat Metab Disord. 1999;23(2):116-25.

68. Kelbaek H, Munck O, Christensen NJ, Godtfredsen J. Central haemodynamic changes after a meal. Br Heart J. 1989;61(6):506-9.

69. Waaler BA, Eriksen M, Toska K. The effect of meal size on postprandial increase in cardiac output. Acta Physiol Scand. 1991;142(1):33-9.

70. Sieber C, Beglinger C, Jaeger K, Hildebrand P, Stalder GA. Regulation of postprandial mesenteric blood flow in humans: evidence for a cholinergic nervous reflex. Gut. 1991;32(4):361-6.

71. Muthusami P, Yoo SJ, Chaturvedi R, Gill N, Windram J, Schantz D, et al. Splanchnic, Thoracoabdominal, and Cerebral Blood Flow Volumes in Healthy Children and Young Adults in Fasting and Postprandial States: Determining Reference Ranges by Using Phase-Contrast MR Imaging. Radiology. 2017;285(1):231-41.

72. Kearney MT, Cowley AJ, Stubbs TA, Perry AJ, MacDonald IA. Central and peripheral haemodynamic responses to high carbohydrate and high fat meals in human cardiac transplant recipients. Clin Sci (Lond). 1996;90(6):473-83.

73. Baron AD, Laakso M, Brechtel G, Hoit B, Watt C, Edelman SV. Reduced postprandial skeletal muscle blood flow contributes to glucose intolerance in human obesity. J Clin Endocrinol Metab. 1990;70(6):1525-33.

74. Gallavan RH, Jr., Chou CC, Kvietys PR, Sit SP. Regional blood flow during digestion in the conscious dog. Am J Physiol. 1980;238(2):H220-5.

75. Chemla D, Hebert JL, Coirault C, Zamani K, Suard I, Colin P, et al. Total arterial compliance estimated by stroke volume-to-aortic pulse pressure ratio in humans. Am J Physiol. 1998;274(2):H500-5.

76. Vatner SF, Patrick TA, Higgins CB, Franklin D. Regional circulatory adjustments to eating and digestion in conscious unrestrained primates. J Appl Physiol. 1974;36(5):524-9.

77. Ziemssen T, Siepmann T. The Investigation of the Cardiovascular and Sudomotor Autonomic Nervous System-A Review. Front Neurol. 2019;10:53.

78. Heesch CM. Reflexes that control cardiovascular function. Am J Physiol. 1999;277(6 Pt 2):S234-43.

79. Barber NJ, Ako EO, Kowalik GT, Steeden JA, Pandya B, Muthurangu V. MR augmented cardiopulmonary exercise testing-a novel approach to assessing cardiovascular function. Physiol Meas. 2015;36(5):N85-94.

80. Cybulski G. Influence of age on the immediate cardiovascular response to orthostatic manoeuvre. Eur J Appl Physiol Occup Physiol. 1996;73(6):563-72.

81. Luciano GL, Brennan MJ, Rothberg MB. Postprandial hypotension. Am J Med. 2010;123(3):281 e1-6.

82. Robertson D, Wade D, Robertson RM. Postprandial alterations in cardiovascular hemodynamics in autonomic dysfunction states. Am J Cardiol. 1981;48(6):1048-52.

83. van Kraaij DJ, Jansen RW, Bouwels LH, Hoefnagels WH. Furosemide withdrawal improves postprandial hypotension in elderly patients with heart failure and preserved left ventricular systolic function. Arch Intern Med. 1999;159(14):1599-605.

84. Berlinerblau R, Shani J. Postprandial angina pectoris: clinical and angiographic correlations. J Am Coll Cardiol. 1994;23(3):627-9.

85. Gilligan DM, Nihoyannopoulos P, Fletcher A, Sbarouni E, Dritsas A, Oakley CM. Symptoms of hypertrophic cardiomyopathy, with special emphasis on syncope and postprandial exacerbation of symptoms. Clin Cardiol. 1996;19(5):371-8.

86. Chung WY, Sohn DW, Kim YJ, Oh S, Chai IH, Park YB, et al. Absence of postprandial surge in coronary blood flow distal to significant stenosis: a possible mechanism of postprandial angina. J Am Coll Cardiol. 2002;40(11):1976-83.

87. Baliga RR, Rosen SD, Camici PG, Kooner JS. Regional myocardial blood flow redistribution as a cause of postprandial angina pectoris. Circulation. 1998;97(12):1144-9.

88. Feiner E, Arabadjian M, Winson G, Kim B, Chaudhry F, Sherrid MV. Post-prandial upright exercise echocardiography in hypertrophic cardiomyopathy. J Am Coll Cardiol. 2013;61(24):2487-8.

89. Sharma N, Okere IC, Duda MK, Chess DJ, O'Shea KM, Stanley WC. Potential impact of carbohydrate and fat intake on pathological left ventricular hypertrophy. Cardiovasc Res. 2007;73(2):257-68.

90. Young JM, Weser E. The metabolism of circulating maltose in man. J Clin Invest. 1971;50(5):986-91.

91. Schwartz JG, Phillips WT, Aghebat-Khairy B. Revision of the oral glucose tolerance test: a pilot study. Clin Chem. 1990;36(1):125-8.

92. https://www.who.int/en/news-room/fact-sheets/detail/cardiovascular-diseases-(cvds).

93. https://ec.europa.eu/eurostat/statistics-explained/index.php/Cardiovascular_diseases_statistics [

94. Weintraub WS, Daniels SR, Burke LE, Franklin BA, Goff DC, Jr., Hayman LL, et al. Value of primordial and primary prevention for cardiovascular disease: a policy statement from the American Heart Association. Circulation. 2011;124(8):967-90.

95. Libby P, Ridker PM, Hansson GK. Progress and challenges in translating the biology of atherosclerosis. Nature. 2011;473(7347):317-25.

96. Conrad N, Judge A, Tran J, Mohseni H, Hedgecott D, Crespillo AP, et al. Temporal trends and patterns in heart failure incidence: a population-based study of 4 million individuals. Lancet. 2018;391(10120):572-80.

97. Berenson GS, Srinivasan SR, Bao W, Newman WP, 3rd, Tracy RE, Wattigney WA. Association between multiple cardiovascular risk factors and atherosclerosis in children and young adults. The Bogalusa Heart Study. N Engl J Med. 1998;338(23):1650-6.

98. Demerath EW, Schubert CM, Maynard LM, Sun SS, Chumlea WC, Pickoff A, et al. Do changes in body mass index percentile reflect changes in body composition in children? Data from the Fels Longitudinal Study. Pediatrics. 2006;117(3):e487-95.

99. Freedman DS, Wang J, Maynard LM, Thornton JC, Mei Z, Pierson RN, et al. Relation of BMI to fat and fat-free mass among children and adolescents. Int J Obes (Lond). 2005;29(1):1-8.

100. Barlow SE, Expert C. Expert committee recommendations regarding the prevention, assessment, and treatment of child and adolescent overweight and obesity: summary report. Pediatrics. 2007;120 Suppl 4:S164-92.

101. McCrindle BW. Cardiovascular consequences of childhood obesity. Can J Cardiol. 2015;31(2):124-30.

102. Morigami H, Morioka T, Yamazaki Y, Imamura S, Numaguchi R, Asada M, et al. Visceral Adiposity is Preferentially Associated with Vascular Stiffness Rather than Thickness in Men with Type 2 Diabetes. J Atheroscler Thromb. 2016;23(9):1067-79.

103. Garrido-Miguel M, Cavero-Redondo I, Alvarez-Bueno C, Rodriguez-Artalejo F, Moreno LA, Ruiz JR, et al. Prevalence and Trends of Overweight and Obesity in European Children From 1999 to 2016: A Systematic Review and Meta-analysis. JAMA Pediatr. 2019:e192430.

104. Bhupathiraju SN, Hu FB. Epidemiology of Obesity and Diabetes and Their Cardiovascular Complications. Circ Res. 2016;118(11):1723-35.

105. Collaboration NCDRF. Worldwide trends in body-mass index, underweight, overweight, and obesity from 1975 to 2016: a pooled analysis of 2416 population-based measurement studies in 128.9 million children, adolescents, and adults. Lancet. 2017;390(10113):2627-42.

106. Ayer J, Charakida M, Deanfield JE, Celermajer DS. Lifetime risk: childhood obesity and cardiovascular risk. Eur Heart J. 2015;36(22):1371-6.

107. Lloyd LJ, Langley-Evans SC, McMullen S. Childhood obesity and adult cardiovascular disease risk: a systematic review. Int J Obes (Lond). 2010;34(1):18-28.

108. Umer A, Kelley GA, Cottrell LE, Giacobbi P, Jr., Innes KE, Lilly CL. Childhood obesity and adult cardiovascular disease risk factors: a systematic review with meta-analysis. BMC Public Health. 2017;17(1):683.

109. Skinner AC, Perrin EM, Moss LA, Skelton JA. Cardiometabolic Risks and Severity of Obesity in Children and Young Adults. N Engl J Med. 2015;373(14):1307-17.

110. Humphrey JD, Harrison DG, Figueroa CA, Lacolley P, Laurent S. Central Artery Stiffness in Hypertension and Aging: A Problem With Cause and Consequence. Circ Res. 2016;118(3):379-81.

111. Middlemiss JE, Miles KL, McDonnell BJ, Yasmin, Maki-Petaja KM, Cockcroft JR, et al. Mechanisms underlying elevated SBP differ with adiposity in young adults: the Enigma study. J Hypertens. 2016;34(2):290-7.

112. Grassi G, Seravalle G, Dell'oro R. Sympathetic activation in obesity: a noninnocent bystander. Hypertension. 2010;56(3):338-40.

113. Corden B, Keenan NG, de Marvao AS, Dawes TJ, Decesare A, Diamond T, et al. Body fat is associated with reduced aortic stiffness until middle age. Hypertension. 2013;61(6):1322-7.

114. Charakida M, Jones A, Falaschetti E, Khan T, Finer N, Sattar N, et al. Childhood obesity and vascular phenotypes: a population study. J Am Coll Cardiol. 2012;60(25):2643-50.

115. Nadruz W. Myocardial remodeling in hypertension. J Hum Hypertens. 2015;29(1):1-6.

116. de Simone G, Devereux RB, Roman MJ, Schlussel Y, Alderman MH, Laragh JH. Echocardiographic left ventricular mass and electrolyte intake predict arterial hypertension. Ann Intern Med. 1991;114(3):202-9.

117. Hoang K, Zhao Y, Gardin JM, Carnethon M, Mukamal K, Yanez D, et al. LV Mass as a Predictor of CVD Events in Older Adults With and Without Metabolic Syndrome and Diabetes. JACC Cardiovasc Imaging. 2015;8(9):1007-15.

118. Stewart MH, Lavie CJ, Shah S, Englert J, Gilliland Y, Qamruddin S, et al. Prognostic Implications of Left Ventricular Hypertrophy. Prog Cardiovasc Dis. 2018;61(5-6):446-55.

119. Wade KH, Chiesa ST, Hughes AD, Chaturvedi N, Charakida M, Rapala A, et al. Assessing the causal role of body mass index on cardiovascular health in young adults: Mendelian randomization and recall-by-genotype analyses. Circulation. 2018;138(20):2187-201.

120. Bluemke DA, Kronmal RA, Lima JA, Liu K, Olson J, Burke GL, et al. The relationship of left ventricular mass and geometry to incident cardiovascular events: the MESA (Multi-Ethnic Study of Atherosclerosis) study. J Am Coll Cardiol. 2008;52(25):2148-55.

121. Rosengren A, Aberg M, Robertson J, Waern M, Schaufelberger M, Kuhn G, et al. Body weight in adolescence and long-term risk of early heart failure in adulthood among men in Sweden. Eur Heart J. 2017;38(24):1926-33.

122. Brady TM. The Role of Obesity in the Development of Left Ventricular Hypertrophy Among Children and Adolescents. Curr Hypertens Rep. 2016;18(1):3.

123. Jing L, Binkley CM, Suever JD, Umasankar N, Haggerty CM, Rich J, et al. Cardiac remodeling and dysfunction in childhood obesity: a cardiovascular magnetic resonance study. J Cardiovasc Magn Reson. 2016;18(1):28.

124. de Onis M, Blossner M, Borghi E. Global prevalence and trends of overweight and obesity among preschool children. Am J Clin Nutr. 2010;92(5):1257-64.

125. How JM, Pumpa TJ, Sartor DM. Renal sympathoinhibitory and regional vasodilator responses to cholecystokinin are altered in obesity-related hypertension. Exp Physiol. 2013;98(3):655-64.

126. Sun Y, Tao FB, Su PY, China Puberty Research C. Self-assessment of pubertal Tanner stage by realistic colour images in representative Chinese obese and non-obese children and adolescents. Acta Paediatr. 2012;101(4):e163-6.

127. Carel JC, Leger J. Clinical practice. Precocious puberty. N Engl J Med. 2008;358(22):2366-77.

128. de Simone G, Devereux RB, Daniels SR, Mureddu G, Roman MJ, Kimball TR, et al. Stroke volume and cardiac output in normotensive children and adults. Assessment of relations with body size and impact of overweight. Circulation. 1997;95(7):1837-43.

129. de Simone G, Devereux RB, Daniels SR, Koren MJ, Meyer RA, Laragh JH. Effect of growth on variability of left ventricular mass: assessment of allometric signals in adults and children and their capacity to predict cardiovascular risk. J Am Coll Cardiol. 1995;25(5):1056-62.

130. Armstrong AC, Gidding S, Gjesdal O, Wu C, Bluemke DA, Lima JA. LV mass assessed by echocardiography and CMR, cardiovascular outcomes, and medical practice. JACC Cardiovasc Imaging. 2012;5(8):837-48.

131. de Onis M, Onyango AW, Borghi E, Siyam A, Nishida C, Siekmann J. Development of a WHO growth reference for school-aged children and adolescents. Bull World Health Organ. 2007;85(9):660-7.

132. Flynn JT, Kaelber DC, Baker-Smith CM, Blowey D, Carroll AE, Daniels SR, et al. Clinical Practice Guideline for Screening and Management of High Blood Pressure in Children and Adolescents. Pediatrics. 2017;140(3).

133. Sfrantzis KD, How JM, Sartor DM. Implications of diet modification on sympathoinhibitory mechanisms and hypertension in obesity. Auton Neurosci. 2015;189:25-30.

134. Sweazea KL, Walker BR. Impaired myogenic tone in mesenteric arteries from overweight rats. Nutr Metab (Lond). 2012;9(1):18.

135. Drazner MH. The progression of hypertensive heart disease. Circulation. 2011;123(3):327-34.

136. Smithwick RH, Thompson JE. Splanchnicectomy for essential hypertension: Results in 1,266 cases. Journal of the American Medical Association. 1953;152(16):1501-4.

137. Smithwick RH. Surgical treatment of hypertension: The effect of radical (lumbodorsal) splanchnicectomy on the hypertensive state of one hundred and fifty-six patients followed one to five years. Arch Surg. 1944;49(3):180-93.

138. Messerli FH, Bangalore S. Renal Denervation for Resistant Hypertension? N Engl J Med. 2014;370(15):1454-7.

139. Khairy P, Poirier N, Mercier LA. Univentricular heart. Circulation. 2007;115(6):800-12.

140. Gewillig M. The Fontan circulation. Heart. 2005;91(6):839-46.

141. Fontan F, Baudet E. Surgical repair of tricuspid atresia. Thorax. 1971;26(3):240-8.

142. Rychik J. The Relentless Effects of the Fontan Paradox. Semin Thorac Cardiovasc Surg Pediatr Card Surg Annu. 2016;19(1):37-43.

143. Krishnan US, Taneja I, Gewitz M, Young R, Stewart J. Peripheral vascular adaptation and orthostatic tolerance in Fontan physiology. Circulation. 2009;120(18):1775-83.

144. Turquetto ALR, Dos Santos MR, Sayegh ALC, de Souza FR, Agostinho DR, de Oliveira PA, et al. Blunted peripheral blood supply and underdeveloped skeletal muscle in Fontan patients: The impact on functional capacity. Int J Cardiol. 2018;271:54-9.

145. Hsia TY, Khambadkone S, Deanfield JE, Taylor JF, Migliavacca F, De Leval MR. Subdiaphragmatic venous hemodynamics in the Fontan circulation. J Thorac Cardiovasc Surg. 2001;121(3):436-47.

146. Eipel C, Abshagen K, Vollmar B. Regulation of hepatic blood flow: the hepatic arterial buffer response revisited. World J Gastroenterol. 2010;16(48):6046-57.

147. Giardini A, Hager A, Pace Napoleone C, Picchio FM. Natural history of exercise capacity after the Fontan operation: a longitudinal study. Ann Thorac Surg. 2008;85(3):818-21.

148. Gewillig MH, Lundstrom UR, Bull C, Wyse RK, Deanfield JE. Exercise responses in patients with congenital heart disease after Fontan repair: patterns and determinants of performance. J Am Coll Cardiol. 1990;15(6):1424-32.

149. Ostrow AM, Freeze H, Rychik J. Protein-losing enteropathy after fontan operation: investigations into possible pathophysiologic mechanisms. Ann Thorac Surg. 2006;82(2):695-700.

150. O'Rourke MF. Vascular impedance in studies of arterial and cardiac function. Physiol Rev. 1982;62(2):570-623.

151. Kroeker EJ, Wood EH. Comparison of simultaneously recorded central and peripheral arterial pressure pulses during rest, exercise and tilted position in man. Circ Res. 1955;3(6):623-32.

152. Hebson CL, McCabe NM, Elder RW, Mahle WT, McConnell M, Kogon BE, et al. Hemodynamic phenotype of the failing Fontan in an adult population. Am J Cardiol. 2013;112(12):1943-7.

153. Scott EM, Greenwood JP, Vacca G, Stoker JB, Gilbey SG, Mary DA. Carbohydrate ingestion, with transient endogenous insulinaemia, produces both sympathetic activation and vasodilatation in normal humans. Clin Sci (Lond). 2002;102(5):523-9.

154. Lipsitz LA, Ryan SM, Parker JA, Freeman R, Wei JY, Goldberger AL. Hemodynamic and autonomic nervous system responses to mixed meal ingestion in healthy young and old subjects and dysautonomic patients with postprandial hypotension. Circulation. 1993;87(2):391-400.

155. Lipsitz LA, Pluchino FC, Wei JY, Minaker KL, Rowe JW. Cardiovascular and norepinephrine responses after meal consumption in elderly (older than 75 years) persons with postprandial hypotension and syncope. Am J Cardiol. 1986;58(9):810-5.

156. Okumura H, Nagaya N, Enomoto M, Nakagawa E, Oya H, Kangawa K. Vasodilatory effect of ghrelin, an endogenous peptide from the stomach. J Cardiovasc Pharmacol. 2002;39(6):779-83.

157. Imai C, Muratani H, Kimura Y, Kanzato N, Takishita S, Fukiyama K. Effects of meal ingestion and active standing on blood pressure in patients > or = 60 years of age. Am J Cardiol. 1998;81(11):1310-4.

158. Du Bois F, Stiller B, Borth-Bruhns T, Unseld B, Kubicki R, Hoehn R, et al. Echocardiographic characteristics in Fontan patients before the onset of protein-losing enteropathy or plastic bronchitis. Echocardiography. 2018;35(1):79-84.

159. Rychik J, Song GY. Relation of Mesenteric Vascular Resistance After Fontan Operation and Protein-Losing Enteropathy. Am J Cardiol. 2002;90:672-4.

160. Mori M, Shioda K, Elder RW, Pernetz MA, Rodriguez FH, 3rd, Rangosch A, et al. Superior Mesenteric Arterial Flow Pattern is Associated with Major Adverse Events in Adults with Fontan Circulation. Pediatr Cardiol. 2016;37(6):1013-21.

161. Kooner JS, Raimbach S, Watson L, Bannister R, Peart S, Mathias CJ. Relationship between splanchnic vasodilation and postprandial hypotension in patients with primary autonomic failure. J Hypertens Suppl. 1989;7(6):S40-1.

162. Totman JJ, Marciani L, Foley S, Campbell E, Hoad CL, Macdonald IA, et al. Characterization of the time course of the superior mesenteric, abdominal aorta, internal carotid and vertebral arteries blood flow response to the oral glucose challenge test using magnetic resonance imaging. Physiol Meas. 2009;30(10):1117-36.

163. Caro-Dominguez P, Chaturvedi R, Chavhan G, Ling SC, Yim D, Porayette P, et al. Magnetic Resonance Imaging Assessment of Blood Flow Distribution in Fenestrated and Completed Fontan Circulation with Special Emphasis on Abdominal Blood Flow. Korean J Radiol. 2019;20(7):1186-94.

164. Abbasi Bavil E, Yang HK, Doyle MG, Kim TK, Karur G, Bhagra C, et al. Cardiovascular and abdominal flow alterations in adults with morphologic evidence of liver disease post Fontan palliation. Int J Cardiol. 2020;317:63-9.

165. Santisteban MM, Qi Y, Zubcevic J, Kim S, Yang T, Shenoy V, et al. Hypertension-Linked Pathophysiological Alterations in the Gut. Circ Res. 2017;120(2):312-23.

166. Marques FZ, Mackay CR, Kaye DM. Beyond gut feelings: how the gut microbiota regulates blood pressure. Nat Rev Cardiol. 2018;15(1):20-32.

167. Rubenstein LZ. Falls in older people: epidemiology, risk factors and strategies for prevention. Age Ageing. 2006;35 Suppl 2:ii37-ii41.

168. Jansen RW, Lipsitz LA. Postprandial hypotension: epidemiology, pathophysiology, and clinical management. Ann Intern Med. 1995;122(4):286-95.

169. Sidery MB, Cowley AJ, MacDonald IA. Cardiovascular responses to a high-fat and a high-carbohydrate meal in healthy elderly subjects. Clin Sci (Lond). 1993;84(3):263-70.

170. Tentolouris N, Tsigos C, Perea D, Koukou E, Kyriaki D, Kitsou E, et al. Differential effects of high-fat and high-carbohydrate isoenergetic meals on cardiac autonomic nervous system activity in lean and obese women. Metabolism. 2003;52(11):1426-32.

171. Hill KD, Suttanon P, Lin SI, Tsang WWN, Ashari A, Hamid TAA, et al. What works in falls prevention in Asia: a systematic review and meta-analysis of randomized controlled trials. BMC Geriatr. 2018;18(1):3.

172. Siebner TH, Fugl Madelung C, Bendtsen F, Lokkegaard A, Hove JD, Siebner HR. Postprandial Increase in Mesenteric Blood Flow is Attenuated in Parkinson's Disease: A Dynamic PC-MRI Study. J Parkinsons Dis. 2021;11(2):545-57.

173. Xiao C, Stahel P, Morgantini C, Nahmias A, Dash S, Lewis GF. Glucagon-like peptide-2 mobilizes lipids from the intestine by a systemic nitric oxide-independent mechanism. Diabetes Obes Metab. 2019;21(11):2535-41.

174. Gentilcore D, Hausken T, Meyer JH, Chapman IM, Horowitz M, Jones KL. Effects of intraduodenal glucose, fat, and protein on blood pressure, heart rate, and splanchnic blood flow in healthy older subjects. Am J Clin Nutr. 2008;87(1):156-61.

175. Pennington N, Soames RW. The anterior visceral branches of the abdominal aorta and their relationship to the renal arteries. Surg Radiol Anat. 2005;27(5):395-403.